Visual Motion Detection in Tethered Flying Flies

Sarah Nicola Jung

München 2011

Visual Motion Detection in Tethered Flying Flies

Sarah Nicola Jung

Dissertation
an der Fakultät für Biologie
der Ludwig-Maximilians-Universität
München

vorgelegt von
Sarah Nicola Jung
aus Engelskirchen

München, 5. September 2011

Erstgutachter: Alexander Borst
Zweitgutachter: Rainer Uhl
Tag der mündlichen Prüfung: 27.10.2011

Table of Contents

Abstract **1**

1 Introduction **4**

1.1 The Role of Sensory Input in Maintaining Flight Stability **5**

1.2 Visually Guided Behavior **6**

1.3 Elementary Motion Detection **9**

1.4 The Optic Lobes and their Role in Motion Computation **12**

1.4.1 Compound Eyes in Insects **14**
1.4.2 Lamina **15**
1.4.3 Medulla **18**
1.4.4 Lobula **19**
1.4.5 Lobula Plate **20**
1.4.6 H1 Cell **22**

1.5 State-Dependent Influences on Sensory Processing **24**

1.5.1 Examples from Various Modalities **24**
1.5.2 State-Dependent Visual Processing in Insects **26**

1.6 Octopamine and its Role in Insects **28**

1.7 Goals and Project Outline **29**

2 Materials & Methods **31**

2.1 Experimental Animals **31**

2.2 Preparation **32**

2.2.1 Preparation for Cutting Experiments **32**
2.2.2 Preparation for Experiments on CDM Application **33**

2.2.3 Preparation for Experiments on Tethered Flying Flies 33
2.2.4 Preparation for Control Experiments on the Influence of Wind 34
2.3 Experimental Set-up and Positioning of the Fly 34
2.4 Stimulation 35
2.5 Cell Identification and Recording 38
2.6 Chlordimeform 39
2.7 Data Analysis 40
2.8 Modeling 41
2.9 Setting up Extracellular Recordings in Tethered Flying Flies 44
2.9.1 Behavioral Pre-Preparations 44
2.9.2 Spike Extraction 45
2.9.3 Control for a Functional Optomotor Response 48
3 Results 49
3.1 Cutting of the Connective 50
3.2 Flight Modulates Visual Processing 52
3.2.1 Flight Changes Neuronal State 54
3.2.2 Flight Increases the Directional Tuning Range 55
3.2.3 Flight Broadens the Temporal Frequency Tuning Curve 57
3.2.4 Control for Wind 59
3.3 Neuromodulation of the Visual Response 60
3.3.1 CDM Changes Neuronal State 61
3.3.2 CDM Broadens the Temporal Frequency Tuning Curve 62
3.3.3 Control for Neuromodulation 63
3.4 Simulations with the Reichardt Detector 64
4 Discussion 72
4.1 Methodology 72
4.1.1 Cut Experiments 72
4.1.2 Extracelluar Recordings in Tethered Flying Flies 75
4.1.3 Application of CDM 77
4.2 State-Dependent Modulation of Visual Processing in the Fly 78

4.2.1 H1 Recordings of Tethered Flying Calliphora **78**
4.2.2 The Behavioral State Changes the Level of Spontaneous Activity and the Directional Tuning Range **78**
4.2.3 State Dependent Broadening of the Temporal Frequency Tuning Curve **83**

4.3 Effect of Neuromodulation on Visual Processing 86

4.3.1 Physiological Action of Octopamine on the Visual System **87**
4.3.2 Differences between Flight and CDM Condition **87**

4.4 Underling Mechanisms for the Observed Change in the Tuning Properties ... 88

4.5 State-Dependent Influences on Neuronal Processing 90

4.6 Effect of Behavioral State on Visual Processing in Invertebrates 91

4.7 Conclusion and Outlook 92

4.7.1 Future Experiments on the Role of Octopamine **92**
4.7.2 Future Experiments on Tethered Flying Flies **93**

5 References 95

6 Curriculum Vitae 106

7 Acknowledgements 108

Table of Figures

Figure 1.1	Optic Flow Fields for Different Flight Maneuvers.	6
Figure 1.2:	Different Elementary Motion Detector Units (EMDs) Building up Variations of the Reichardt Detector Model.	11
Figure 1.3:	Visual Processing in the Fly Brain.	13
Figure 1.4:	Three Different Types of Compound Eyes in Insects.	15
Figure 1.5:	Drawings of Receptor Cell Axons and of Neurons Connecting the Lamina with the Medulla.	16
Figure 1.6:	Motion Detection Models.	18
Figure 1.7.	Summary Diagram of Synaptic Connections between Input Terminals to the Medulla.	19
Figure 1.8:	VS Cells as Rotation Detectors.	21
Figure 1.9:	Network circuitry of selected tangential cells of the blowfly lobula plate.	22
Figure 1.10:	Anatomy of H1 together with a Vector Field of its Response Properties to Visual Motion.	23
Figure 1.11:	Behavioral Choice by Presynaptic Inhibition of Tactile Terminal.	25
Figure 1.12	Visual Motion Processing is Modulated during Running.	26
Figure 1.13:	Effects of Octopamine on Different Tissues of Invertebrates.	29
Figure 2.1:	Preparation for Tethered Flying Flies.	34
Figure 2.2:	Positioning of the Fly in the Experimental Set-up	35
Figure 2.3	Stimulus Protocols used for Different Experiments.	37
Figure 2.4:	H1 Anatomy and Response Properties to Visual Stimulation.	39
Figure 2.5:	High-Pass Model.	42
Figure 2.6:	Behavioral Test to Increase Willingness of Flies to Fly.	45
Figure 2.7:	Spike Extraction Protocol.	47
Figure 2.8:	Spontaneous Activity Recorded before, during, and post Flight, together with the Waveforms of the Extracted Spikes.	48
Figure 3.1:	Response of H1 before and after Cutting the Connective.	51
Figure 3.2:	Response of V1 before and after Cutting the Connective.	52

Figure 3.3:	Wingbeat Amplitude during Tethered Flight.	53
Figure 3.4:	Spontaneous Activity during Non-Flight and Flight Conditions.	55
Figure 3.5:	Firing Rate in Response to Different Patterns Moving in Preferred and Null Directions of H1.	56
Figure 3.6:	Response of H1 to Different Temporal Frequencies during Flight and Non-Flight Condition.	58
Figure 3.7:	Temporal Frequency Tuning Curve.	59
Figure 3.8:	Control of Wind-Induced Changes in the Response of H1.	60
Figure 3.9:	Spontaneous Activity before and after the Application of CDM.	61
Figure 3.10:	Response of H1 to Different Temporal Frequencies before and after the Application of CDM.	62
Figure 3.11:	Temporal Frequency Tuning Curve.	63
Figure 3.12:	Control for Neuromodulation Experiments.	64
Figure 3.13:	Impulse Response before and after the Presentation of a Moving Sine Grating.	66
Figure 3.14:	Impulse Response before and after the Presentation of a Moving Sine Grating.	68
Figure 3.15:	Comparison between the Experimentally Measured and Fitted Temporal Frequency Tuning Curves.	69
Figure 3.16:	Error Function of the Low-pass Time Constant.	70
Figure 3.17:	Model Prediction of the Step Response to Visual Stimulation.	71
Figure 4.1:	Intracellular Recording of Lobula Plate Tangential Cells before and after Cutting the Connective.	74
Figure 4.2:	Behavioral and Cellular Temporal Frequency Tuning Curve.	86

Abstract

Sensory systems are the interface between an animal and its environment. Therefore, it is essential for the survival of a species that its sensory neurons are optimized for encoding all behaviorally relevant information contained in a stimulus. However, the characteristics of the sensory input perceived by an animal change over time depending on both the external world and the behavioral state of the animal. In the visual system of vertebrates and invertebrates the question of how sensory neurons adapt to different stimulus statistics has been investigated to a great extent, including information theoretical work on synthetic as well as natural stimuli. However, little is known about the influence of the behavioral state on sensory processing, because most work on sensory processing has been restricted to immobilized and/or anesthetized animal preparations. Since the behavior of an animal has a strong influence on the perceived stimulus, it might be of evolutionary advantage to adapt the response properties of sensory neurons to the behavioral state. Recent work, in vertebrates as well as insects, demonstrated that the behavioral state of an animal indeed has an influence on sensory processing.

Motion vision in flies is especially suitable for studying how the motor-activity of an animal can change sensory processing. The dynamic range of visual input in flies changes dramatically from the values at rest, through walking, to flying. Furthermore, lobula plate tangential cells (LPTCs), the neurons coding for self-motion based on optic-flow, are well described. In this work I investigated whether and how visual response properties of LPTCs depend on the behavioral state. I focused on the response

properties of H1, a well-described cell responding to horizontal motion, as it is easy to access and to identify with extracellular methods.

In the first set of experiments, I investigated the influence of ascending projections from the motor-system onto H1. The experiments were based on previous work, in which cutting of the neck connective resulted in a loss of response to visual stimuli in different LPTCs. However, these findings could not be confirmed for H1.

In the second set of experiments, I compared the neuronal responses of H1 to visual stimulation during non-flight and during flight. LPTCs are thought to control different behavioral responses, including the optomotor response. The optomotor response functions most likely as a mechanism for course stabilization during flight. One of its major characteristics is its tuning to a particular temporal frequency [the number of cycles passing a given point on the retina per unit time] of the moving visual environment. Previous comparisons between electrophysiological data obtained from LPTCs and behavioral studies on the optomotor response have revealed a discrepancy in the velocity tuning. The behavioral response was shifted to higher temporal frequencies compared to the response of LPTCs recorded from immobilized flies. Hence, I was particularly interested in the effect of flying on the velocity tuning curve of H1. The results demonstrated that during flight the temporal frequency tuning curve is broadened towards higher frequencies, solving the discrepancy between behavioral observations and electrophysiological measurements in fixed flies.

Next, I wanted to investigate what physiological mechanisms are responsible for the changes observed during flight. Octopamine is a neuromodulator known to change the behavioral state of an animal. In addition, octopaminergic projections into the optic lobe have been described. Using the same visual motion stimuli as beforehand, I applied the octopamine agonist CDM into the hemolymphe of fixed flies and recorded the change in activity of H1. Similar to flight, the application of CDM broadened the temporal frequency tuning curve of H1 towards higher frequencies. This indicates that octopamine is involved in the observed effects of flying.

Where do the octopamine-mediated changes in motion-processing take place? To address this question, I made use of the fact, that visual motion detection in flies is well

described by a phenomenological model called the Reichardt detector, thought to be implemented presynaptic to LPTCs. Although the cellular mechanisms of the Reichardt detector are not yet fully understood, the different processing steps – filtering, multiplication and subtraction – can at least coarsely be related to specific visual neuropils. I evaluated how the parameters of the Reichardt model have to be adjusted for different behavioral states to explain the difference in the temporal frequency tuning of the response of H1 to visual stimulation. The results indicate that the low-pass time constant is shortened during flight and after the application of CDM. Hence, the observed behavioral state dependent effects most likely have their origin in the circuitry presynaptic to H1.

My work is among several pioneering studies conducted in parallel that found that behavior has a strong influence on sensory processing in the fly visual system. By using a combination of different approaches – electrophysiology, pharmacology and modeling – it is one of a few studies not only describing the difference in neuronal processing linked to the behavioral state but also yielding insights into the underlying mechanisms.

1. Introduction

Insects – flies, beetles, wasps, and moths – account for the majority of animal life on Earth. The history of fly evolution can be traced back over 260 million years. During this time flies experienced three episodes of rapid radiation — lower Diptera (220 Ma), lower Brachycera (180 Ma), and Schizophora (65 Ma) — and a number of life history transitions to hematophagy, phytophagy, and parasitism (Wiegmann et al., 2011). Since flies occur in almost every ecological niche, one can easily imagine that they must show great diversification and adaptation to different life styles. However, what has been most fascinating to human beings is probably their amazing ability to fly and to perform acrobatic flight maneuvers. This behavior has created interest regarding many different aspects of flight control, ranging from aerodynamic principles to sensory and motor control. For flight control, sensory feedback is obviously a very important aspect (Frye and Dickinson, 2001). The importance of visual information for flying insects becomes even more evident when one considers the amount of neural hardware these organisms dedicate to vision. In flies, the optic lobes account for approximately a third of the brain's volume (Strausfeld, 1976). The following paragraphs provide the reader with some basic background about vision in flies.

1.1 The Role of Sensory Input in Maintaining Flight Stability

As mentioned above, flies are known for their amazing maneuverability during flight. While chasing mates, for example, they encounter turning velocities of more than 3000 deg/sec. There are several important tasks an animal has to perform to keep flight stable. First, a fly needs to maintain its flight equilibrium, for example by maintaining a certain angle of attack. Second, it needs to control various aspects of its movement in space, such as flight speed and direction.

To control this complex behavior, the fly has access to three different sensory modalities: inertial and gyroscopic forces, wind, and visual input. Coriolis forces can be measured by halteres (Hengstenberg, 1988; Nalbach, 1993; Nalbach and Hengstenberg, 1994). Halteres are transformed hindwings (Weismann, 1964). They consist of an end knob, a thin stiff stalk and an innervated basal swelling containing hundreds of mechanoreceptors. Several studies have investigated how halteres are involved in controlling flight equilibrium (Hengstenberg, 1988; Nalbach, 1993; Nalbach and Hengstenberg, 1994; Sherman and Dickinson, 2003; Sherman and Dickinson, 2004). They demonstrated that the haltere-mediated response to mechanical rotation increases with rising angular velocity, whereas visual input is tuned to lower frequencies. Therefore, integration of feedback from both modalities may enable the fly to stabilize flight over a wide range of angular velocities (Sherman and Dickinson, 2003; Sherman and Dickinson, 2004).

Wind has been shown to be involved in stabilizing aspects of the animal's position during flight, such as its angle of pitch (Reichert et al., 1985; Simmons, 1980). An animal supported by moving air is unlikely to use mechnosensory cues, but rather relies on vision to determine ground speed (David, 1982). However, mechanosensory cues might play a critical role in determining the detection of an insect’s self-induced velocity relative to the ambient air. Johnston’s organs, the chordotonal organs in the antennae of the fly, are involved in regulating the wind beat amplitude and contribute to the stabilization of the flight direction in the horizontal plane (Gewecke, 1967). Furthermore, a recent behavioral study has demonstrated the importance of Johnston’s organs to sustain forward flight (Budick et al., 2007). Wind stimuli transduced via

mechanosensory means can compensate for visual expansion stimuli that have been shown previously to elicit avoidance responses (Tammero and Dickinson, 2002).

The visual system is generally considered as the most important aspect for guiding flight behavior (Borst et al., 2010). Whereas wind and gyroscopic forces give information about flight stability, vision in addition relates the animal's flight to the physical structure of its immediate environment. It has been demonstrated that vision is used for various aspects of flight control including the regulation of speed (Fry et al., 2009) and of flight altitude (Straw et al., 2010) as well as object fixation (Kimmerle and Egelhaaf, 2000).

1.2 Visually Guided Behavior

The current work is focused on motion vision of the fly during different behavioral states. When a fly is flying through a textured environment, self-motion creates an optic flow on the retina (Borst et al., 2010; Franz and Krapp, 2000). The optic flow provides three-dimensional information about how the fly is moving through its environment. When flying through the air, the movement of a fly can be separated into two basic components: translation (thrust, sideslip, lift) and rotation (pitch, roll, yaw). All these movements create distinct optic flow patterns on the retina of the fly's eye (fig. 1.1). A specific set of cells in the fly's visual system, the lobula plate tangential cells, have receptive fields acting as matched filters of the optic flow created during self-motion (Franz and Krapp, 2000; Krapp et al., 1998).

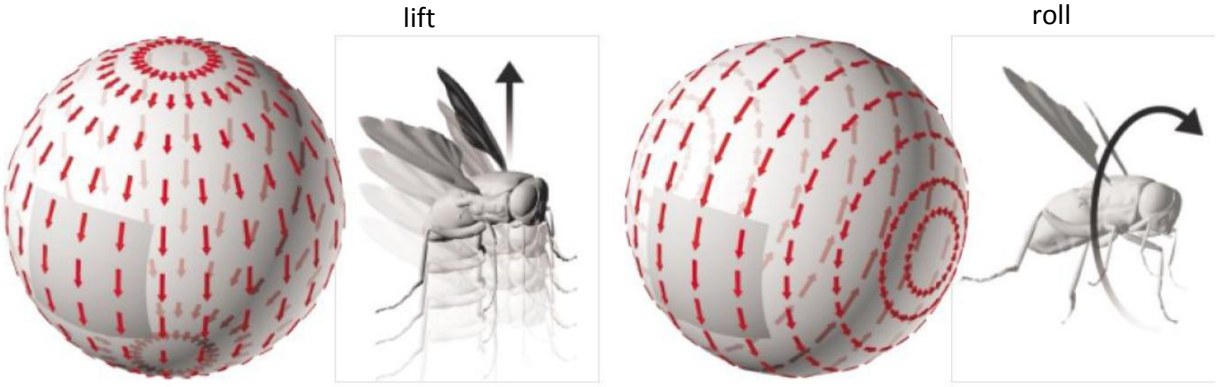

Figure 1.1 Optic Flow Fields for Different Flight Maneuvers. Although locally the optic flow field created by the different flight maneuvers might be ambiguous, integrating information over the entire visual space gives distinct information about the movement (from Zbikowski, 2005).

Behavioral studies on various invertebrate species have shown that, by using specific optic flow stimuli, stereotypic behaviors can be elicited, including visual odometry, peering behavior, the centering response, the landing response, visual regulation of flight speed and the optomotor response (Srinivasan et al., 1999).

The ability to navigate to a specific location like a food source by measuring the distance and direction to fly in order to reach it is called visual odometry (Srinivasan et al., 1996). Bees share this information with conspecifics through the well-known waggle dance (von Frisch, 1947; von Frisch, 1993). The peering response is a behavior used to measure a target distance. A nice example of this behavior can be found in the desert locust. It sways its head from side to side before jumping onto a nearby object (Wallace, 1959). Studies related to the peering responses suggest that this behavior is used to estimate the distance of a target by a movement-detecting mechanism that measures for example the speed/displacement of the target's image and compares this information with the speed/displacement of the eyes (Collett and Paterson, 1991; Kral and Poteser, 1997; Wallace, 1959). In vertebrates, small eye movements might be enough to create a displacement sufficient for object detection. Arthropods, however, have to move their whole head since the eyes are immobile.

Bees are able to fly through the middle of a narrow gap by balancing the distances to the boundary on either side. The so-called centering response can be manipulated by presenting patterns at the adjacent borders of the gap that move with different speed. This, together with additional observations, indicates that bees estimate the distances of surfaces in terms of the apparent motion of patterns by measuring their angular speed (Srinivasan et al., 1991; Srinivasan et al., 1996). Little is known about the centering response in flies. However, most likely similar mechanisms are used (Sugiura and Dickinson, 2009). On the other hand, the landing response has been described in detail in tethered flying flies. It consists mainly of the extension of the forelegs in preparation to land. The landing response can be elicited when flies encounter, for example, looming stimuli representing an approaching object (Borst and Bahde, 1986; Braitenberg and Ferretti, 1966; Goodman, 1960).

Many insect species can regulate the speed of their flight by monitoring and holding constant the velocity with which the image of the environment moves on the eyes (Srinivasan et al., 1999). In bees it has been shown that the speed of flight is controlled by a motion-detecting system which measures and holds constant the speeds of the images of the walls accurately regardless of their spatial structure (Srinivasan et al., 1996). A similar dependence of flight speed on pattern velocity has also been suggested for flies (David, 1982; Fry et al., 2009).

The optomotor response can be described as the turning response evoked by the apparent motion of the visual environment. This behavior was first described in studies of beetles (Hassenstein and Reichardt, 1951; Hassenstein and Reichardt, 1956b). The most important characteristic feature of the optomotor response is its tuning to a particular temporal frequency [the number of cycles passing a given point on the retina per unit time] (Borst and Egelhaaf, 1989; Buchner, 1984; Reichardt, 1961; Reichardt, 1987). It serves to stabilize the insect's orientation with respect to the environment (Goetz et al., 1979; Goetz, 1968). The optomotor response can be elicited by several types of stimuli, ranging from moving stripe patterns to movement of randomly constructed patterns of shades from white through black (Reichardt and Varjú, 1959, Reichardt, 1969).

Traditionally it has been thought that motion vision in flies in general can be computed by a correlation type motion detector model (see below) (Borst and Haag, 2002; Borst, 2007; Srinivasan et al., 1999). As predicted by the model, the optomotor response clearly shows a strong dependence on the temporal frequency and hence on particular pattern characteristics (Borst and Bahde, 1987; Duistermars et al., 2007). The measurement of flight speed is supposed to be independent of the pattern size (Fry et al., 2009; Srinivasan et al., 1991). This raises the issue of identifying the neuronal stage at which the two pathways segregate (Fry et al., 2009). Different solutions have been suggested in recent years (Fry et al., 2009; Katsov and Clandinin, 2008; Srinivasan et al., 1999; Zanker et al., 1999). Zanker et al. (1999), for example, demonstrated that different weighting of the Reichardt detector subunits (see below) can produce responses which vary with image speed and display tuning curves that are substantially independent of

the spatial structure of an image. Srinivasan et al. (1999) suggested mechanisms based on multiple correlators with different temporal frequency optima.

1.3 Elementary Motion Detection

There are different possibilities for how motion information might be computed in the fly brain. The most common models are the *gradient type* and the *correlation type* motion detector (Borst, 2007). While the gradient detector provides an estimate of the local retinal image velocity by dividing the spatial and the temporal luminance gradient (Hildreth and Koch, 1987; Srinivasan, V, 1990), the correlation type motion detector – also called Reichardt detector - correlates the luminance levels derived from two adjacent image points (Hassenstein and Reichardt, 1956a; Hassenstein and Reichardt, 1956b; Reichardt, 1961). In flies, there is strong evidence that the mathematical operation underlying motion detection can best be explained by the Reichardt detector (Borst, 2007). In its simplest form, the Reichardt detector consists of two mirror-symmetrical subunits (Borst and Egelhaaf, 1989; Haag et al., 2004; Hassenstein and Reichardt, 1956a; Hassenstein and Reichardt, 1956b; Reichardt, 1961). In each subunit, the luminance values as measured in two adjacent image locations become multiplied (M) by each other after one of them is delayed by a low-pass filter with time constant τ [s]. This operation is performed twice in a mirror-symmetrical form and the resulting output signals are then subtracted (fig. 1.2). In particular, the bell-shaped steady-state velocity dependence of the response is faithfully described with this model. Furthermore as the optomotor response, the Reichardt detector exhibits an inherent dependence on the spatial pattern wavelength such that the ratio of the optimum velocity and the spatial wavelength remains at a constant temporal frequency (Borst and Egelhaaf, 1989). However, there are several points which are not captured by the model, in particular adaptive properties (Borst et al., 2003; Harris et al., 1999). This can be demonstrated by the example of the so-called impulse response elicited by a brief motion stimulus. The impulse response is characterized by a transient excitation that decays exponentially. The time constant of this decay is supposed to reflect the time constant of the low-pass filter in the simple version of the Reichardt detector (fig 1.2 a).

The impulse response shortens after presenting an adaptation stimulus such as movement or flicker (Borst and Egelhaaf, 1987). However, there is a strong discrepancy between the temporal frequency tuning curves predicted from these experiments and the observed tuning of motion-sensitive cells. A shortening of the low-pass filter would shift the temporal frequency optimum to higher values after motion adaptation; this has not been confirmed by experimental results (Harris et al., 1999).

This discrepancy can be resolved by using an extended version of the model (Borst et al., 2003). In agreement with the original model, the signal coming from the retina is low-pass filtered in one cross-arm of the detector; in the other cross-arm, however, an additional high-pass filter is added (fig. 1.2 c). According to the 'High-pass' model the time constant of the impulse response is identical to the high-pass time constant of the model. Changing the time constant of the high-pass filter by an adapting stimulus will only have little effect on the temporal frequency tuning curve (Borst et al., 2003; Reisenman et al., 2003).

How the Reichardt detector is implemented on a cellular level is not yet well understood. However, there are several cell types in the fly visual system which might be suitable to compute one of the different steps that are necessary for a motion detection mechanism based on the Reichardt detector (Higgins et al., 2004). I will use the following section to introduce the visual system of the fly, with special focus on motion computation.

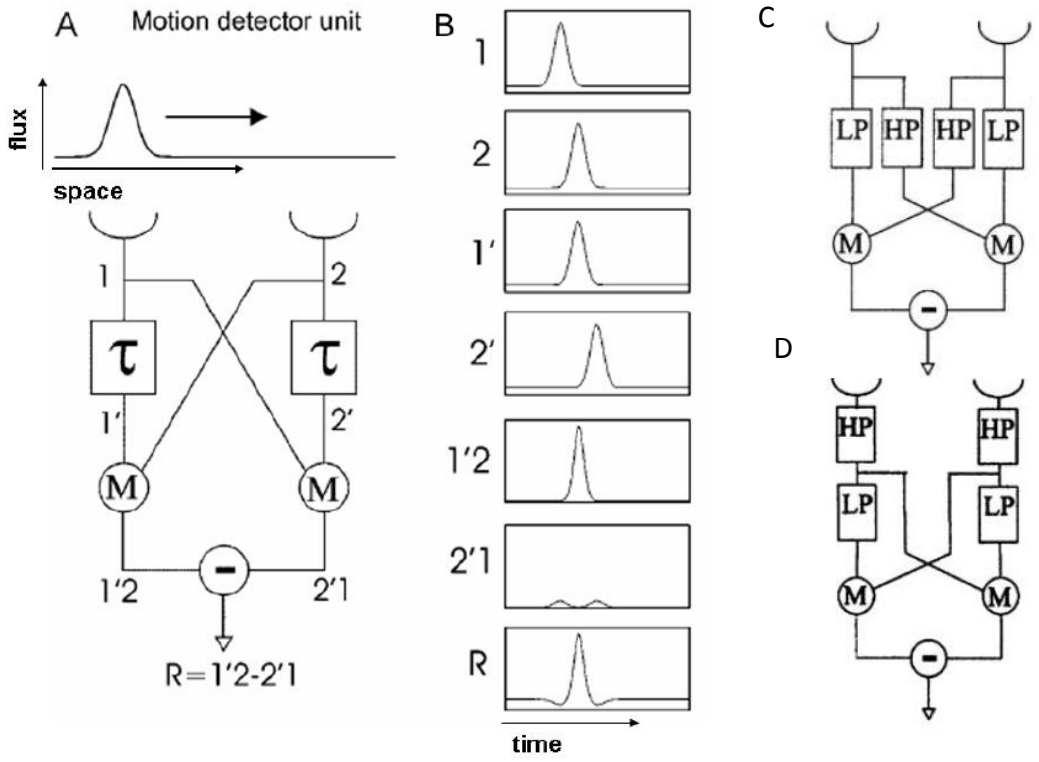

Figure 1.2: Different Elementary Motion Detector Units (EMDs) Building up Variations of the Reichardt Detector Model. a) Reichardt and Hassenstein model for directionally selective motion detection (from Borst and Haag, 2002). b) The intermediate signals from the Reichardt detector at the corresponding positions in (a). A light bar passes the detector unit in its preferred direction. First the left photoreceptor is stimulated (1); the signal is delayed while passing through the left arm of the unit (1'), but not while passing through the crossarm (1). The light bar needs some time to travel to the second photoreceptor (2). Here again the signal is delayed when passing through the right arm (2'), but not when passing through the crossarm (2). When the temporal delay induced by the filter in the left arm is equivalent to the temporal delay induced by the spatial distance between the photoreceptors, the signals arrive at the same time and lead to a maximum output after the multiplication step (1'*2). Since, in the right half of the detector unit, the signals do not arrive together, the output is minimal (2'*1). The last subtraction step (R=1'*2-2'*1) increases the direction selectivity of the detector and also determines the polarity of the output (from Borst and Haag, 2002). c) 'High-pass' detector model - modified version of the Reichardt detector model with a high-pass filter added to the cross arm of the detector unit (from Borst et al., 2003). d) A detector version with a high-pass filter added to the input lines (from Borst et al., 2003).

1.4 The Optic Lobes and their Role in Motion Computation

Like most insects, flies have a compound eye built up from hundreds to thousands of ommatidia, depending on the species. Each ommatidium possesses its own lens and its own set of photoreceptors. The axons of the photoreceptors project into a brain area called the optic lobe. The optic lobe is composed of three visual ganglia: the lamina, the medulla and the lobula complex, which itself is divided into the lobula and the lobula plate (fig. 1.3 a). The visual neuropil are composed of columnar elements. The specific elements are called ommatidia (compound eye/retina), cartridges (lamina) and columns (lobula complex). Two chiasms exist in the visual track of the fly, one between the lamina and the medulla and one between the medulla and the lobula complex, which reverse the order along the anterior-posterior axis of visual space. The visual input is organized in a retinotopic fashion. This means that the spatial relationship between neighboring image points is preserved throughout the visual neuropil (Borst and Haag, 2002; Borst et al., 2010; Braitenberg, 1970).

Each ommatidium is composed of eight photoreceptors (R1-R8). There is a strong separation between different visual pathways. The different absorption spectra of the photoreceptors leads to a spilt of visual information into a chromatic and an achromatic channel (Cook and Desplan, 2001; Hardie, 1979; Sanes and Zipursky, 2010; Yamaguchi et al., 2008).

The chromatic channel starts with the photoreceptors R7 and R8 (Montell et al., 1987; Sanes and Zipursky, 2010; Zuker et al., 1987). R7-R8 do not form synapses in the lamina, but directly project to the medulla. Here, they aborize in distinct layers. In the medulla the information is further processed by local neurons and transmedullary neurons innervating the lobula, the lobula plate, or both. Visual projection neurons (VPNs) link the medulla, lobula, and lobula plate with the central brain (Otsuna and Ito, 2006; Sanes and Zipursky, 2010).

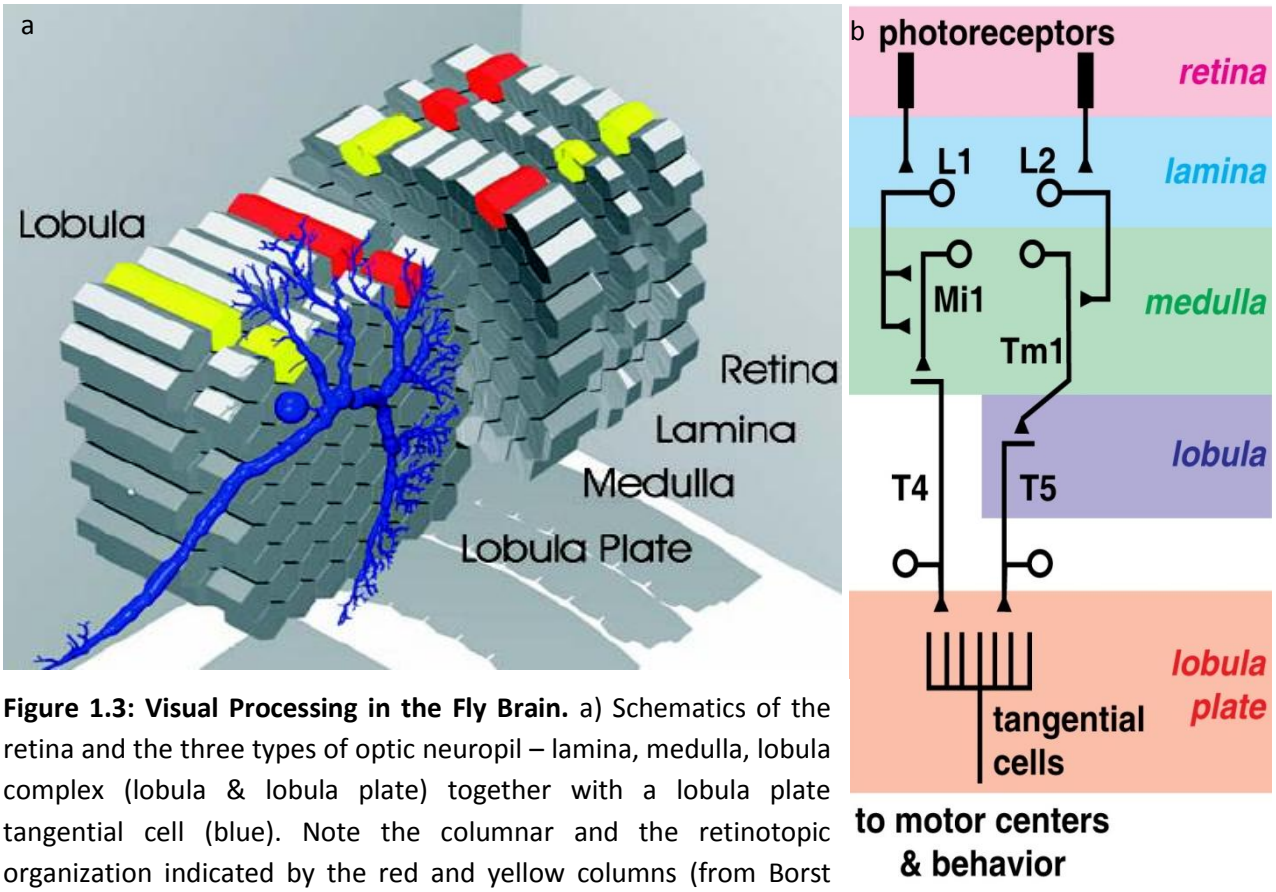

Figure 1.3: Visual Processing in the Fly Brain. a) Schematics of the retina and the three types of optic neuropil – lamina, medulla, lobula complex (lobula & lobula plate) together with a lobula plate tangential cell (blue). Note the columnar and the retinotopic organization indicated by the red and yellow columns (from Borst and Haag, 2002). b) Schematics of minimal circuitry candidate to implement the Reichardt model (from Gabbiani and Jones, 2011).

R1-R6 neurons provide an achromatic channel which is further divided into multiple information pathways including circuits for motion computation and phototaxis behavior (Hardie, 1979; Sanes and Zipursky, 2010; Yamaguchi et al., 2008; Zhu et al., 2009). The minimal circuitry presumed to be involved in motion detection starts with the photoreceptors R1-R6 which project into the lamina (fig. 1.2 b). Here, large monopolar cells – L1 and L2 – further transfer information to the medulla cells Mi1 and Tm1, respectively (Meinertzhagen and O'Neil, 1991; Takemura et al., 2008). Within the medulla, Mi1 is thought to project onto the dentrites of T4 cells. Tm1 projects into the lobula where it likely synapses onto T5 cells. Therefore, there exist two different pathways involved in motion computation, starting with L1 and L2, respectively. Both pathways merge again in the lobula plate where T4 and T5 innervate the so-called lobula plate tangential cells (Bausenwein and Fischbach, 1992; Douglass and Strausfeld, 2003; Fischbach and Dittrich, 1989). The latter cells are directionally selective and involved in the visual course control of the fly (Borst and Haag, 2002; Borst et al., 2010).

1.4.1 Compound Eyes in Insects

The compound eye is the most common eye design found in animals, including most species of insects, crustaceans, myriapods and even some clams and polychaetes (Exner, 1981; Land and Fernald, 1992). There are several very interesting aspects related to the optics of compound eyes. The most striking one is the strong relationship between the size of the eye and its spatial resolution. All compound eyes are composed of ommatida consisting of a corneal facet lens, a crystalline cone, screening pigments and a rhabdom which contains the photoreceptor molecules. The anatomical resolution is given by the interommatidial angle ϕ and is defined by $1/(2*\phi)$ (Land, 1997). The visual acuity, however, is determined by the photoreceptor's spatial receptive field, which also depends on the specific eye design (Land, 1997).

There is a trade-off between spatial resolution and light sensitivity that led to two different major designs for compound eyes: the apposition eye (1.4 a) and the superposition eye (1.4 b). The apposition eye is best adapted to bright light and is mostly found in animals active during daylight. Each ommatidium is isolated from its neighbors by a sleeve of light-absorbing screening pigments to prevent light from adjacent ommatidia reaching its photoreceptors (Land, 1999). The rhabdomeres are often fused (e.g., in honeybees) such that all photoreceptors within one ommatidia receive light from the same direction in space (Borst, 2009). Higher flies also possess an apposition eye; however, they have a special adaption to increase sensitivity while losing only little spatial resolution, called neuronal superposition (Kirschfeld, 1973). Each ommatidium has a distinct optical axis. The same is true for the different photoreceptors in one ommatidium, since the rhabdomeres are segregated. Within neighboring ommatidia certain groups of photoreceptors have parallel optical axes. By connecting these groups of photoreceptor to a common postsynaptic target, sensitivity of the system increases without the drawback of losing spatial resolution (fig. 1.4 c) (Braitenberg, 1967; Braitenberg, 1970; Kirschfeld, 1973).

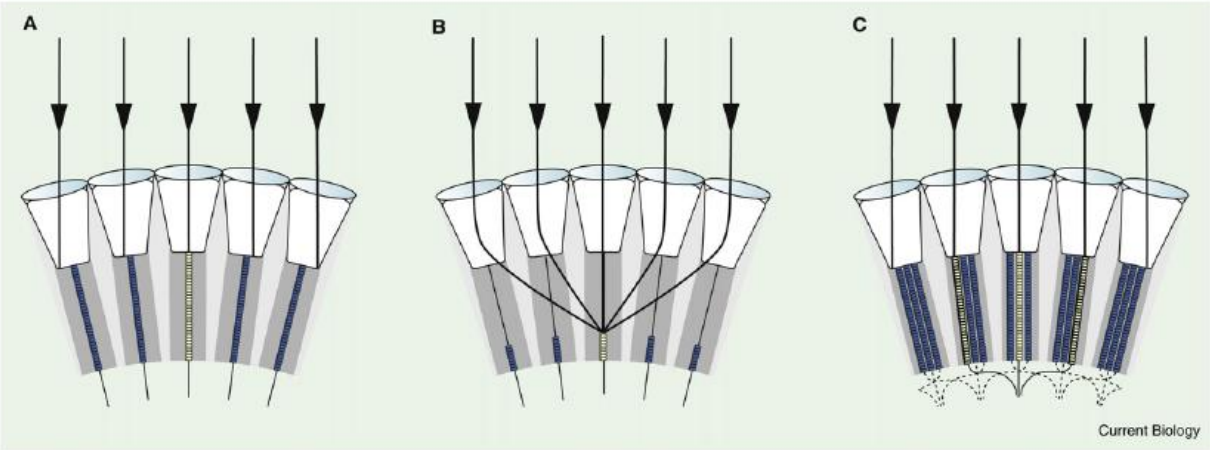

Figure 1.4: Three Different Types of Compound Eyes in Insects. a) Apposition eye. A light absorbing pigment between the ommatidia prevents light from entering any neighboring rhabdomere. b) Superposition eye. The lower parts of the ommatidia are only separated by a transparent material. Therefore, light from neighboring ommatidia can reach the rhabdomere from the central ommatidia. c) Neural superposition eye. As in the apposition eye, only light entering one ommatidium can reach the rhabdomere. However, on a neuronal level, photoreceptors located in neighboring ommatidia pointing into the same direction are pooled together at the next processing stage, leading to an increase in sensitivity without losing spatial resolution (from Borst, 2009).

In the second major design type of the compound eyes – the superposition eye – the pigment sleeve is withdrawn and a wide optically transparent area is interposed between the lenses and the photoreceptors. Light traveling between ommatidia is focused on one rhabdomere which increases the sensitivity of the eye to light but decreases the spatial resolution. This eye design is mainly found in animals active during dim light or night (Warrant, 1999; Land, 1999).

1.4.2 Lamina

The lamina is organized in cartridges. Anatomical studies have shown that each cartridge is composed of 12 neuron types that include 11 narrow-field elements and one wide-field/amacrine cell (Fischbach and Dittrich, 1989; Meinertzhagen and O'Neil, 1991). The narrow-field elements are composed of one of the receptor terminals R1-6, two fibers from the receptors R7 and R8 that do not ramify in the lamina, five types of monopolar cells L1-5 and three types of medulla cells C2, C3 and T1 (fig. 1.5). There is little known about L3, L4 and L5 neurons, but L1-L2 cells and, to some extent, L4 cells are thought to

be involved in motion processing. The neuronal superposition principle reveals itself by the fact that in each cartridge, L1 and L2 receive input from each of the R1-R6 photoreceptor cell types originating from different ommatidia but pointing to the same direction in space (Braitenberg, 1967; Braitenberg, 1970; Kirschfeld, 1973).

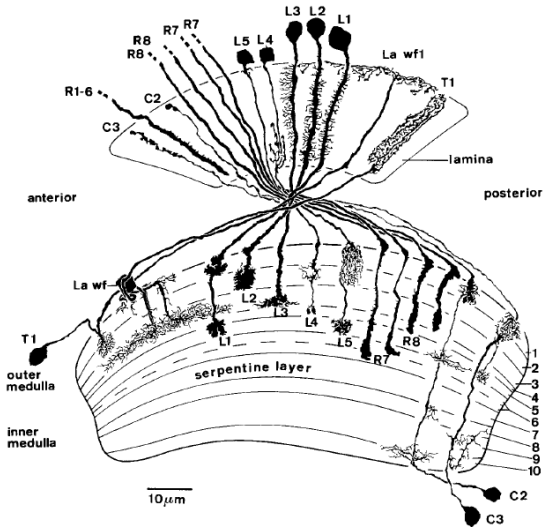

Figure 1.5: Drawings of Receptor Cell Axons and of Neurons Connecting the Lamina with the Medulla. R1-R6 terminate in the lamina, while the axons of R7 and R8 project into the medulla. Nine interneurons are shown, which arborize in lamina and medulla. The Lawf neuron corresponds to the wide-field neuron (from Fischbach and Dittrich, 1989).

Although electrophysiological data from lamina neurons (L1-5) exist, it is difficult to assess from this data the contribution of these neurons to motion processing (Jarvileh and Zellter, 1971; Laughlin and Osorio, 1989; Skingsley et al., 1995; Straka and Ammermuller, 1991; Uusitalo et al., 1995; Uusitalo and Weckstrom, 2000). However, it has been proposed that they take part in high-pass filtering the visual input before it reaches further motion processing stages (Higgins et al., 2004; Jarvileh and Zettler, 1973). Genetic tools have given some interesting insights into information processing in the lamina, including direct evidence of the role of lamina cells in motion vision. Inactivation studies have revealed that information is segregated into multiple information streams for the general sensitivity to light and specific motion computations that arise in higher-order brain regions. It could be demonstrated for example that inactivating L4 cells result in a complete loss of motion vision without comprising phototaxis behavior (Zhu et al., 2009). The importance of the L1 and the L2 pathway has been shown by genetically silencing either one or both of them. It was suggested that L1 and L2 together are necessary and largely sufficient for motion-dependent behavior (Rister et al., 2007). A recent study confirmed the importance of L1 and L2 for motion

detection (Joesch et al., 2010). Joesch et al. (2010) further concluded that, similar to the processes taking place in the retina of vertebrates, L1 and L2 neurons provide the input to separate on- and off-channels. The response of L2 to motion stimuli has also been studied by using calcium imaging (Reiff et al., 2010). It was concluded that half-wave rectification takes place at the level of the L2 neurons because brightness decrements induced a strong increase in the intracellular Ca-signals, but brightness increments induced only small changes. Based on these recent studies, new experiments and modeling studies were performed to gain insight into the internal structure of the Reichardt detector (Eichner et al., 2011). The new model, proposed by Eichner et al. (2011), is a modification of the so-called 2-Quadrant model originally suggested by Franceschini et al. (1989). Here, the input to each subunit of the Reichardt detector is split into ON (brightness increment) and OFF (brightness decrement) components. Only input combinations of the same sign (ON-ON, OFF-OFF) are further processed. Therefore, the 2-Quadrant model is not mathematically identical to the original Reichardt detector. Nevertheless, the 2-Quadrant model can still account for its major characteristics. However, recordings from lobula plate tangential cells revealed strong directionally-selective responses to sequences of same sign (ON-ON, OFF-OFF) and inverted responses to sequences of opposite sign (ON-OFF, OFF-ON) (Eichner et al., 2011). The latter is a clear contradiction to the original proposed 2-Quadrant model. However, Eichner et al. (2011) found persistent directionally selective responses, indicative of a tonic representation of the brightness level at the input of the motion detector. By preprocessing the input by a filter stage that feeds the signal through a first-order high-pass filter but in parallel allows 10% of the original signal to pass (DC), the authors could reproduce all measured responses including the directionally selective response to sequences of opposite sign (fig. 1.6 a). However, Clark et al. (2011) came to a contradictory conclusion regarding the internal structure of the Reichardt detector. Similar to Reiff et al. (2010), they performed calcium imaging in lamina cells. Using random brightness changes, they found that the encoding of L1 and L2 is largely linear, arguing against the half-wave rectification within L1 and L2. For their experiments, Clark et al. (2011) used a combination of specific genetic silencing, minimal motion stimuli and in vivo calcium imaging, as well as behavioral experiments. Based on the experimental findings, they proposed a weighted 4-Quadrant model (fig. 1.6 b). The functional role for

L1 and L2 is still under discussion, since the modified 2-Quadrant model, as well as the weighted 4-Quadrant model, could reproduce a wide range of experimental data.

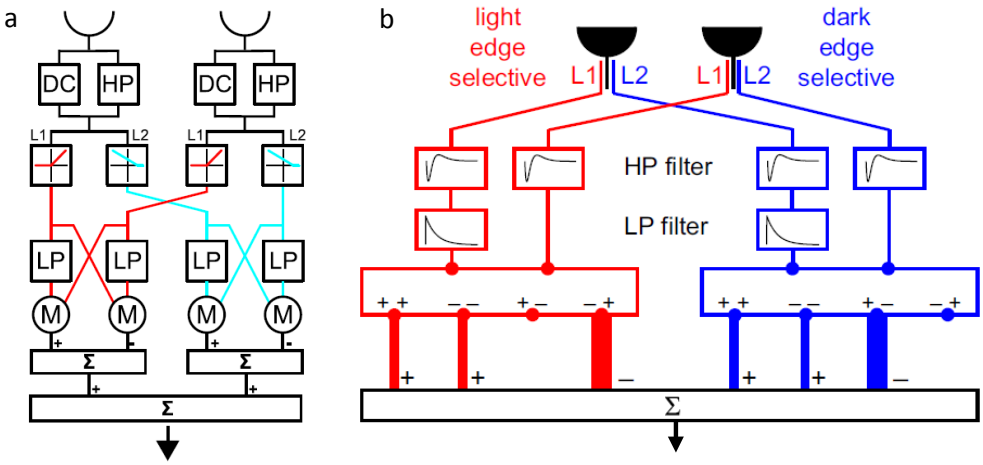

Figure 1.6: Motion Detection Models. a) '2-Quadrant-Detector' with an additional preprocessing stage including a DC component and a high-pass filter step in parallel. The two signals are added before the rectification step takes place. The ON pathway is depicted in red; the OFF pathway is depicted in blue (from Eichner et al., 2011). b) Weighted quadrant model. The inputs are filtered before being split into four multiplication steps that are weighted differently in the two pathways. The weighting is indicated by the thickness of the lines (from Clark et al., 2011).

1.4.3 Medulla

The medulla is divided into ten layers (M1-M10). The first 6 outer layers (M1-M6) receive direct input from the lamina neurons (L1-L5) or the photoreceptors R7 and R8 (fig. 1.5). The input is cartridge-specific, resulting in a retinotopic organization of the medulla. In addition, the separation of the chromatic and the achromatic channels is preserved, because the different pathways innervate distinct layers. Also, the postsynaptic neurons, such as medulla tangential cells and interneurons, ramify in distinct layers. However, the strong retinotopy becomes diluted because some of the postsynaptic neurons extend their arborizations beyond cartridge boundaries. A few major classes of medulla cells send information further to the lobula complex. TM cells innervate the lobula, T-cells innervate either lobula (T2-3) or lobula plate (T4), whereas TmY neurons bifurcate and innervate both lobula as well as lobula plate (Bausenwein and Fischbach, 1992; Fischbach and Dittrich, 1989).

Recent work using serial-section electron microscopy closely matches previously reported Golgi-staining results concerning the anatomy of the cells (Takemura et al., 2008). However, in addition, synaptic connectivity could be shown (fig. 1.7). In the chromatic channel, R8 forms contacts upon R7 and thus these two spectral inputs are interconnected. L3 provides input upon both R6 and R7, adding an achromatic input. In the achromatic the channel the terminal of L5 reciprocally connects to that of L1. Importantly, input cells L1 and L2 lack direct interconnection, which speaks in favor of a strong separation of the two motion-processing pathways. However, L1 and L2 cells both receive input from C2 and C3 cells.

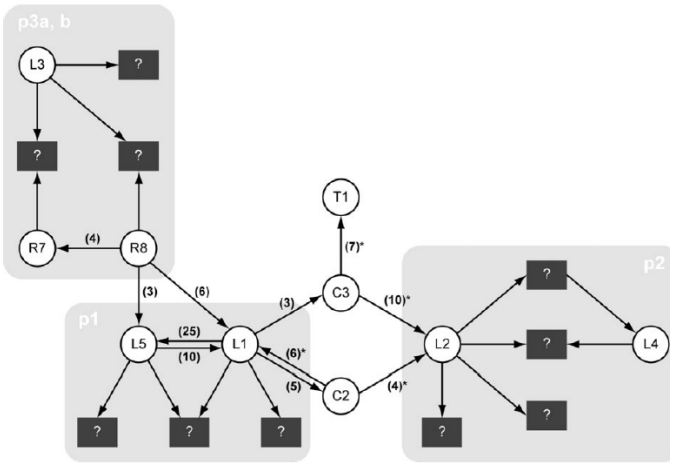

Figure 1.7. Summary Diagram of Synaptic Connections between Input Terminals to the Medulla. The terminals are also presynaptic to many unknown cells, probably mostly medulla neurons. The numbers of synapses found in a specific column are indicated by each arrow. The gray shaded panels (p1, p2, p3 a,b) represent previously proposed visual pathways (Bausenwein and Fischbach, 1992) (from Takemura et al., 2008).

1.4.4 Lobula

The lobula forms the anterior part of the lobula complex. Compared to the lobula plate, the lobula is a less well-studied optic neuropil. It receives input directely from the medulla (Fischbach and Dittrich, 1989). Like the preceeding neuropil, the lobula is organized in a retinotopic fashion, but the number of columns is reduced compared to the number of cartridges. This results in a coarser visual resolution (Strausfeld, 1976). The lobula is divided into six layers. It is assumed that the lobula processes colour as well as motion. Indication for a colour vision channel comes from the fact that certain transmedulla neurons which arborize in medulla layers receive input from R7 or R8 and terminate in discrete layers of the lobula (Gao et al., 2008).

Three of the six layers were labeled with 2-Deoxyglucose in response to a motion stimulus (Buchner et al., 1984). The most posterior layer of the lobula contains the axonal arborizations of the Tm1 cells from the medulla as well as the T5 dendritic arborizations. The T5 neurons are one of a few cell types which interconnect the lobula with the lobula plate (Fischbach and Dittrich, 1989). T5 cells are assumed to be crucial for motion vision (Douglass and Strausfeld, 1995). They project to distinct layers of the lobula plate containing cells selective for motion (Buchner et al., 1984; Douglass and Strausfeld, 1995; Douglass and Strausfeld, 2003; Strausfeld, 1976).

1.4.5 Lobula Plate

The lobula plate forms the posterior part of the lobula complex. This brain area is also often refered to as the cockpit of the fly because it contains neurons – the lobula plate tangential cells (LPTCs) – that have been shown to be involved in the visual course control of flies (Borst and Haag, 2002; Borst et al., 2010). The later idea has its origin from experiments that showed that the optomotor response is strongly effected when LPTCs are ablated (Geiger and Nassel, 1981; Hausen and Wehrhahn, 1983; Heisenberg et al., 1978). In blowflies each hemisphere contains about 60 different LPTCs which are individually identifiable based on their anatomy and response properties to visual stimulation. The principal output elements of the lobula plate are thought to be the 'horizontal system' (HS) cells and the 'vertical system' (VS) cells. As indicated by their names, they receive information about large-field horizontal (HS cells) and vertical (VS cells) motion which they further transmit onto descending neurons (Haag et al., 2007; Hausen, 1982a; Hausen, 1982b; Hengstenberg, 1982; Hengstenberg et al., 1982; Krapp et al., 1998; Wertz et al., 2008). Interestingly, however, looking more closely at the response properties of theses neurons reveals that they are not only direction-selective to visual motion but, more specifically, tuned to certain axes of rotation of the fly (fig. 1.8). This rotation selectivity is thought to represent certain movements such as yaw, roll and pitch occuring during flight or other locomotor behaviors (Franz and Krapp, 2000; Krapp et al., 1998). How do these complex receptive fields arise? This has been investigated in great detail by analysing the vertical system in flies (fig. 1.8 a-c). The receptive field of these cells is composed of two components (Haag and Borst, 2004):

one from local motion detectors on their dendrites, and one from other large-field neurons (fig. 1.9). For the first component, the dendritic organization and the layered structure of the lobula plate is of critical importance. First of all, the lobula plate forms a map of direction-selective small-field elements as a result of the retinotopic organisation, where a specific location on the lobula plate corresponds to a particular position in the visual world. There exists a segregation of the input into different layers of the lobula plate. In total, four direction-specific input layers exist, representing the four main directions of motion (Buchner et al., 1984). The LPTCs run perpendicular to the columns, covering many hundreds or thousands of them with their dendrites. The dendrites only obtain input from specific layers of the lobula plate and this explains a large part of the directional selectivity of the particular LPTCs (Hausen, 1982a; Hausen, 1982b; Hengstenberg et al., 1982). Theoretically, it would be possible to build up neurons matching the receptive field properties of VS cells by only using small-field elements. However, the receptive fields predicted from the anatomy of VS cells do not match the measured receptive fields (Hengstenberg et al., 1982; Krapp et al., 1998; Krapp and Hengstenberg, 1996). Consequently, the receptive fields of VS cells cannot be explained only by their retinotopic input from local elementary motion detectors (EMDs). It turns out that network connectivity within the lobula plate plays a critical role (Borst and Weber, 2011). The coupling of neighboring VS-cells through gap junctions leads to a broadening of their receptive fields (Elyada et al., 2009; Farrow et al., 2005). Inhibitory chemical synapses play a role in sign reversal in a few of these cells; in addition, indirect coupling to the HS-system adds a horizontal component to the receptive field of VS cells (Haag and Borst, 2004).

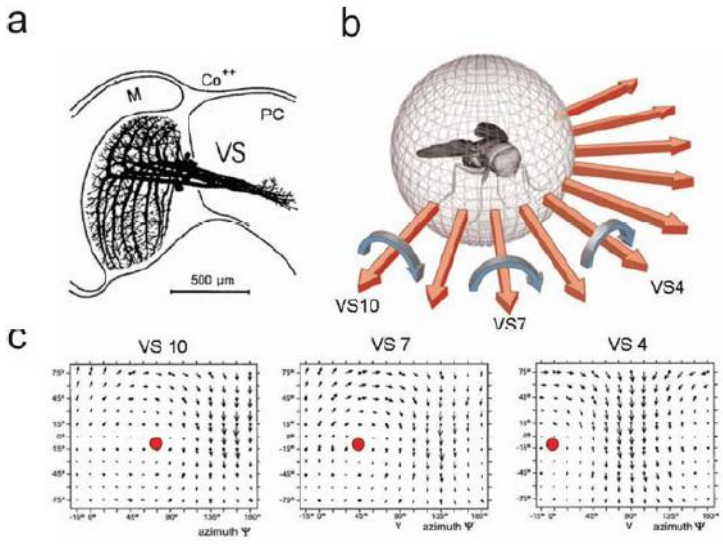

Figure 1.8: VS Cells as Rotation Detectors. a) Anatomy of VS cells as obtained from cobalt fills. b) Schematic fly with various axes of rotation. c) Receptive fields of VS cells. Note that receptive fields match different axes of rotation around different poles (red dot) (from Borst and Haag, 2007).

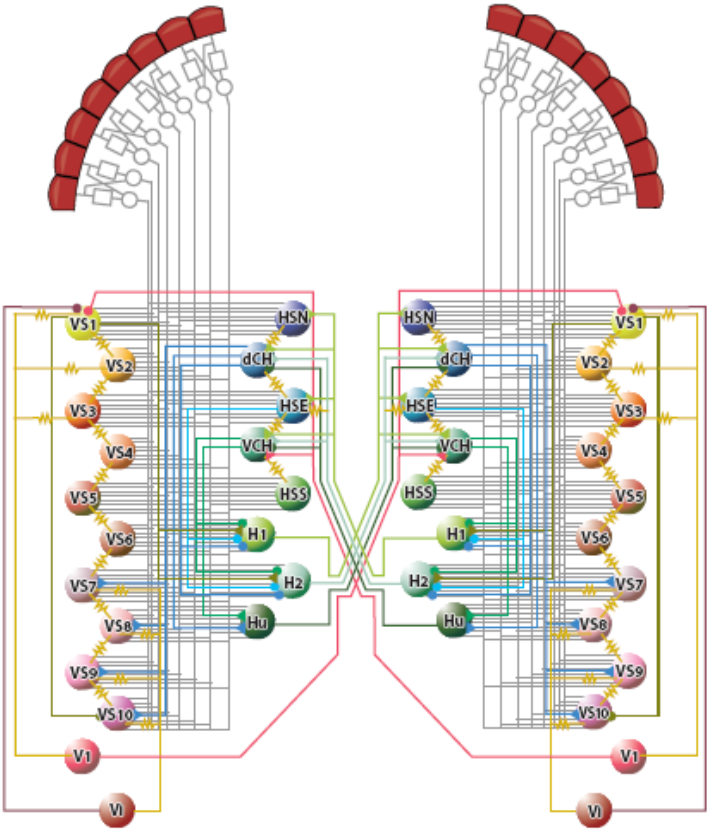

Figure 1.9: Network circuitry of selected tangential cells of the blowfly lobula plate. In addition to receiving retinotopic input from arrays of local motion detectors, cells are strongly interconnected with each other. Excitatory and inhibitory chemical synapses are symbolized by triangles and circles, and electrical synapses are represented by resistor symbols (from Borst and Haag, 2007).

1.4.6. H1 Cell

Almost all data in this work are obtained from the lobula plate tangential cell H1. Anatomically, H1 is interesting because its aborizations span over the lobula plate of both brain hemispheres (fig. 1.10 inset). The dendritic input and the receptive field, however, are restricted to only one hemisphere (Eckert, 1980). The axon crosses along the dorsal surface of the central protocerebrum to the opposite side, where it finally enters into the contralateral lobula plate.

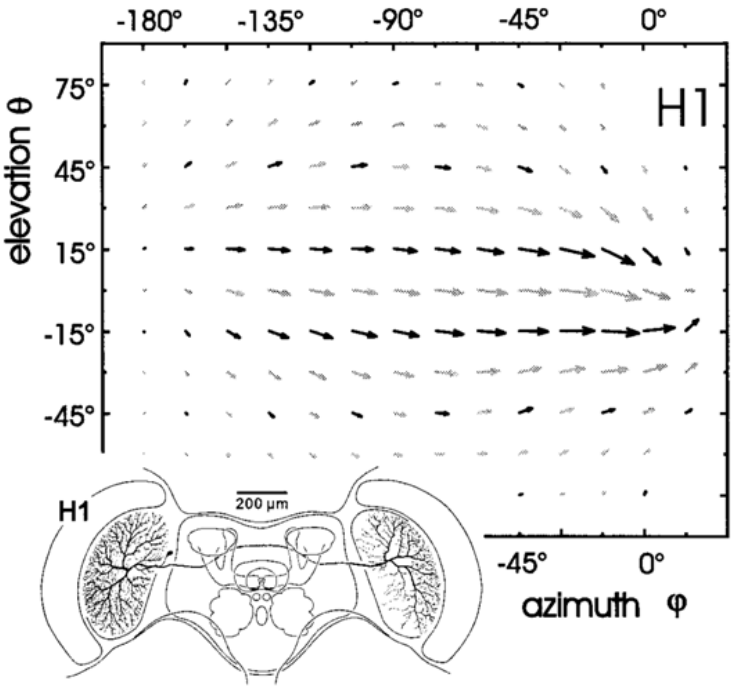

Figure 1.10: Anatomy of H1 together with a Vector Field of its Response Properties to Visual Motion. The anatomy (inset, modified from Hausen 1993) as well as the response field are shown as depicted from a neuron that receives its retinotopic input in the left visual hemisphere. The neuron's local preferred direction (LPD) is indicated by the direction of the arrow. The local motion sensitivity (LMS) is reflected by the length of the arrows (from Krapp et al., 2001).

In contrast to HS and VS cells, H1 is a spiking neuron. It responds with an increase in firing rate when the pattern is moved horizontally from back to front in the receptive field (preferred direction) and with a decrease in firing rate when the pattern is moved in the opposite direction (null direction) (Eckert, 1980). It is generally assumed that H1 receives input mainly from columnar EMDs (Borst and Haag, 2007; Borst et al., 2010). The receptive field of the cell was measured using local stimuli (fig. 1.10) (Krapp et al., 2001). In addition to the input from the EMDs, a few connections to other lobula plate tangential cells are known (fig. 1.9) (Borst and Weber, 2011). The H1 in the left lobula plate excites the HS and CH cell of the right lobula plate (Haag and Borst, 2001; Hausen, 1984; Horstmann et al., 2000), which in turn inhibits the right H1 (Haag and Borst, 2001). Thus, the two H1 cells mutually inhibit each other via HS and CH cells. Furthermore, H1 also receives excitatory input from VS1 (Haag and Borst, 2003).

1.5 State-Dependent Influences on Sensory Processing

Most electrophysiological work in vivo has been conducted in immobilized or even anesthetized animal preparations. It has been generally assumed that the response properties of sensory neurons are the same, whether the animal is immobilized and passively perceiving a stimulus or whether it is freely moving around. Considering how different the tasks are an animal has to solve when it is passively receiving a stimulus and during active sensation, it is not surprising that this assumption has been challenged in the past years.

1.5.1 Examples from Various Modalities

The behavioral state of an animal has a strong influence on sensory processing. This has been shown not only throughout the animal kingdom but also throughout sensory modalities.

In the olfactory cortex of rats it has been shown that odorant-evoked responses are changed dependent on whether brain activity of the neocortex is characterized by slow wave (SWS) or fast wave (FWS) oscillations (Murakami et al., 2005). In the olfactory cortex the majority of units showed a robust spike response to adequate odorants during FWS but only a weak response during SWS. Interestingly, this state-dependent change in odorant-evoked responses was only observed in a small fraction of units recorded in the olfactory bulb.

Another interesting example comes from the electrosensory system of weakly electric fish (Rose, 2004). These fish produce via electric organs in their tails periodic, electrical signals (EOD) that can be used, for example, for prey localization (Nelson and Maciver, 1999). The summation of EOD signals of two fish in the vicinity of each other can cause EOD amplitude modulations. These amplitude modulations reduce the ability to detect objects if the fish have a similar EOD frequency (Matsubara and Heiligenberg, 1978). One of the fish usually shows a so-called jamming avoidance behavior and changes its EOD frequency to improve object localization (Bullock et al., 1975; Bullock et al., 1972; Watanabe and Takeda, 1963). This example illustrates a completely different aspect of

behavioral modulation of sensory processing because sensory information is actively changed before even reaching the receptors.

Behavioral studies in the leech have shown that feeding suppresses different sets of locomotor activities such as shortening, swimming, crawling or even local bending. A recent study demonstrated that the lack of such locomotor behavior normally induced by touch is likely suppressed by presynaptic inhibition of sensory terminals (Gaudry and Kristan, 2009). P cells are touch-sensitive neurons. They are presynapitic to many neurons involved in locomotion, e.g., to cell 212, which is known to be involved in local bending. During feeding the amplitude of EPSPs decreases at P cell synapses (fig. 1.11). This process is most likely mediated by serotonin.

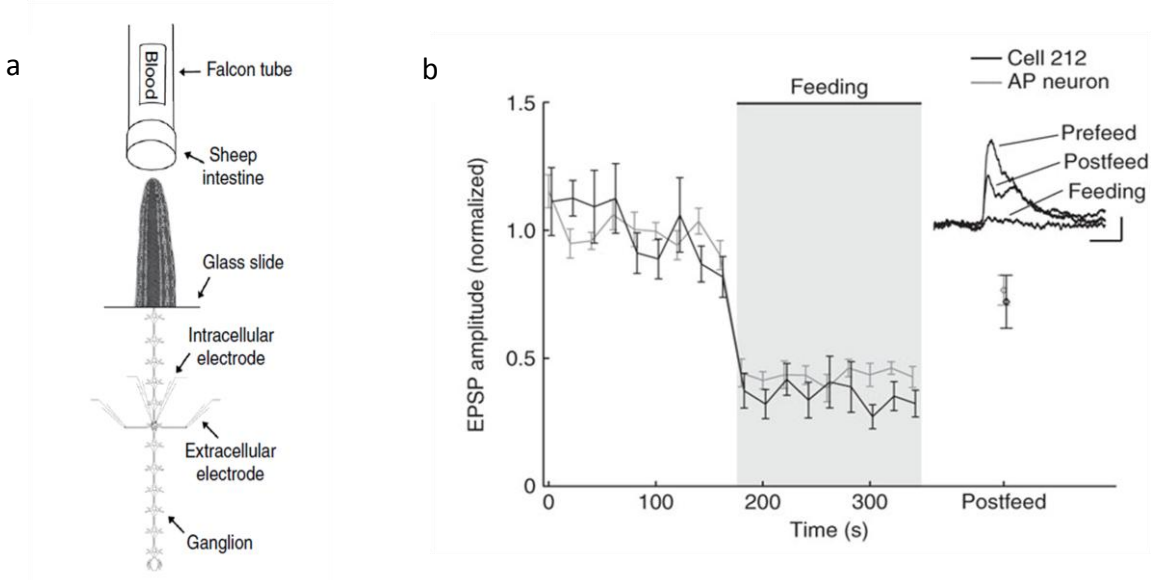

Figure 1.11: Behavioral Choice by Presynaptic Inhibition of Tactile Terminal. a) Preparation of the leech. Leeches still perform normal feeding behavior even though most of their nervous system is dissected for electrophysiological recordings. b) EPSP amplitude of P-cell synapses before, during and after feeding. During feeding, the EPSP in the postsynaptic neurons 212 and AP is strongly reduced. The inset shows an average EPSP form under the three conditions (from Gaudry and Kristan, 2009).

It has been shown that visual processing is also strongly modulated by the behavioral state of an animal. In monkeys, it has been demonstrated that visual motion processing is regulated by behavior (Treue and Maunsell, 1996). The responses of direction-selective neurons are greatly influenced by attention. An interesting finding of this study

was that attentional modulation of the neuronal response already appeared on the level of the middle temporal visual area – a relatively early visual area.

In mice, visual processing is modulated in a cell-type specific manner when they are running on a treadmill (Niell and Stryker, 2010). In the primary visual cortex (V1) one can distinguish between broad-spiking, excitatory neurons and narrow-spiking, inhibitory interneurons. The authors demonstrated that broad-spiking neurons increase their response to motion stimuli while running. Narrow-spiking neurons often increase their activity in response to both self-movement and visual stimulation, but, in a subset of these neurons, the activity during visual stimulation was suppressed while running (fig. 1.12).

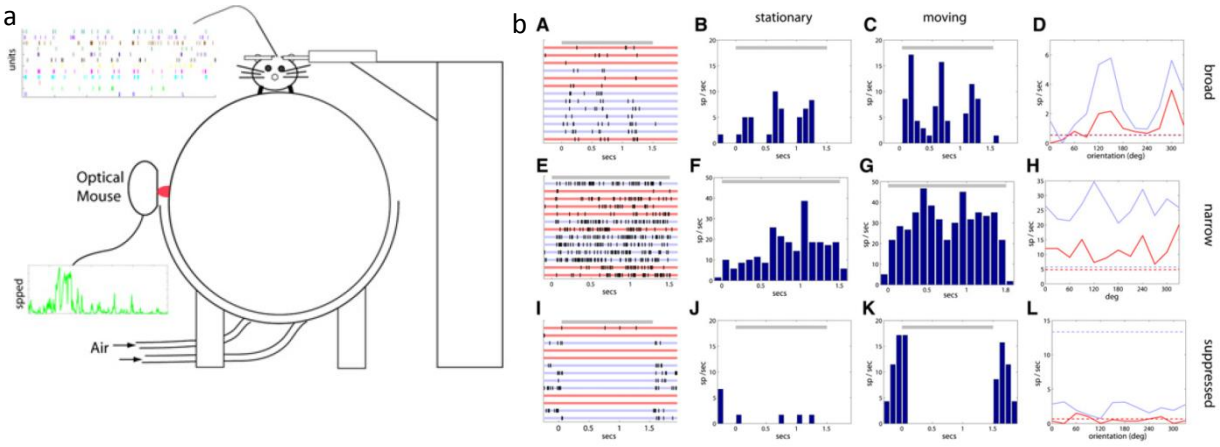

Figure 1.12 Visual Motion Processing is Modulated during Running. a) Experimental setup. A mouse is running on a ball while different visual patterns are presented. Neural activity is measured extracellularly; the running speed is measured using an optical mouse. b) Cell response to visual stimulation during different behavioral states. The gray bar indicates the onset of a visual stimulus in the preferred direction of the cell. Trials in which the mouse was running are depicted in blue, trials in which the mouse was inactive in red. left: Raster plot of the spiking activity (A,E,I). middle: PSTH for non-moving mice (B,F,J), and running mice (C,G,K). right: Visual motion tuning curves (D,H,L) (from Niell and Stryker, 2010).

1.5.2 State-Dependent Visual Processing in Insects

In insect neurobiology, the question of how behavior influences sensory processing has received more and more attention in recent years (Chiappe et al., 2010; Haag et al., 2010; Maimon et al., 2010; Rind et al., 2008; Rosner et al., 2010). Using motion-sensitive

lobula plate tangential cells (LPTCs) of blowflies, Rosner et al. (2010) investigated how information processing changes for two different states of motor activity based on haltere movements. Halteres oscillate when the animals walk or fly, and are therefore associated with locomotion (Schneider, 1953; Miller, 1977; Sandeman and Markl, 1980). Rosner et al. (2010) observed a response gain in LPTCs when the halteres oscillated. LPTCs are known to mediate the head optomotor response. Therefore, a behavioral equivalent of the response gain in the LPTCs is an enhanced head optomotor response in walking flies. However, haltere activity itself did not change the activity of LPTCs. In addition, the response gain observed in the cells was not strong enough to account for the observed gain in the optomotor response. Instead, a central signal associated with motor activity was proposed to change both the gain of the response of LPTCs as well as the gain of the head optomotor response. Regarding the role of a central input on the head optomotor response in flies, a recent study by Haag et al. (2010) came to a similar conclusion. The work focused on integration of multisensory and central inputs at the level of the ventral cervical nerve motorneuron (VCNM), which controls head movement in flies. Visual motion only leads to a subthreshold response in these cells. The combination with wind stimuli or haltere movement resulted in a modulation of the spike activity to visual motion in a directionally selective way. In a subset of flies, both the response of HS cells as well as the response of VCNM cells were measured to active haltere beating. Interestingly, based on the changes in the membrane potential as well as the time course of the responses, the results suggested that excitation spreads from the VCNM to HS cells through electrical synapses. Haltere movements resulted in only a relatively small change of the response properties of LPTCs to visual stimulation (Rosner et al., 2010). In contrary, during walking (Chiappe et al., 2010) and flying (Maimon et al., 2010) the response gain of LPTCs was greatly increased. In a recent study, calcium imaging was used to measure responses of LPTCs in walking flies (Chiappe et al., 2010). The response gain of the cells was strongly dependent on the temporal frequency with which the pattern was presented, resulting in a shift of the temporal frequency optimum. The amplified responses were also correlated with the walking speed, suggesting that all the observed changes are modulated to specific behavioral requirements. Similar to the results in LPTCs during haltere beating, the membrane potential was observed to increase slightly during flight (Maimon et al., 2010). However,

stimulus presentation in different spatial orientations revealed an increased response gain of LPTCs for null as well as for the preferred direction of the specific cell. One additional finding is especially interesting. When the fly stops flying, both the resting potential and the visual response go back to baseline. However, the time courses underlying these effects are different. Maimon et al. (2010) therefore suggested a different mechanism for the baseline shift and the response gain. The baseline shift in the membrane potential might be explained by mechanosensory afferents, whereas the increase in response gain might be a result of neuromodulator release during flight.

1.6 Octopamine and its Role in Insects

The physiological role of octopamine is restricted to invertebrates (fig. 1.13). Considering the functional similarity, the octopaminergic system of invertebrates and the noradrenergic system of vertebrates seem to be analogous. Octopamine modulates almost every physiological process in invertebrates and acts a neuromodulator, neurotransmitter and neurohormone (Farooqui, 2007; Roeder, 1999). It has been known for decades that it changes the behavioral state of an animal. The level of octopamine is increased during stress and aggression (Davenport and Evans, 1984; Stevenson et al., 2005). The effects of octopamine on the flight system of the locust has been studied in detail ranging from work on adaptation to energy demanding processes to single-cell physiology (Morris et al., 1999; Orchard and Lange, 1984; Orchard et al., 1993; Ramirez and Pearson, 1991). Also, work in *Drosophila* has indicated that octopamine plays an important role during flight (Brembs et al., 2007). Early evidence that octopamine might play a role in motion detection comes from work on the crab. The experiments showed an enhancement of the optokinetic responses after application of octopamine (Erber and Sandeman, 1989). Behavioral studies on the antennal reflex and electrophysiological studies on motion-sensitive neurons in the lobula have shown that the visual system of the honey bee is modulated by octopamine (Erber and Kloppenburg, 1995; Kloppenburg and Erber, 1995). In addition, anatomical studies in flies have shown that the visual system is highly innervated by octopaminergic neurons originating in the central brain (Sinakevitch and Strausfeld, 2006, Busch et al., 2009). Altogether, these results give a strong hint that octopamine modulates the visual system involved in motion detection in

flies. A recent paper has confirmed that octopamine modulates the cell response of lobula plate tangential cells. After the application of chlordimeform (CDM), an octopamine agonist, the response to visual stimuli is greatly enhanced (Longden and Krapp, 2009). In addition, later work showed that octopamine also modulates temporal frequency tuning (Longden and Krapp, 2010). The strong similarities between the results of the behavioral state studies mentioned in the previous section and the results from the work on octopamine clearly indicates that neuromodulation plays a critical role in state-dependent changes of visual processing.

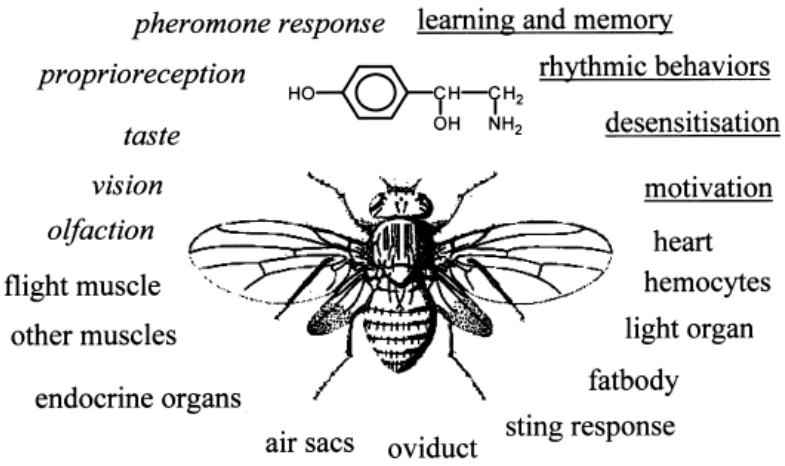

Figure 1.13: Effects of Octopamine on Different Tissues of Invertebrates. Octopamine is a multipotent substance in invertebrates. It modulates numerous peripheral tissues as well as sense organs. Also, central systems (underlined) are modulated by octopamine (from Roeder, 1999).

1.7 Goals and Project Outline

The dynamic range of visual input in flies changes dramatically from the values at rest, through walking, to flying. How does the visual system adapt to these changes? Only very few studies have addressed the question of how behavior changes the response of lobula plate tangential cells. I investigated how the response properties of lobula plate tangential cells are modulated during flight.

To study how H1 changes its response characteristics during flight is especially interesting, since H1 is one of the most studied cells in insect physiology (Brenner et al., 2000; Haag and Borst, 1997; Maddess and Laughlin, 1985; vanSteveninck et al., 1997). I

investigated how the response properties of the lobula plate tangential cell H1 changes during flight using extracellular recording. Therefore, I had to adapt the preparation commonly used for recording H1 in blowflies to allow for tethered flying of the animal without restricting the wing beat amplitude and for simultaneous recording of H1 without destruction of the lobula plate due to brain movements.

During flight the fly has to deal with much faster image speeds compared to non-moving conditions. In addition, it has to compensate fast for involuntary movements, such as those induced by wind. Therefore, I investigated whether LPTCs show a difference in their response properties as a result of the behavioral state of the fly. First, I measured the spontaneous activity and the directional tuning range of the cells. The latter might increase during flight as an adaptation to a broader velocity range. There exists a mismatch between the behavioral measured optomotor response and the temporal frequency tuning curve obtained from electrophysiological recordings of LPTCs (Borst and Bahde, 1987; Haag et al., 2004; Hausen and Wehrhahn, 1989). Therefore, I analyzed the temporal frequency tuning of H1 during non-flight and during flight in detail.

In further experiments, I investigated whether octopamine is involved in changing the response properties of H1 to visual stimuli. This hypothesis was tested because, as described in the previous section, octopamine is thought to be a major player in regulating the behavioral state of insects. In addition, it is known to be involved in visual motion processing in blowflies (Longden and Krapp, 2009). I compared the response of flying flies with fixed flies before and after CDM application using the same stimulation protocol as for the flight experiments to figure out whether CDM can mimic some of the effects attributed to the flight condition.

Finally, I addressed the question of which parameters of the Reichardt detector model have to be changed to explain the behavioral state dependent differences in the visual response (Hassenstein and Reichardt, 1956a; Hassenstein and Reichardt, 1956b; Reichardt and Varjú, 1959).

2. Materials & Methods

Three different preparations were used to perform the experiments presented in the next chapter. Originally, the work was based on previous observation that lobula plate tangential cells lose their responsiveness to visual motion stimuli when the connective is cut. To test whether this holds also true for H1, the experiments were repeated in a slightly different manner and the response of the cells to visual stimulation before and after cutting of the connective was compared. The main focus of the work, however, is on the question of how the neuronal response of H1 changes with the behavioral state of the fly. To address this question, in the second set of experiments I recorded extracellularly from tethered flying flies and compared the cell response with non-flying flies. Since the standard preparation has been modified for tethered flying flies during the thesis, I will use the last section of this chapter to describe it in further detail. The third set of experiments was conducted in fixed flies. Here, the cell response was compared before and after the application of the octopamine agonist CDM.

2.1 Experimental Animals

Blow flies (Lucilia spp.) were purchased weekly from a local pet shop and subsequently maintained in the departmental stock. The animals were delivered at a larval stage and started to pupate within the next 2-3 days. During that time, the larvae were not fed. Once the flies were hatched they received water and sugar ad libitum.

Flies were kept in a plastic container of size 25cm x 25cm. The room temperature was kept around 20°C and the relative humidity between 50% and 60%. The animals were kept under a 12h-12h light-dark cycle. Only female blowflies were used for experiments. The age varied between 3-10 days after eclosion.

2.2 Preparation

2.2.1 Preparation for Cutting Experiments

The aim of this experiment was to cut the connective of the fly while recording extracellularly from H1. The animals were briefly anesthetized with CO_2. Then, their dorsal part of the thorax was attached to a small glass platform with wax. After the legs were removed with scissors, the body was covered with wax to reduce strong movements. The halteres, stigmen and proboscis were left open. Next, the head was waxed onto the ventral thorax at an angle of approximately 90°, so that the neck of the fly was slightly stretched but no strong forces were created. An injection needle was used to open the head capsule on both sides. In contrast to the following experiments, no care was taken on the size of the holes. After that, the needle was used to open the skin of the neck from behind. In order to obtain access to the cervical connective, the oesophagus had to be removed. Therefore, it was cut with a scissor as close to the head as possible. The part of the oesophagus ending in the stomach was pulled out and waxed to the thorax. Now, the connective was visible and a hair was pushed gently under the connective using forceps. After that, both ends of the hair were waxed together to form a ring. Throughout the whole procedure, care was taken that the air sacs and other important supply circuits were as little harmed as possible; however, the air sacs were usually damaged slightly. It was also of critical importance that no further forces were put onto the hair in order to ensure that the connective was not damaged before the actual recording. Ringer's solution was added to keep the brain as well as the connective moist, to keep both in an isotonic solution and to ensure sufficient contact with the reference electrode.

2.2.2 Preparation for Experiments on CDM Application

Regarding anesthetizing and fixation, the preparation was done in a similar way as described in the cutting experiment. However, the head was waxed onto the ventral thorax at an angle of about 20°-30°. This angle was shallower compared to standard conditions to allow the use of the same experimental set-up as in the tethered flight experiments. In addition, the ocelli were covered with wax. Finally, an injection needle was used to open the head capsule on both sides. The right side of the head (viewing the fly's head from the back) was opened from the most lateral limit to the midline. The vertical length of the opening extended from the upper part of the head to approximately the middle. Extending the opening further in the dorsal direction often resulted in a loss of Ringer's solution or hemolymphe. The left side of the head was opened in a similar way; however, the exact size of the opening did not seem to play a critical role. The openings left sufficient space for the recording as well as the reference electrode. Ringer's solution was added to keep the brain moist, to keep it in an isotonic solution and to ensure contact with the reference electrode.

2.2.3 Preparation for Experiments on Tethered Flying Flies

The preparation consisted of two steps. The first part of the preparation was conducted at least 12 hours before the actual experiments. The animals were briefly anesthetized with CO_2. A small piece of cardboard was waxed perpendicularly onto the dorsal thorax of the fly, keeping the wings free to move. The ocelli were covered with wax. The head fixation was the most critical part which had to be changed from the commonly conducted preparation procedure (described above). The head was fixed to the thorax with a very shallow angle of approximately 20°-30° and was fixed to the dorsal part of the thorax instead of to the ventral part. During this procedure, the ocelli were covered with wax (fig. 2.1). After the pre-preparation, the flies were put back into the holding tank to recover for at least 12 hours. The actual recordings were performed within the next two days. At that time, the head capsule was opened as described above and Ringer's solution was added.

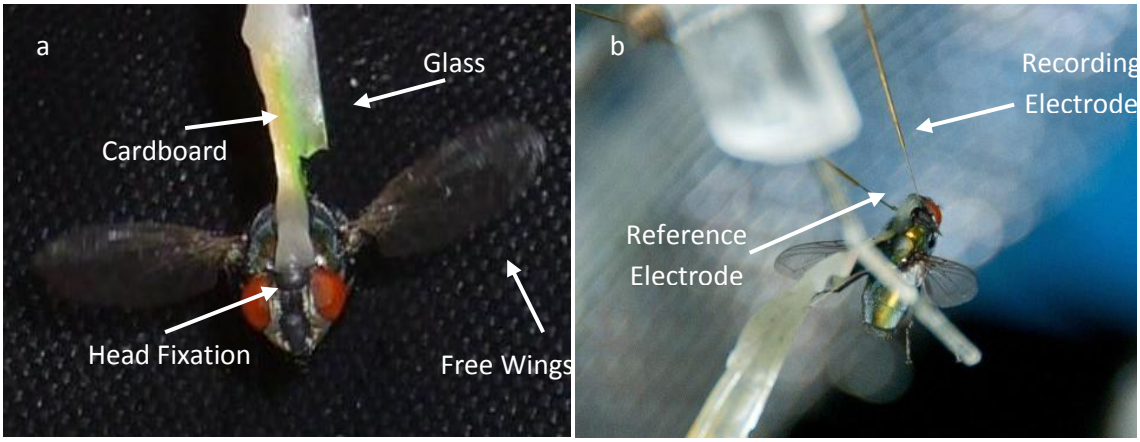

Figure 2.1: Preparation for Tethered Flying Flies. a) View onto the front of the fly. To get a strong enough connection between the head of the fly and the back of the thorax the ocelli were covered with wax. A piece of cardboard was mounted perpendicularly onto the thorax. The wings were free to move. b) View onto the back of the fly while it was in the setup (picture taken by R. Schorner).

2.2.4 Preparation for Control Experiments on the Influence of Wind

For the control experiments on the influence of wind on the neuronal response the same preparation was made as for the CDM application, except that the legs were free to move and the body was not covered with wax. This kept other wind-sensitive body parts such as hairs free for sensation, in addition to the antenna.

2.3 Experimental Set-up and Positioning of the Fly

The fly was mounted on a heavy recording table with the stimulus monitor in front of it. The fly was fixed in a slightly forward bend position to mimic the angle of flight a fly would have under free flight conditions (fig. 2.1 b). The LED-Arena used for stimulation (described below) was tilted forward until the fly faced the visual stimulation frontally (fig. 2.2). For the experiments on flying flies, a constant air flow had to be delivered to the fly through a plastic tube in order to keep the fly flying. The opening was approximately 4 cm away from the fly and pointed towards its head. At the head of the fly, the air velocity was approximately 2.5 m/s. Under these conditions, flies flew steadily for about 20 min. Flight was stopped by giving the flies a piece of paper to the legs and

stopping the air flow. The reference electrode was always inserted into the left side of the head capsule; the recording electrode was inserted into the right side. The fly brain was viewed from behind through a Zeiss dissection scope.

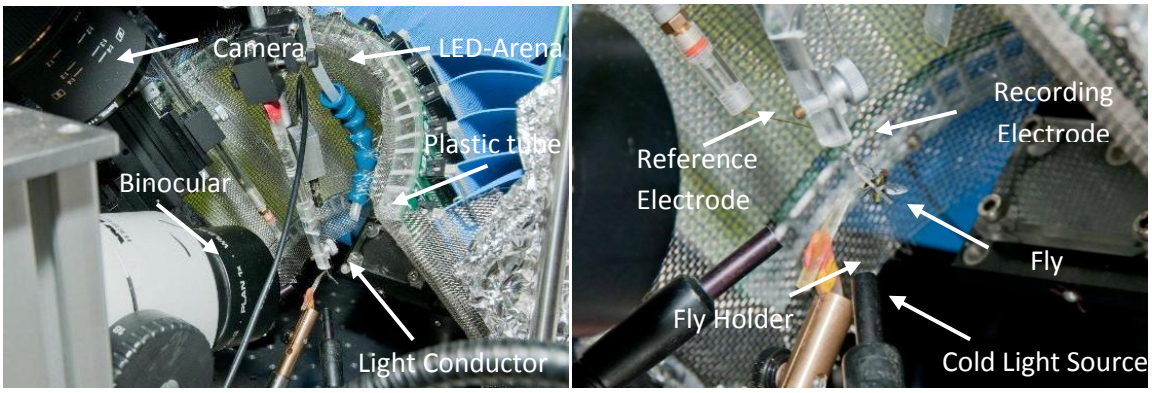

Figure 2.2: Positioning of the Fly in the Experimental Set-up. Stimulus arena and fly were tilted towards each other so that the fly was flying in an angle comparable to free flight conditions. The reference electrode and the recording electrode were placed on the left and right side of the fly, respectively. Air was delivered through a plastic tube. The fly brain was viewed from behind through a Zeiss dissection scope (picture taken by R. Schorner).

2.4 Stimulation

The stimuli were presented using a cylinder-shaped LED-Arena that was custom built based on the open-source information of the Dickinson Laboratory (Reiser and Dickinson, 2008). The arena consists of 15x 8 TA08-81GWA dot matrix displays (Kingbright, CA, USA), each harboring 8 x 8 individual green (568 nm) LEDs. The arena covered 170° and 60° of the horizontal and vertical visual field, respectively. The angle between adjacent LEDs was 1.7°. It was possible with the arena to show patterns with a refresh rate of 600 Hz and 16 intensity values. Each dot matrix display was controlled by an ATmega644 microcontroller (Atmel) that obtains pattern information from one central ATmega128-based main controller board. The main controller reads in pattern information from a compact flash memory card. For achieving high frame rates, each panel controller was equipped with an external AT45DB041B flash memory chip for local pattern buffering. Matlab was used for programming and generation of the patterns as well as for sending the serial command sequences via RS-232 to the main controller board.

The stimulus pattern consisted of a vertical two-dimensional sine wave grating of either 20° or 40° spatial wavelength. The mean luminosity of the screen was 5.3 cd/m². The stimuli had either a low (17.4%) or a high (approximately 90%) contrast. For low contrast stimuli, patterns were generated by two consecutive frames. This resulted in 32 equidistant intensity levels available per image; however, only 8 intensity levels were used. Since two frames were used to create one picture, the actual picture rate was half the frame rate. Given a frame rate of 400 Hz, this resulted in a picture rate of 200 Hz. For high contrast stimulus the frame rate and picture rate were identically 400 Hz. The number of intensity levels used was 16.

The spontaneous firing of H1 was measured after the fly was adapted to light for at least 5 min. The response of H1 to stimuli moving in preferred and null directions was measured using all four possible combinations of contrast and wavelength (high contrast: 20° & 40° wavelength; low contrast: 20° & 40° wavelength; fig. 2.3 b). The pattern was presented with a temporal frequency of 5 Hz for 3 s in either the preferred or the null direction in an alternating fashion. The inter-stimulus time interval was 3 s. The temporal frequency tuning was measured in a different set of flies. To measure the temporal frequency tuning, a pattern of a spatial wavelength of 40° and low contrast was used. The pattern moved at temporal frequencies ranging from 0.3 Hz to 20 Hz in the preferred direction of H1 (fig. 2.3 a). For each stimulus trial 10 different temporal frequencies were presented in a pseudo-random fashion. Each temporal frequency was presented for 3 s; the interval between each stimulus presentation consisted of a stationary pattern presented for 3 s. This stimulus protocol was repeated 10 times, so that for each frequency 10 measurements were performed.

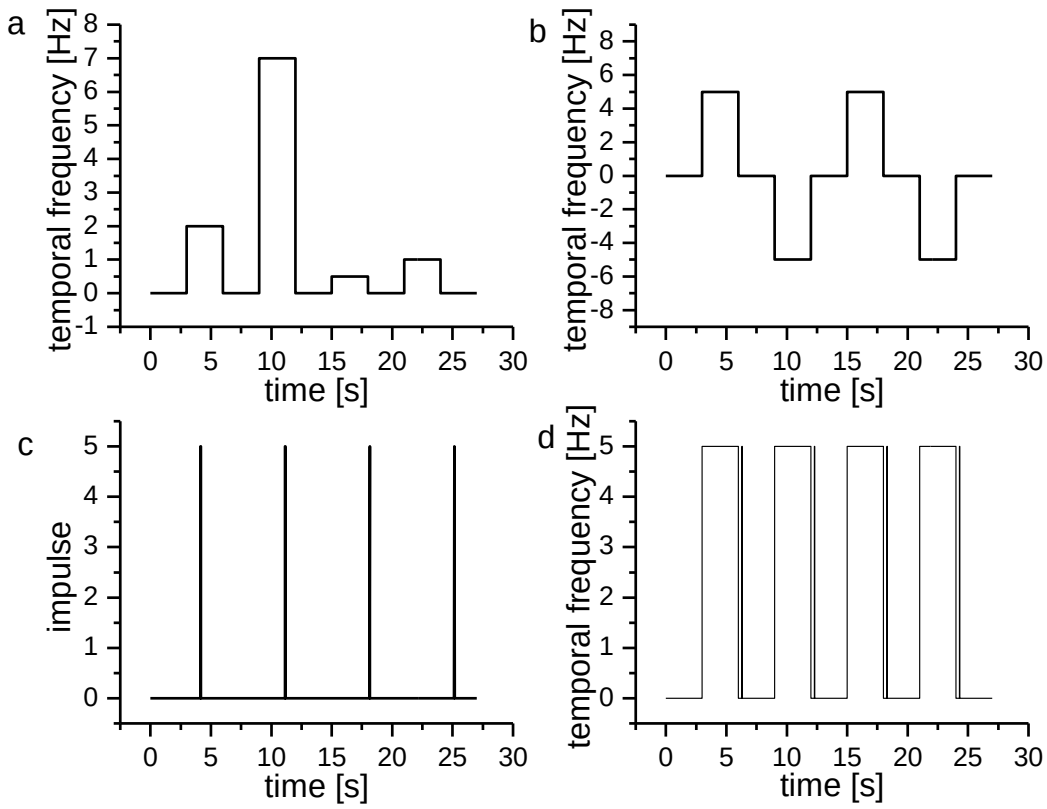

Figure 2.3 Stimulus Protocols used for Different Experiments. a: Stimulus protocol to measure the temporal frequency tuning curve for the preferred direction of H1. b: Stimulus protocol to measure the response to the preferred and null direction of H1. c: Stimulus protocol to measure the isolated impulse response. d: Stimulus protocol to measure the impulse response after the presentation of an adaptation stimulus.

In order to measure the impulse response of H1, a brief motion stimulus was delivered. The impulse response of H1 was analyzed before and after the presentation of constant motion stimuli ('adaptation stimulus'). Apparent motion was used as a test stimulus. Both the adaptation and the test stimulus were delivered at low contrast. The displacement of the pattern was 180°. For each fly, the test stimulus was repeated 100 times with an inter-stimulus interval of 7 s to evaluate the response of H1 to an isolated impulse (fig. 2.3 c). As for the velocity tuning measurement, the inter-stimulus time interval between each presentation of the adaptation stimulus was 3 s. The adaptation stimuli lasted 3 s and had a temporal frequency of 5 Hz; a test stimulus was presented 200 ms after the adaptation stimulus (fig. 2.3 d).

2.5 Cell Identification and Recording

H1 is one of a few spiking interneurons in the fly's lobula plate which crosses the midline (fig. 2.4 a). This property, in addition to the specific directional motion sensitivity, makes it possible to identify the cell (Eckert, 1980). I always recorded extracellularly from the axonal arborizations in the right brain hemisphere and measured the firing rate in response to visual stimuli on the contralateral side. The reference electrode was inserted into the left head capsule. H1 was identified during the non-flight or before-CDM condition. In order to identify the cell, a different sine-wave grating was shown than for the actual experiments. The spatial wavelength of the pattern was 20°; the contrast was above 90% and the stimulus velocity was 5 Hz. The direction of movement alternated between preferred direction (PD) and null direction (ND). Movement in PD led to a strong increase in firing frequency, whereas movement in ND led to a strong reduction of H1 activity (fig. 2.4 b). Since the stimulus arena covered most of the receptive field of both eyes, it was ensured by waving a hand in front of the eye that the receptive field of the cell was always contralateral to the recording site.

For electrical recording, tungsten electrodes were used with a resistance of 0.5-1 MOhm. Spikes were transferred at 30 kHz temporal resolution to a computer to allow offline spike extraction. Spike extraction was performed via threshold detection based on the digital band-pass filtered recording and its first derivative.

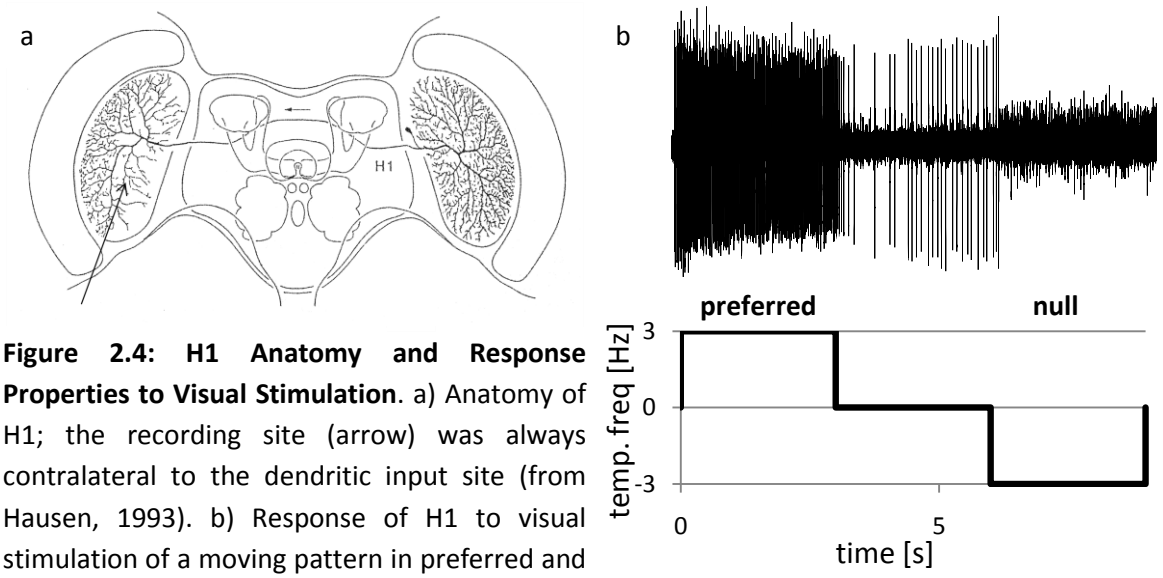

Figure 2.4: H1 Anatomy and Response Properties to Visual Stimulation. a) Anatomy of H1; the recording site (arrow) was always contralateral to the dendritic input site (from Hausen, 1993). b) Response of H1 to visual stimulation of a moving pattern in preferred and null direction.

To enable recordings in tethered flying flies, the recording procedure had to be adjusted slightly compared to previous work done in immobilized flies. Since the small angle between head and thorax blocked access to the lobula plate with straight electrodes, the tip of the tungsten electrodes was bent beforehand using forceps. The same kind of electrodes were used as a reference because they turned out to be relatively thin but stable compared to the normal silver wires used for H1 recordings. To get a low resistance, the tip of the electrode was cut and the tip of the electrode was polished.

2.6 Chlordimeform

Chlordimeform-HCl (CDM; Sigma–Aldrich) is a tissue-permeable octopamine agonist (Hiripi et al., 1999). It has been used already in many insect preparations to test, for example, the functional role of octopamine in locomotion (Rosenberg et al., 2007; Vierk et al., 2009). CDM was dissolved in water and stored as a 1 M stock solution at 4° C. Before each experiment the CDM solution was diluted in Ringer's solution to give a final concentration of 20 µM. 2 µl of the CDM solution was applied to the lobula plate contralateral to the recording site. Before application of CDM, the reference electrode had to be removed from the head capsule of the fly. For the delivery of CDM, a micropipette was used. After that, the reference electrode was put back into place. It

was taken care that during this procedure the fly was neither touched by the reference electrode nor by the micropipette. The recording electrode was not moved at all, so that H1 could be recorded after the application of CDM without reorientation of the recording electrode.

The amount of CDM used in each experiment was about 1.5x higher than that used in previous studies on arousal in flies (Longden and Krapp, 2009). Given the different size of *Calliphora* and *Lucilia* the difference in total concentration per brain volume is assumed to be even higher and was approximated at 7.2×10^{-10} mol/g. However, considering the broad range of concentrations in bath solutions used in other insects studies I consider the concentration well within the range of physiologically relevant concentrations for CDM (Duch and Pfluger, 1999; Kinnamon et al., 1984; Stevenson et al., 2005; Vierk et al., 2009). The spontaneous spike rate of H1 was reliable increased within 5 min after application and remained so throughout the duration of the stimulus presentation (20 min).

2.7 Data Analysis

To calculate the spontaneous activity, the firing rate was recorded for 1 min while presenting the stationary visual pattern described above. In the experiments in which the effect of CDM was studied I measured the spontaneous firing rate before and after recording the velocity tuning and averaged the results.

In response to the onset of a constant velocity stimulus, H1 exhibits transient oscillations before settling to a steady-state value. The response transients are characterized by oscillations that have the same frequency as the temporal frequency of the periodic pattern and are only observed when the visual pattern has been shown before stimulus onset (Egelhaaf and Borst, 1989; Maddess, 1986). The steady-state response is, in contrast, independent of the presence or absence of a visual pattern before stimulus presentation (Maddess, 1986; Reisenman et al., 2003). The data under different stimulus conditions were analyzed by plotting either the *firing rate* or the *response* defined as the firing rate minus the average firing rate during the last second before stimulus

presentation. The instantaneous firing rate was always calculated using a bin width of 10 ms.

To describe the temporal frequency tuning curves, two different parameters were calculated. The *steady-state firing rate* was defined as the average firing rate during the last second of stimulus movement; the *steady-state response* was defined as the difference between the steady-state firing rate and the average firing rate during the last second before stimulus onset.

Before the Reichardt detector model could be used for fitting the experimental results, the data had to be normalized. For the data set on flying flies normalization was performed within each single fly. The temporal frequency-tuning curve of the steady-state response of H1 was calculated for the non-flight as well as for the flight condition. The maximum value of the steady-state response curve of the non-flight condition was then used to normalize the data set. After normalization, all curves were averaged across flies. The same procedure was repeated for the CDM experiments. Here, the condition 'before-CDM application' was used as reference.

2.8 Modeling

The Reichardt detector – a correlation based motion detector model, described above – can account for many properties observed in fly motion vision (Hassenstein and Reichardt, 1951, Reichardt, 1969; Borst, 2007). In particular, the bell-shaped steady-state velocity dependence is faithfully described with this model. However, adaptive properties – such as the shortening of the impulse response after the presentation of a motion stimulus – are not captured with the original model (Borst and Bahde, 1986; Goetz, 1972). For my simulations, I used an extended version of the Reichardt detector model. In agreement with the original model, the signal coming from the retina was low-pass filtered in one cross-arm of the detector; in the other cross-arm, however, an additional high-pass filter was added (fig. 2.5). Following the original publication, the model will be referred to as the 'High-pass' model (Reisenman et al., 2003). According to the High-pass model the time constant of the impulse response is identical with the

high-pass time constant of the model. It has been observed that visual motion leads to an adaptation and hence shortening of the time constant (Borst et al., 2003; Reisenman et al., 2003). Therefore, I used the adapted high-pass time constant for all experimental conditions (non-flight, flight, before-CDM, CDM) as a parameter for the model. The steady-state response of the High-pass model was calculated by Borst et al. (2003):

$$\langle R \rangle_{\varphi} = \Delta I^2 \cdot \sin(2\pi\Delta\varphi/\lambda) \cdot \frac{\tau_h \omega \cdot (1 + \tau_l \tau_h \omega^2)}{(1 + \tau_l^2 \omega^2) \cdot (1 + \tau_h^2 \omega^2)} \quad (1)$$

where λ represents the wavelength of the pattern [°], Δφ the sampling base [°], ΔI the pattern contrast, τ_h the high-pass and τ_l the low-pass time constant [s], the angular frequency of the pattern [Hz] and v the stimulus velocity. As can be seen from the above equation, the steady-state velocity tuning of this detector depends only on the time constants of the internal filters, since the first two terms are independent of stimulus velocity, affecting the overall amplitude of the response only.

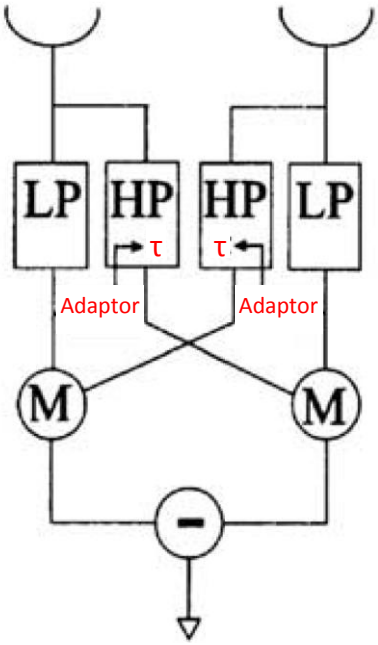

Figure 2.5: High-Pass Model. The High-pass model was based on the original Reichardt detector model with an additional HP filter in the input line. To fit the temporal frequency tuning curves, the measured adapted high-pass constant (red) was set as a fixed value, whereas the low-pass time constant was fitted. To calculate the transient response, the High-pass model was used. The adapted high-pass time constant and the fitted low-pass time constant were used as input parameters (adapted from Borst at al. (2003).

I investigated to what extent which filter time constants had to be adjusted in order to explain the differences observed in the response to visual stimulation under various conditions (e.g., when the flies are at rest or during tethered flight, and before or after CDM application). Since for both types of experiments the same fitting procedure was performed, it will be explained only once for the experiments on flying flies. I used the adapted high-pass time-constant during non-flight and during flight as one parameter of

the model. To estimate the other parameter, i.e., the time constant of the low-pass filter, I fit the tuning curve of the model to the tuning curve of the fly obtained under both conditions by minimizing the mean square error between the model response and the experimental data. Values of the low-pass time constant were tested ranging from 0.005 to 0.25 s at a resolution of 0.001 s. The model values and the experimental data do differ by a constant. In this work the results are presented in which this constant could be different for the non-flight and flight condition (or before-CDM vs. CDM condition). However, the fits only change slightly, when for both conditions the same multiplication factor is used to map the model data onto the experimental data.

To verify whether the High-pass model can also reproduce the transient response characteristics of H1 to different temporal frequencies, the measured and fitted parameters were used to calculate the transient response. The step response to a grating moving with constant velocity is given by Borst et al. (2003):

$$\begin{aligned}\langle R(t)\rangle_{\varphi} = {} & \Delta I^2 \cdot \sin(2\pi\Delta\varphi/\lambda) \\ & \cdot \frac{\tau_h \omega}{(1+(\tau_l\omega)^2)\cdot(1+(\tau_h\omega)^2)} \\ & \cdot [K + F_1 \cdot \exp(-t/\tau_l) \ * \ \exp(-t/\tau_h) \\ & \quad + F_2 \cdot \sin(\omega t) - F_3 \cos(\omega t)]\end{aligned} \tag{2}$$

with

$$K = 1 + \omega^2 \cdot \tau_h \cdot \tau_l,$$

$$F_1 = \tau_l \omega^2 \cdot (\tau_h - \tau_l),$$

$$\begin{aligned}F_2 = {} & \omega \cdot \lfloor (\tau_h \tau_l \omega^2 + 1)\tau_l \exp(-t/\tau_l) \\ & + (\tau_h - \tau_l)\exp(-t/\tau_h)\rfloor,\end{aligned}$$

$$\begin{aligned}F_3 = {} & \tau_l \omega^2 (\tau_h - \tau_l)\exp(-t/\tau_l) \\ & + (\tau_h \tau_l \omega^2 + 1)\cdot \exp(-t/\tau_h).\end{aligned}$$

2.9 Setting up Extracellular Recordings in Tethered Flying Flies

2.9.1 Behavioral Pre-Preparations

To record from flying flies, the standard preparation for H1 recordings had to be adapted (Eckert, 1980; Reisenman et al., 2003; Weber et al., 2010). To enable the wings of the flies to move freely a piece of paper was waxed perpendicular to the thorax (figure 2.1). Instead of fixing the head to the front of the thorax a wax bridge was built from the head to the back of the thorax. The latter step had two advantages: first, the back of the thorax is more rigid during flight, which reduced vibration of the head, and, second, the front legs were free to move. Nevertheless, it turned out that under these conditions the flies did not fly when recording extracellularly from H1. To entangle whether this was due to the fact that flies do not like electrodes in their head or because particular aspects of the preparation reduced their willingness to fly, initial behavioral experiments were performed. The first parameter tested was the angle between thorax and head. In former behavioral studies on the response of flies to visual stimulation, the head of the fly was directly fixed to the thorax (Geiger, 1974; Mayer et al., 1988; Wehrhahn and Hausen, 1980)**.** The flight duration of 13 flies of the species *Calliphora vicina* was measured with an angle between thorax and head of either <30 or 45 degrees. It turned out that a smaller angle between head and thorax was favorable for longer flight periods (fig. 2.6 a). However, long flight periods were rarely observed in *Calliphora vicina* (fig. 2.6 c). Therefore, another species, *Lucilia*, was tested (n=16). Assuming that also in this species a small angle between thorax and head is favourable for flight willingness; the next parameter tested was the age of the fly at the day of preparation (fig. 2.6 b). If the flies were too young at the time of the preparation – most likely because the cuticula was not yet hardened and in general the flies were more fragile – flies did not fly very well. A comparison between *Calliphora vicina* and *Lucilia* showed that the duration of flight was longer when *Lucilia* were used for experiment instead of *Calliphora vicina* (fig. 2.6 c). It has to be noted, however, that within these two groups, beside species type, other parameters were also different such as the average age during testing. Nevertheless, further experience confirmed that *Lucilia* fly better in this experimental setting than *Calliphora vicina*.

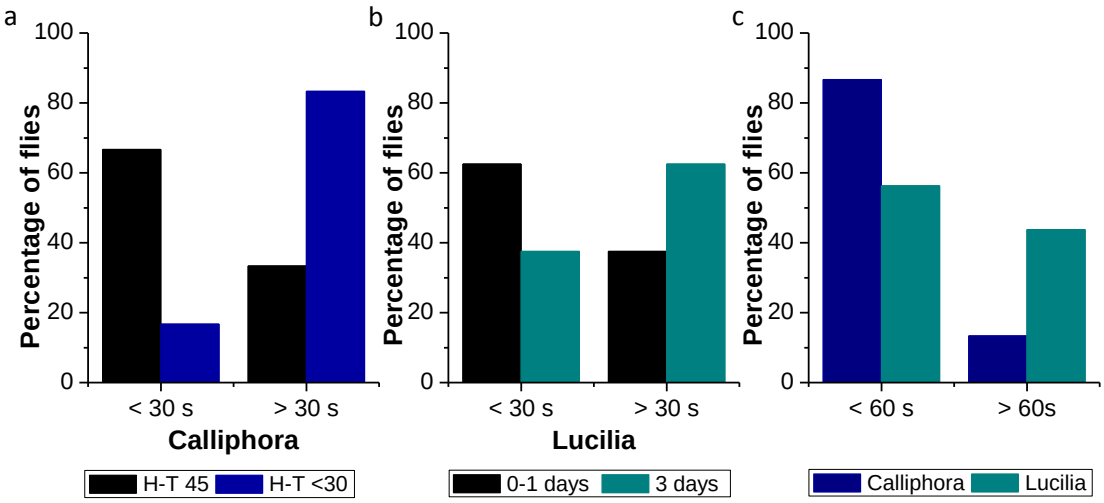

Figure 2.6: Behavioral Test to Increase Willingness of Flies to Fly. a) Originally, *Calliphora* were use for flight experiments. Here, preliminary results showed that a small angle between head and thorax was favorable for getting the flies to fly. b) The dependence of flight duration on age of the fly (*Lucilia*) at the day of preparation is shown. c) A general comparison between the duration of flight in *Calliphora* and *Lucilia* is shown. Long periods of flight are rarely seen in *Calliphora*. Note however, parameters other than the species were changed as well.

2.9.2 Spike Extraction

To extract action potentials from extracellular recordings with a high reliability, the signal to noise ratio is of critical importance. In the experiments on tethered flying flies the signal strength might decrease during flight, whereas the noise level might increase during flight. First of all, the brain could move during recording because of the forces created by flight. It turned out that a reduction in spike amplitude was rarely observed during flight. Most likely, strong brain movements decreased the willingness to fly when an electrode was inserted into the brain. Therefore, no recordings could be performed in these flies anyway. However, an increased noise level caused further experimental difficulties. One critical aspect was that vibrations due to wing/body movements could be captured by both the reference as well as the recording electrodes as an increase in noise level with wing beat frequency. Hence, even small vibrations within the Ringer's solution on top of the brain should be avoided. Another aspect which had to be taken into account was that not only might H1 change its pattern of activity during flight, but

other cells in the lobula plate might as well. As an ‘online criterion’ for single cell recording a strong stimulus pattern (the same as used for cell identification) was presented in the preferred as well as in the null direction. If the spiking activity was completely suppressed in the null direction a single cell recording was very likely. As an off-line criterion, after spike extraction the interspike interval (ISI) was checked for consistency with the refractory period of a cell.

In the following, the spike separation process is outlined using one example data set. This particular data set was chosen because it consisted of a long stretch of recording of the spontaneous activity in which non-flight, flight and non-flight conditions were alternated. For each condition before, during and after flight a 60 s long recording trace was evaluated. First, the recording trace was digitally band-pass filtered between 200 Hz and 4800 Hz. The high-pass threshold was set to remove some of the motion artifacts (e.g., movements of the legs); the low-pass threshold was set to smooth the recording. After that, the derivative of the signal was taken. The recording was then binned into segments of 0.001 s. For each segment the maximum of the filter signal and the maximum of the first derivative are plotted against each other in a scatter plot (fig. 2.7). Based on the scatter plot, thresholds were chosen to separate spikes from noise. In order to be counted as a spike, a data point had to lie above both criteria. The histograms of the signal and derivative height are also shown, in order to give a more qualitative overview. For example, even though the spike separation for the flight condition does not appear well-resolved on the scatter plot, the histograms show clear and distinct peaks for spikes and noise. The ISI in the last column of the figure indicates a good spike separation since, for all conditions, no spikes are detected within the refractory period of the cell.

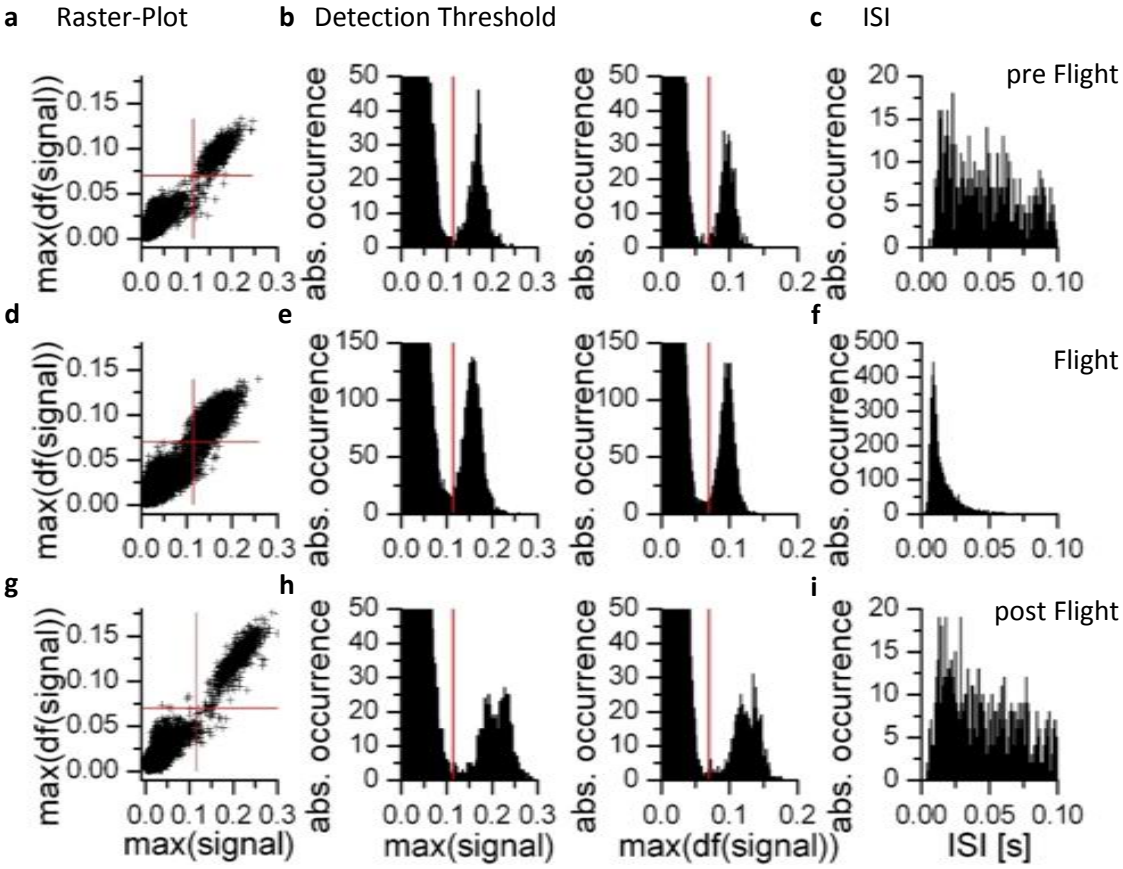

Figure 2.7: Spike Extraction Protocol. Spike were extracted from 60 s long recording stretches obtained during before (a-c), during (d-f), and post (g-i) flight condition. a,d,g) scatter plot of the maximum and the maximum of the derivative of the recording trace based on 0.001 s long time bins. b,e,h) the same data are presented as in the first column, but plotted as histograms. c,f,i) ISI histograms based on the extracted spikes. Note that the criterion of a refractory period is fulfilled.

A two-second long recording stretch for each condition is shown in figure 2.8. Note that during flight the noise level seems to rise slightly. However, it is difficult to tell whether this is only due to an increase of activity within the lobula plate or whether the noise is caused by slight vibrations of the brain. The waveform of the extracted spike was the same for each condition.

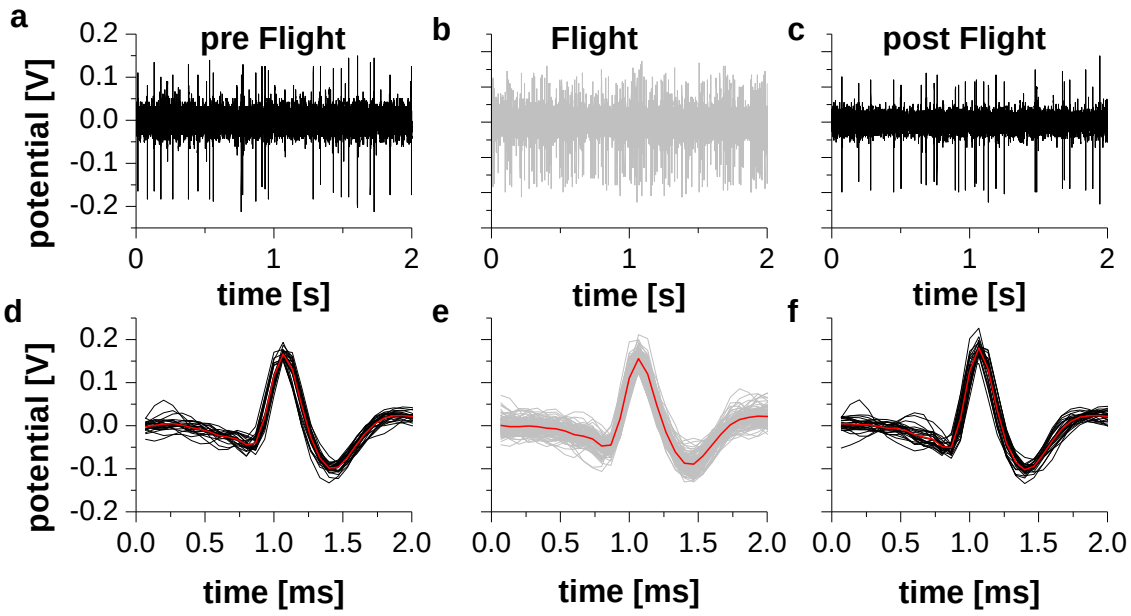

Figure 2.8: Spontaneous Activity Recorded before, during, and post Flight, together with the Waveforms of the Extracted Spikes. a-c) 2 s long segments of spontaneous activity pre (a), during (b) and post flight (c). d-f) the corresponding waveform from the spikes shown in a-c. Note that the waveform does not change throughout the recording.

2.9.3 Control for a Functional Optomotor Response

To assure that the flies were still behaving normally, the wingbeat frequency and the optomotor response were measured. In order to do this, the flies were filmed with a high-speed camera (MotionPro Y3, Redlake) with a macro objective (Sigma, 105mm F2,8 EX DG). To measure the wingbeat frequency, a frame rate of 1000 Hz was used. In order to test whether the fly shows a normal optomotor response during flight, the fly was filmed at a frame rate of 90 Hz while a visual motion stimulus was displayed. To elicit the optomotor response a high pattern contrast was used. After one second exposure to a stationary pattern, a moving pattern (temporal frequency 2 Hz) was displayed which changed direction every 5 seconds. The acquired movies were tracked manually (ImageJ, Manual Tracking plug-in). From the acquired movies, the wingbeat frequency and wingbeat amplitude of the left and right wing were determined.

3. Results

The main focus of my dissertation is the investigation of how lobula plate tangential cells change their response properties with the behavioral state of the animal. To address this question I used three different experimental approaches.

The first set of experiments regard the clarification of previous observations in which the response properties of lobula plate tangential cells where tested after cutting the connective. Previous results indicated that lobula plate tangential cells lose their responsiveness to visual stimuli when the main connective is cut. This indicates a feedback mechanism from the motor system to the optic neuropil. However, the results obtained by cutting the connective while recording extracellularly from H1 revealed that the response properties of the cell to visual motion stimuli did not alter dramatically.

In the next set of experiments I investigated how H1 changes its response to visual stimuli while the fly was flying compared to the non-flight condition. I demonstrated that H1 increases its firing rate dramatically when the flies started to fly, and maintained an elevated firing rate throughout the duration of flight. Next, I demonstrated that the directional tuning range is increased during flight. However, this effect depended on different parameters such as pattern wavelength and contrast. Furthermore, I found that the temporal frequency tuning of the steady-state response of the cell is broadened towards higher frequencies. This effect was due to a reduced adaptation to higher stimulus velocities when fast patterns were presented.

The last sets of experiments were performed to investigate functional mechanisms involved in the changes of the response properties of H1. The current literature suggests that octopamine is a promising candidate for being involved in inducing behavioral state-dependent changes in the response properties of lobula plate tangential cells. By applying the octopamine agonist Chlordimeform-HCl (CDM; Sigma–Aldrich) the effects induced by flight could be mimicked to some extent; the baseline firing rate increased and the temporal frequency tuning curve was shifted to higher frequencies.

Octopaminergic projections can be found in the lobula plate as well as in the medulla. Therefore, the question remains whether the observed effects are a result of changes in the properties of H1 itself of whether the presynaptic circuitry is altered. Using the Reichardt detector as a model, the conclusion could be drawn that the most likely scenario is that the broadening of the tuning curve results from changes in the presynaptic circuitry of H1. The changes in the tuning curve could be fit by decreasing the low-pass time constant of the model.

3.1 Cutting of the Connective

Previous experiments have suggested that lobula plate tangential cells lose their ability to respond to visual motion after the connective between the central brain and the thoracic ganglia is cut (Haag, unpubished). This suggests a strong interaction between the motor system and the optic neuropil. The experiments were conducted on cells belonging to the horizontal system and vertical system in flies (HS and VS) which respond to motion stimuli with a graded change in their potential. Working on spiking cells allowed repeating the previous experiments with the additional possibility of recording while the connective was cut. The cutting was performed by pulling on a hair which had been previously attached to the connective. Most of the time the cell was lost after cutting the connective and often it could not be found again. In most of these cases, the lobula plate appeared to be relatively silent: no other spiking cells were located after the initial spiking cell was lost. This is in agreement with the previous results; however, after some practice it was possible to identify H1 after cutting the connective, though the recording quality was often not good enough for spike

extraction. In a few cases, however, the recording quality was good and spike extraction could be performed throughout the experiments. During the cutting procedure the firing rate increased (figure 3.1). In addition, the adaptation to a moving grating appeared to be less strong. However, the increase in activity and the reduction in adaptation was only a temporary change in firing pattern. After 5 min the cell recovered back to baseline activity and the response properties to a moving grating recovered completely as well. Therefore, previous observations from J. Haag could not be confirmed.

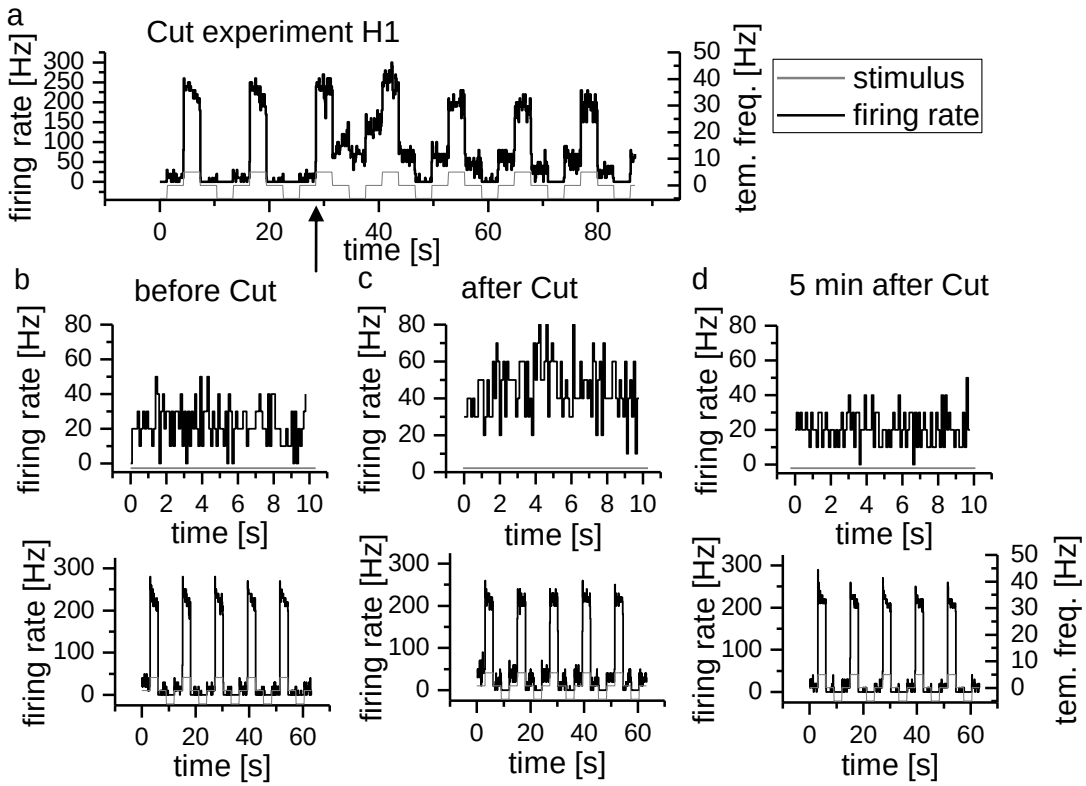

Figure 3.1: Response of H1 before and after Cutting the Connective. a) The black trace shows the firing rate (bin-width: 0.01 s) of H1 in response to a visual stimulus. An alternating moving grating was shown while the connective was cut (indicated by the arrow). The visual pattern was changed from a stationary sine grating, to a sine grating moving in the preferred direction of H1, then back to a stationary grating, and finally to a sine grating moving in the null direction of H1 (gray trace). b) The recordings were performed before the connective was cut; upper panel: the spontaneous activity is shown; lower panel: the response of H1 to an alternating moving grating (same as in a) is shown. c-d) same as in b) but the data were obtained approximately 1 min after cutting the connective (c), or after a recovery period of 5 min (d). Note that directly after cutting (c), the baseline activity is increased.

The experiments were repeated with V1, which is another spiking lobula plate tangential cell (fig. 3.2). Since the directional selectivity of V1 is shifted by 90° compared to H1, a vertical moving grating was presented. V1 was chosen because it is electrically coupled to VS1, and therefore any changes in the VS-cell should be reflected in V1. Again, an increase in baseline activity could be observed after cutting the connective, but nevertheless the response properties to a moving grating before and after cutting the connective were qualitatively similar (fig. 3.2 b&c).

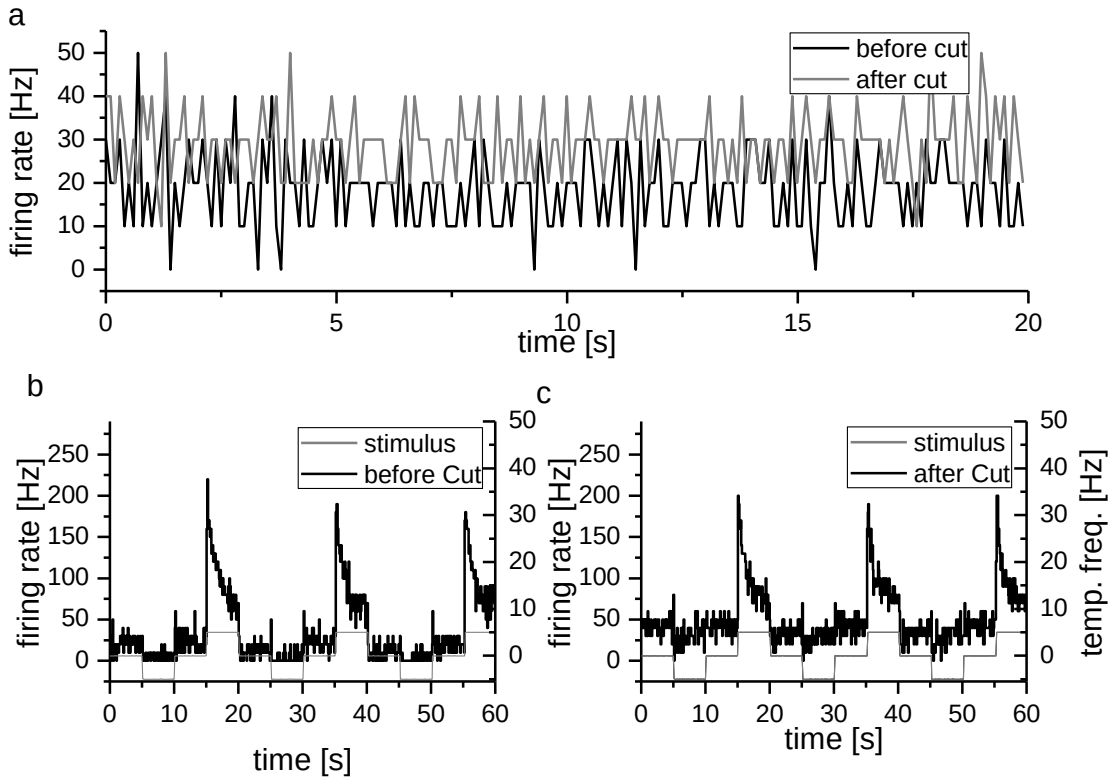

Figure 3.2: Response of V1 before and after Cutting the Connective. a) Spontanous activity of V1 before (black) and after cutting the connective (gray). b-c) The black trace shows the firing rate (bin-width: 0.01 s) of V1 in response to a visual stimulus. The gray trace indicates the visual stimulation. The response of V1 looks does not change significantly when the connective is severed. However, a slight offset between the baseline activity and the firing rate during the presentation of the null-direction could be observed.

3.2 Flight Modulates Visual Processing

In order to study how the visual motion processing is modulated during flight, I recorded extracellularly from the lobula plate tangential cell H1 during flight and compared the

results with data from the same animals when they were not moving. To confirm that the flies show normal flight behavior, wingbeat frequencies and the optomotor response were measured in a dissected preparation, simultaneous with H1 recordings.

The average wingbeat frequency during flight was 153 ± 5 Hz (n=5). The optomotor response was elicited by showing a high contrast pattern moving in the preferred and null directions of H1. The amplitudes of the left and right wing were modulated in counterphase depending on the direction of pattern motion (fig. 3.3 a, n=1). The difference in wing amplitude between left and right wing reflected the turning tendency of the fly (fig. 2.9 b) which was syndirectional with the pattern motion. This result demonstrates that the tethered flying flies showed a normal optomotor response. The higher contrast pattern parameters presented during the measurement of the optomotor response were used to measure the temporal frequency tuning curve of H1 in the same fly. The results did not qualitatively differ from the temporal frequency tuning curve measured at low contrast frequencies.

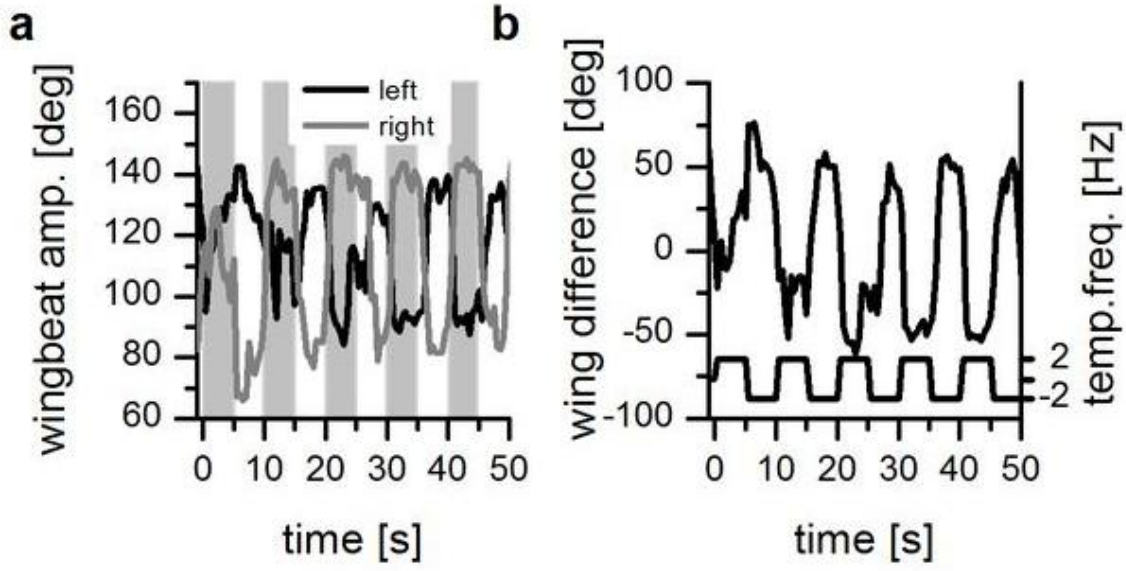

Figure 3.3: Wingbeat Amplitude during Tethered Flight. The direction of pattern movement alternated every five seconds from left to right and from right to left. a) Wingbeat amplitude of the left (black line) and the right wing (gray line) are shown. Pattern motion to the left is indicated by the gray boxes. b) Difference in wingbeat amplitude of left and right wing (wingbeat amplitude of left wing – wingbeat amplitude of right wing). The fly was trying to compensate for the visual stimulus. Square wave corresponds to the frequency of the pattern motion indicated by the gray boxes in 3.3a (picture by J. Haag).

3.2.1 Flight Changes Neuronal State

To characterize the influence of flight on the response properties of the H1 cell, first the spontaneous activity was measured under light adapted conditions. Therefore, I presented a stationary sine-wave grating which was later used as the motion stimulus (mean luminance: 5.2 cd/m²; contrast: 17.4%; wavelength: 40°).

Figure 3.4 a shows the firing rate of a single fly under flight and non-flight conditions. Note that the data for the non-flight condition were acquired approximately 5 min after flying. The firing rate was measured over a duration of 60 seconds and calculated over a time interval of 0.5 seconds. Throughout the recording, the firing rate during flight remained at a much higher level than during non-flight. In general, the standard deviation of the firing rate between flight and non-flight conditions was very similar (non-flight: 6.7 Hz; flight: 8 Hz); however, whereas, during flight, changes in the firing rate remained at the same order of magnitude throughout the recording, during non-flight sudden peaks in the firing rate occurred. These sudden increases in firing rate during non-flight most likely had their origin in movement of the antennae, halteres or legs.

The ISI-Histogram (fig. 3.4 b) shows a much narrower peak during flight, which corresponds to a comparably low standard deviation (non-flight: 0.049 s; flight: 0.009 s); however, the coefficient of variance (CV) is very similar (non-flight: 0.7253; flight: 0.6365). Note that for both conditions the CV is below 1, which indicates a relatively regular spike train compared to a Poisson distribution. Whether the regularity in the spike train is a consequence of cell-specific properties or is due to a regular input cannot be discriminated.

The average spontaneous activity over all flies is shown in figure 3.4 c. The mean spontaneous firing rate was increased dramatically by almost a factor of nine from 8.39 Hz ± 1.65 to 75.54 Hz ± 6.48 (mean±sem; n=8; $P<0.05$; paired t-test).

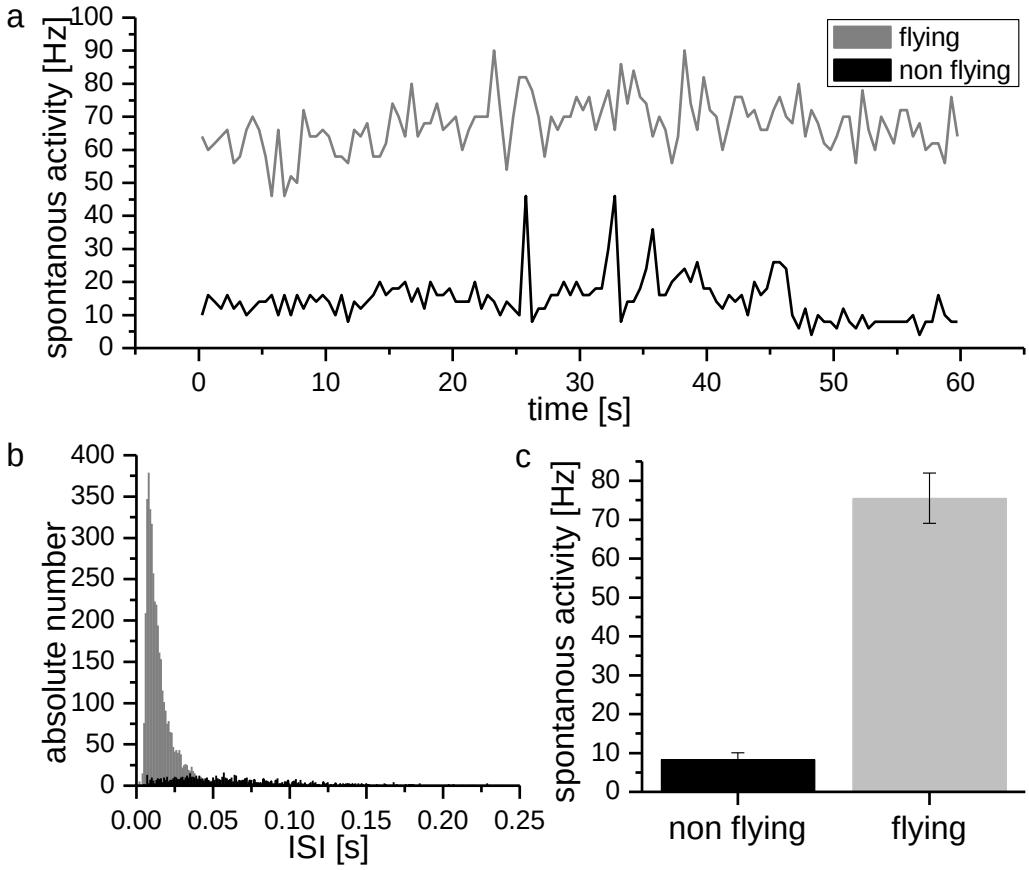

Figure 3.4: Spontaneous Activity during Non-Flight and Flight Conditions. a) Spontaneous firing rate of a single fly during flight and 5 min after flight. b) Interspike-Interval-Histogram calculated from the same spike train used to measure the firing rate in a. c) Average spontaneous activity calculated from 8 different flies under non-flight and flight conditions. Error bars indicate standard error of the mean.

3.2.2 Flight Increases the Directional Tuning Range

Work on Drosophila has shown that during flight the directional tuning range of lobula plate tangential (VS) cells – the difference between the response of cells to motion stimuli in the preferred vs. the null direction – is increased (Maimon et al., 2010). To test whether this holds true for H1 in *Lucilia* the firing rate in response to stimuli in the preferred and null directions was measured using a sine wave pattern moving with a temporal frequency of 5 Hz.

Figure 3.5 shows the average firing rate in response to four different stimulus conditions, each delivered both in the preferred and the null direction. Throughout the experiments the firing rate in the flight condition was clearly elevated. Also the response to pattern movement in the preferred direction of H1 was higher during the flight condition. The response increased between 10 - 20 Hz during flight, except for the strongest stimulus condition (high contrast + 20°) where only a small increase of 2.5 Hz could be observed. This is likely a result of a saturation of the firing rate of H1, which was close to 300 Hz during the flight condition. For the low contrast condition the response to the null direction was close to zero for the non-flight as well as for the flight condition. However, for the high contrast condition an increase of the negative tuning range could be observed during flight; this increase was most pronounced for the strongest stimulus (non-flight: high contrast + 20° = -3.73 Hz; flight: high contrast + 20° = -40.25 Hz).

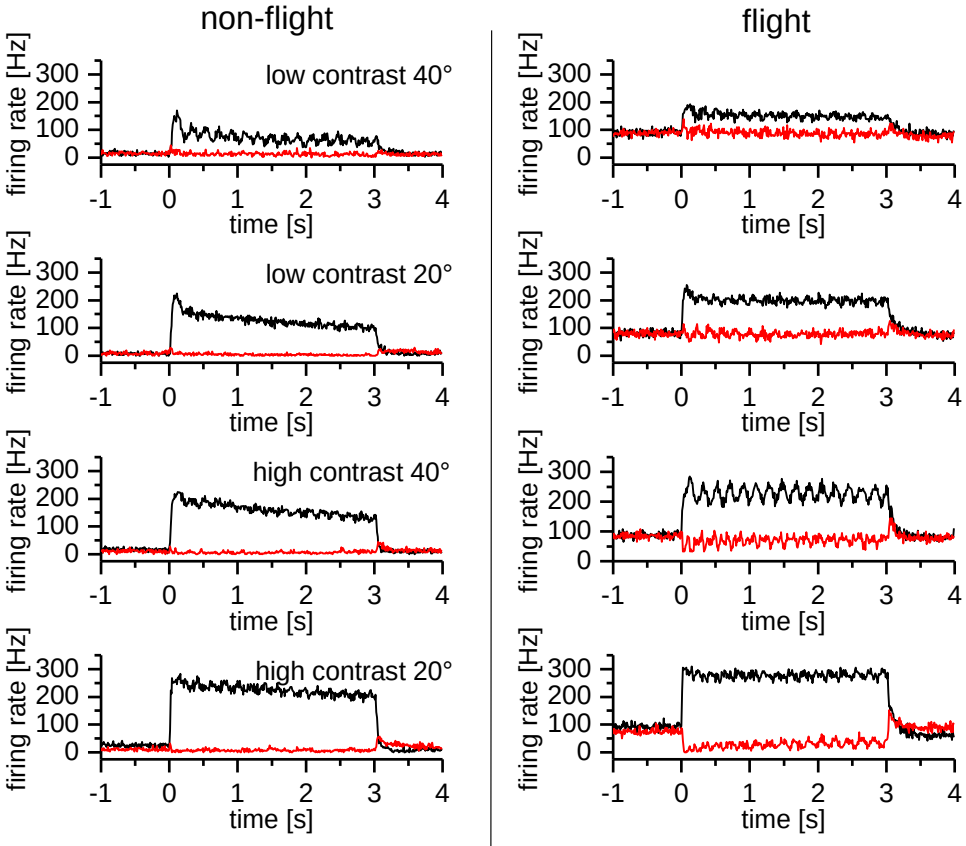

Figure 3.5: Firing Rate in Response to Different Patterns Moving in Preferred and Null Directions of H1. As indicated, four different patterns, varying in contrast and spatial wavelength, were used. The firing rates for stimulus presentations in the preferred and null directions are shown in black and red, respectively. Left: Results for the non-flight condition are shown (n=4). Right: Results for the flight conditions are shown (n=4).

3.2.3 Flight Broadens the Temporal Frequency Tuning Curve

One important aspect of motion detection is that the dynamic range of the visual input changes strongly depending on whether the animal is at rest, walking or in flight. Therefore, it is particularly interesting to ask whether the cells' temporal frequency tuning properties are changed in addition to the observed elevated spontaneous spike rate and the increased directional tuning range. The temporal frequency is defined as the pattern wavelength divided by the pattern velocity. To measure the temporal frequency tuning curve a moving sine-wave grating was shown for 3 sec with different temporal frequencies ranging from 0.3 Hz to 20 Hz.

The firing rate recorded during the presentation of different temporal frequencies (fig. 3.6 a & b) revealed two major differences between non-flight and flight conditions. First, the overall firing rate for low (e.g., 1 Hz) as well as for high (e.g., 10 Hz) frequencies is elevated over the entire duration of pattern presentation during flight (fig. 3.6 a & b). Second, for high frequencies the time course of the firing rate during prolonged stimulus presentation seems to be changed as well. Note, however, that during flight the maximum firing rate might already be influenced by saturation effects.

For low frequencies the responses of H1 during non-flight and during flight look very similar (fig. 3.6 c & d). However, one interesting observation can be made. During flight the response at pattern movement onset seems to rise faster. This phenomenon might have its explanation in the fact that H1 is closer to threshold during flight, as suggested by its increased spontaneous activity. The largest state-dependent difference between the response properties of H1 was observed for high frequencies, whereas the peak response was almost unchanged. The response adapted more slowly and stayed at a higher steady-state value during flight. This finding was further analyzed by calculation of the steady-state firing rate and the steady-state response of the cell.

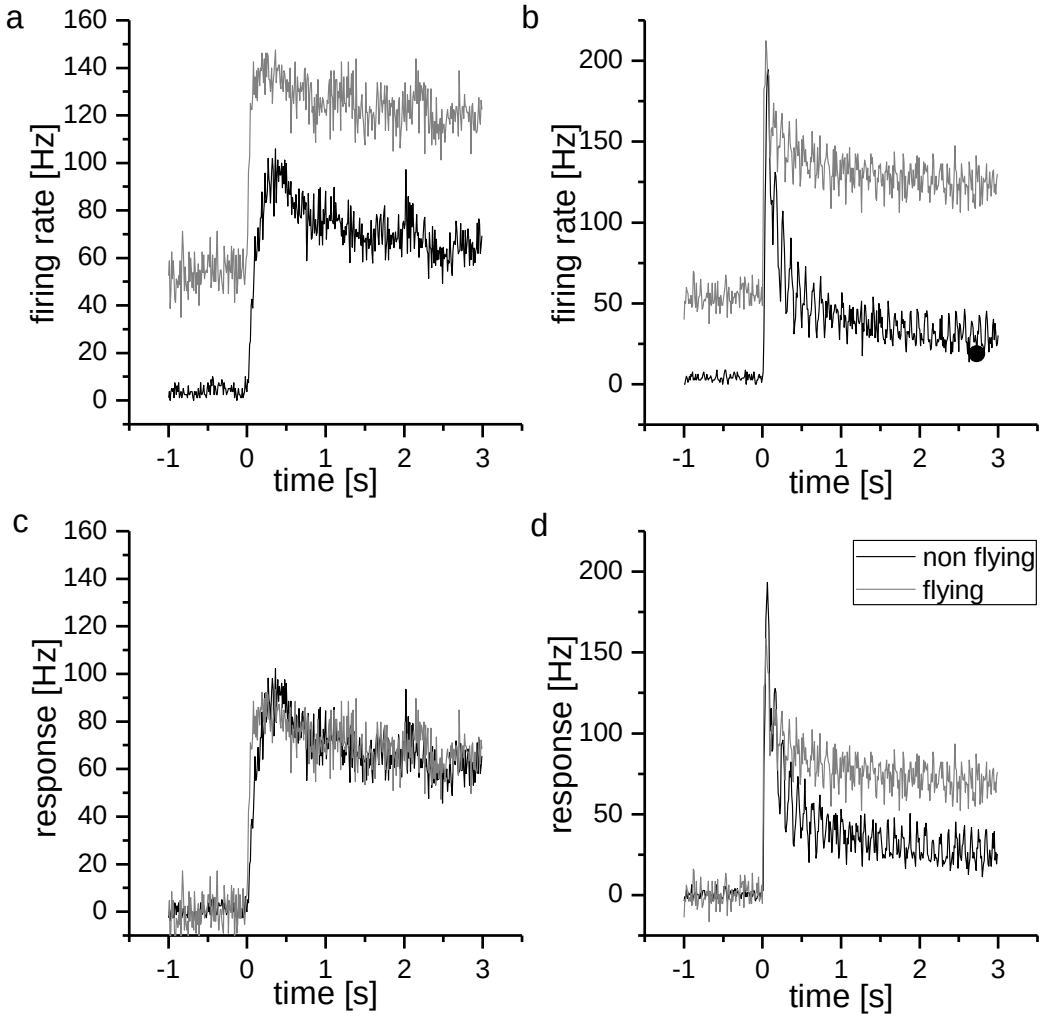

Figure 3.6: Response of H1 to Different Temporal Frequencies during Flight and Non-Flight Condition. a & b) Average firing rate to a 1 Hz (a) or 10 Hz (b) stimulus presentation during flight and non-flight conditions (n=8). c & d) Average response to a 1 Hz (c) or 10 Hz (d) stimulus presentation during flight and non-flight conditions (n=8).

The steady-state firing rate of H1 was significantly higher during flight than during non-flight (fig. 3.7 a) over the whole frequency range tested. However, the picture looks very different when one considers the steady-state response. At low frequencies, as one might already suspect from the results presented in figure 3.6, there was no significant change between the flight and the non-flight condition (fig. 3.7 b). This changed when the pattern frequency was increased. The response to high frequencies was, in contrast to the responses to low frequencies, higher during flight than during non-flight. Hence, both the steady-state firing rate and response of H1 to high frequencies were increased during flight.

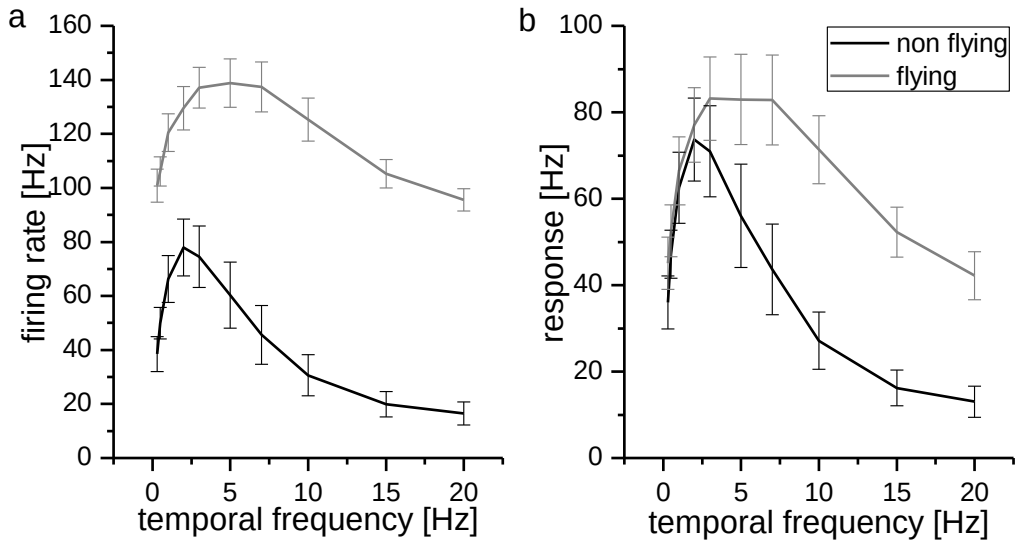

Figure 3.7: Temporal Frequency Tuning Curve. a) Average of the steady-state firing rate in response to a stimulus presentation in preferred direction under flight and non-flight condition (n=8 flies). Each temporal frequency was presented 10 times to every fly. Error bars are indicating the standard error of the mean. b) same as in a, but the steady-state response is plotted.

In summary, one can describe the steady-state response tuning curve as follows: Whereas in non-flying flies the response of H1 reached a maximum around 2 Hz, during flight the response further increased slightly and stayed at an almost constant level until a pattern frequency of 7 Hz was reached. For higher temporal frequencies the response decline was relatively small, so that even at 20 Hz the response was still significantly higher than during non-flight. These results show that the temporal frequency curve changes with the behavioral state of the fly.

3.2.4 Control for Wind

To induce and maintain flight behavior, it was necessary to use wind as an additional stimulation for flight. It is therefore possible that the wind stimulus is responsible for the observed change in the neuronal response of H1. The influence of wind on the neuronal response of H1 was tested in fixed flies (fig. 3.8). The spontaneous rate increased slightly when the wind was turned on. The effect, however, was much lower than the effect of flying. A reason for this increase could be a stronger movement of antennae, halteres or

legs during wind stimulation. The frequency tuning curve did not shift, and only a small increase in the overall gain was observed.

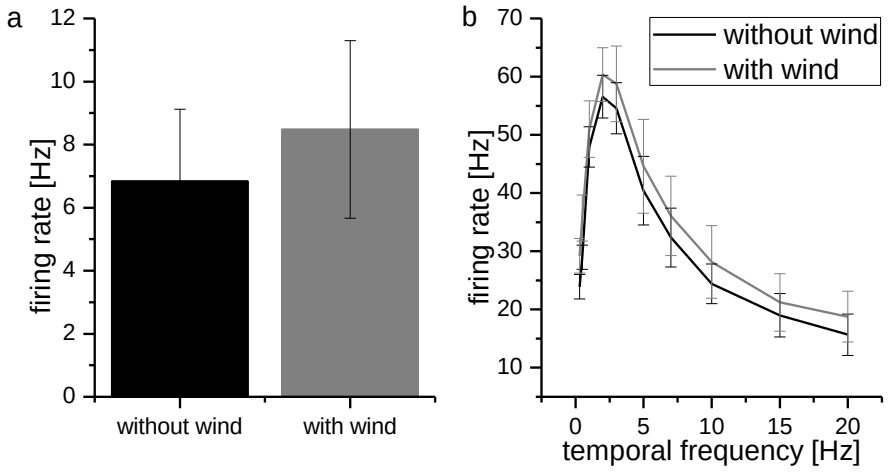

Figure 3.8: Control of Wind-Induced Changes in the Response of H1. a) The average spontaneous activity is shown with and without wind stimulation (n=4). b) Average of the steady-state firing rate of H1 to different temporal frequencies presented in the preferred direction (n=4). The same flies as in (a) were used. Each temporal frequency was presented 10 times to every fly. Error bars indicate the standard error of the mean.

3.3 Neuromodulation of the Visual Response

It is commonly assumed that octopamine plays an important role in the arousal state of insects (Davenport and Evans, 1984; Roeder, 1999) and it has been shown that it changes the response properties of lobula plate tangential cells in flies (Longden and Krapp, 2009; Longden and Krapp, 2010). Therefore, it is a reasonable assumption that some of the observed effects of flying on the response properties of H1 can be mimicked by the application of octopamine into the hemolymphe.

To test this hypothesis I applied the octopamine agonist CDM (Hiripi et al., 1999) to the hemolymphe of the fly. The stimulus protocol before and after the application of CDM consisted of three steps: first: recording of the spontaneous firing rate; second: measuring the response to different temporal frequencies (same stimulus protocol as for the flight experiments); third: recording of the spontaneous firing rate. The second measurement of the spontaneous activity was performed in order to ensure that the

influence of CDM application was relatively constant over the whole duration of the protocol.

3.3.1 CDM Changes Neuronal State

In all flies the application of CDM resulted in an increase in spontaneous activity. As can be seen from the example of the spontaneous activity of a single fly (fig. 3.9 a), the increase in activity remained relatively constant over the whole duration of recording (std – before-CDM: 3.55 Hz; std - CDM: 7.56 Hz). For both conditions the CV calculated from the Interspike-Interval-Histogram was very close to 1 (fig. 3.9 b; before-CDM: 0.97; CDM: 0.84). After the application of CDM, the spontaneous firing rate increased on average from about 10.5 Hz to 37.6 Hz (fig. 3.9 c, $P<0.05$, paired t-test, n=10).

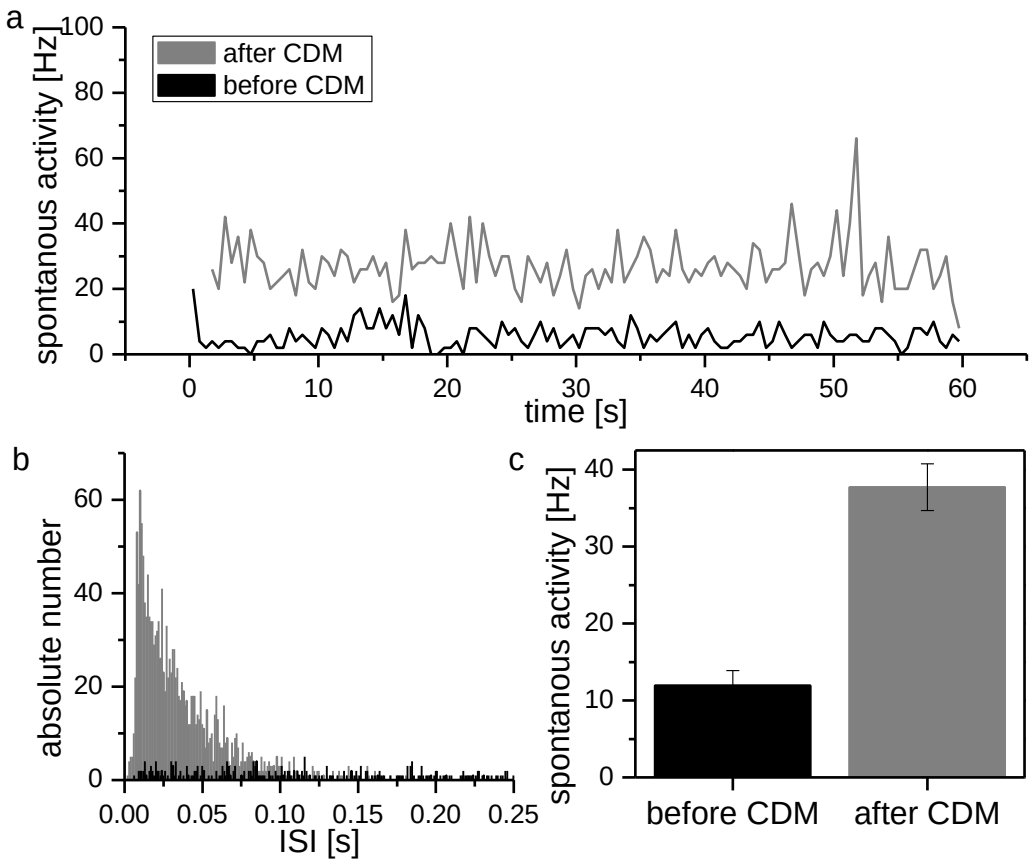

Figure 3.9: Spontaneous Activity before and after the Application of CDM. a) Spontaneous firing rate of a single fly during flight and 5 min after flight. b) Interspike-Interval-Histogram calculated from the same spike train used in (a) to measure the firing rate. c) Average spontaneous activity calculated from 8 different flies under both conditions.

3.3.2 CDM Broadens the Temporal Frequency Tuning Curve

In addition to the increase in spontaneous firing rate, I also observed that several aspects of the changes in the response of H1 to different pattern frequencies between non-flying and flying animals could be mimicked with CDM. Throughout the stimulus protocol the firing rate was elevated after the application of CDM (fig. 3.10 a & b). As for the experiment on flying flies, the responses to a 1 Hz stimulation is very similar between both conditions. For a 10 Hz stimulation the response, however, stays at higher level after the application of CDM. However, the differences in steady-state level are not as pronounced as for the flight condition.

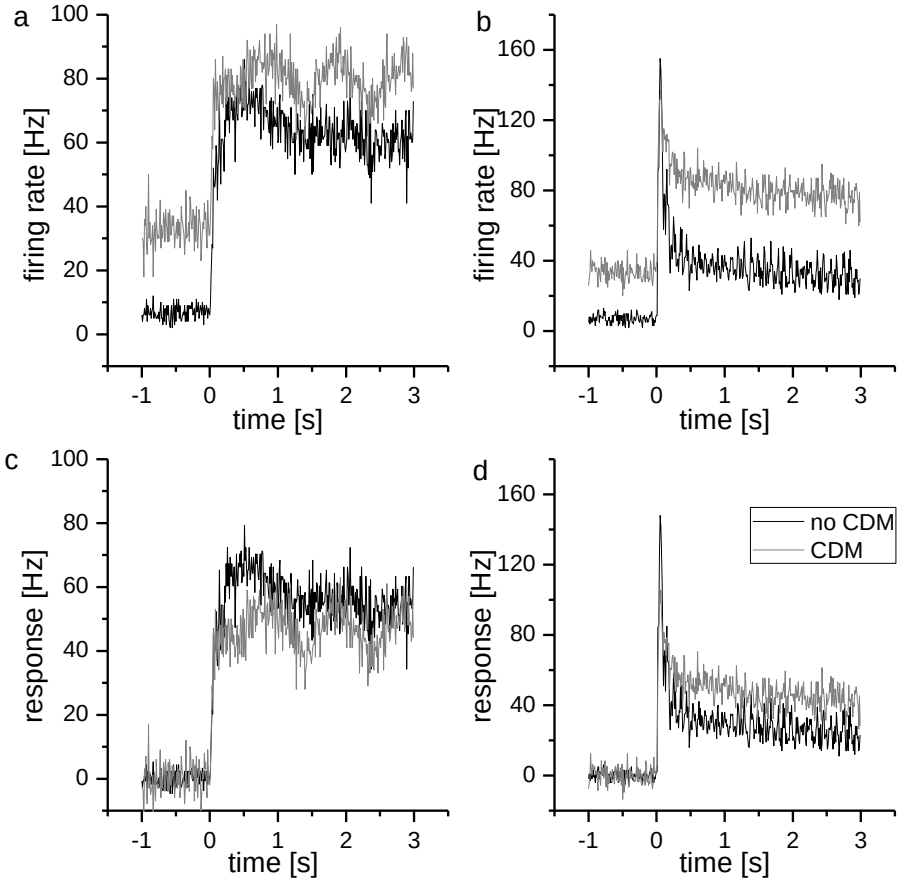

Figure 3.10: Response of H1 to Different Temporal Frequencies before and after the Application of CDM. a & b) Average firing rate to a 1 Hz (a) or 10 Hz (b) stimulus presentation before and after the application of CDM (n=10). c & d) Average response to a 1 Hz (c) or 10 Hz (d) stimulus presentation before and after the application of CDM (n=10).

The increased steady-state firing rate after CDM application is also observed when one looks at the temporal frequency tuning curve (fig. 3.11 a). Further analyzing the steady-state response revealed that the application of CDM led to a broadening of the temporal frequency tuning curve (Fig. 3.11 b). Overall, the changes in the activity of H1 were not as pronounced as during flight conditions; however, both effects (increase in spontaneous activity & broadening of the temporal frequency tuning curve towards higher frequencies) could be observed.

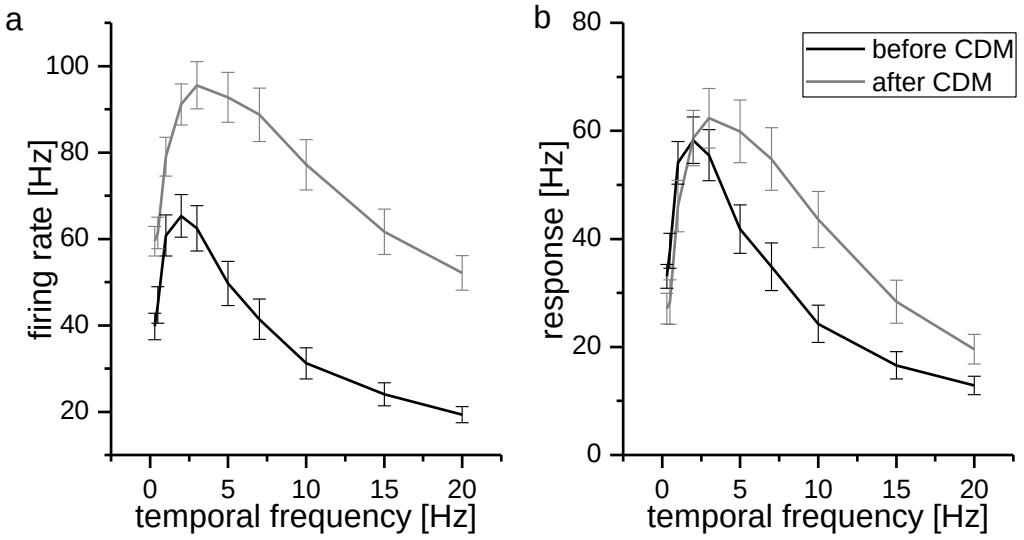

Figure 3.11: Temporal Frequency Tuning Curve. a) Average steady-state firing rate in response to a stimulus presentation in preferred direction before and after the application of CDM (n=10 flies). Each temporal frequency was presented 10 times to every fly. Error bars indicate the standard error of the mean. b) same as in a, but the steady-state response is plotted.

3.3.3 Control for Neuromodulation

As a control for the application of CDM, exactly the same experimental procedure was applied except that no CDM was added to the Ringer's solution. The application of Ringer's onto the fly brain is a standard method to keep it from drying out during the experiment. Therefore, no change in the activity of H1 was expected when Ringer's was applied during the experiment. Nevertheless, small effects might be possible since the Ringer's in the pipette might have a different temperature as the Ringer's already

previously applied to the fly's head. Moreover, it is possible that the fly becomes slightly aroused by the procedure, though care was taken that the pipette never touched the fly while applying the Ringer's. In addition to the test for effects induced by the experimental procedure, this control also shows that the stimulus protocol is short enough so that the preparation is still in good condition at the end of the experiment. Neither the spontaneous activity nor the steady-state firing rate measured for different temporal frequencies showed any difference after the Ringer's was applied to the head capsule (fig. 3.12).

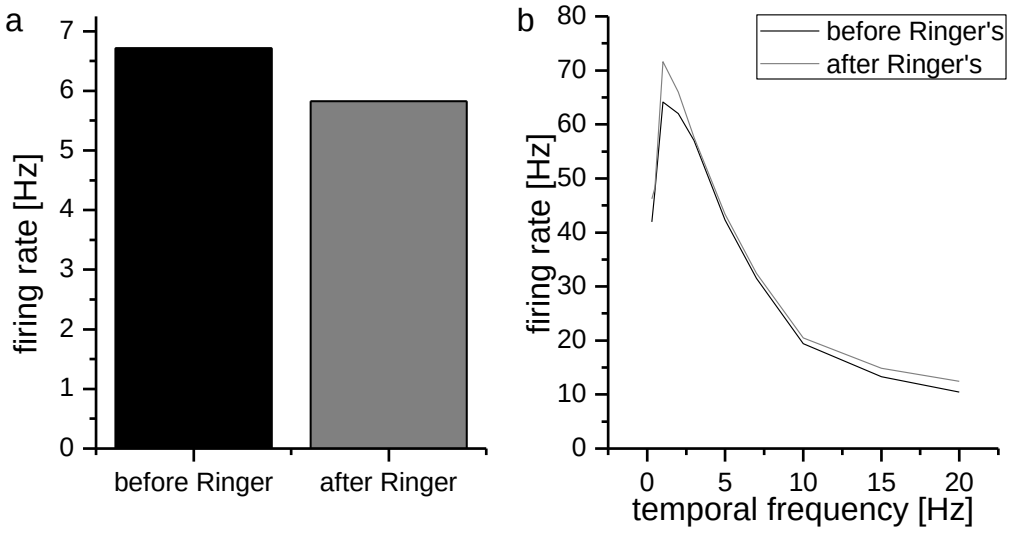

Figure 3.12: Control for Neuromodulation Experiments. a) Average spontaneous activity measured before and after the application of Ringer's (n=2) b) Average steady-state firing rate for different temporal frequencies before and after the application of Ringer's (n=2).

3.4 Simulations with the Reichardt Detector

To test whether a change in the filter parameters of the Reichardt detector model could explain the observed broadening of the tuning curve, I used the 'High-pass' model (fig. 2.5) to fit the results. The 'High-pass' model has, in addition to the low-pass filter in one input line, a high-pass filter in the cross-arm of the detector unit. The high-pass time constant in this model is given by the time constant of the impulse response (Borst et al., 2003). Since the high-pass constant adapts during stimulus presentation I measured the

impulse response after presenting an adaptive stimulus (de Ruyter van Steveninck et al., 1986; Reisenman et al., 2003). The low-pass time constant can then be fitted using the model.

For non-flight as well as during flight I measured the impulse response in isolation and 200 ms after the presentation of a sine grating moving for 3 sec with a temporal frequency of 5 Hz in the preferred direction of the cell (fig. 3.13). The latter stimulus protocol was used to obtain an estimate for the high-pass filter time constant after adaptation. Figure 3.13 (a-c) shows the experimental results and the respective fits for the impulse response of a single fly. The impulse response had a similar maximum for non-flight and for flight. However, if one considers the time course of the response it can be seen that during flight the time constant of the impulse response is increased. The impulse response measured after the presentation of the adaptive stimulus was very different between the two conditions (fig. 3.13 d). The response decreased compared to the isolated impulse response for the non-flight condition, whereas for the flight condition the response stayed on a relatively high level. The time courses of the impulse response after the presentation of a moving grating shortened for both conditions. However, the effect was much more pronounced for the flight condition, resulting in a relatively small difference of the high-pass time constant in the adapted state (fig. 3.13 e-f).

On average the time constant of the impulse response decreased after the presentation of a moving grating to about 2/3 of the value of the isolated impulse response for non-flight as well as for the flight condition (fig. 3.13 g). The absolute decrease was more dramatic for the flight condition.

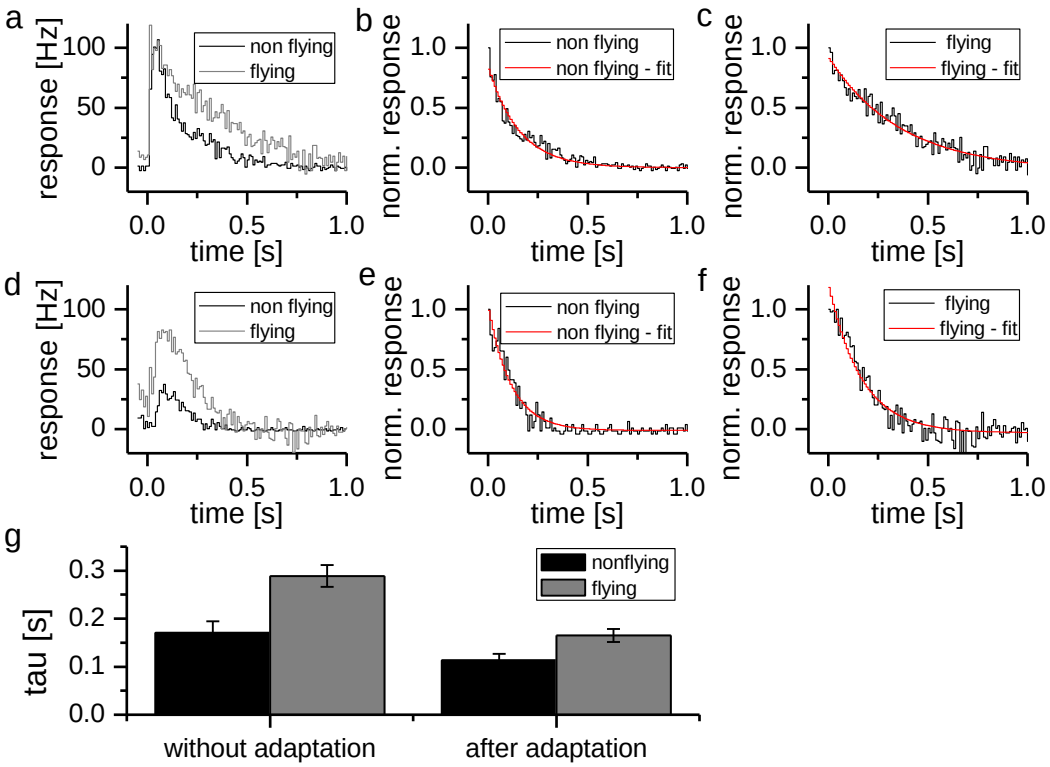

Figure 3.13: Impulse Response before and after the Presentation of a Moving Sine Grating. a-f) Impulse responses and fits obtained from a single fly are shown. a) Impulse response during non-flight and flight conditions. b) Data and fit to the impulse response during the non-flight condition. c) Data and fit to the impulse response during the flight condition. d) Impulse response 200 ms after the presentation of a moving grating (5 Hz) during non-flight and flight conditions. e) Data and fit to the impulse response 200 ms after the presentation of a moving grating (5 Hz) during the non-flight condition. f) Data and fit to the impulse response 200 ms after the presentation of a moving grating (5 Hz) during the flight condition. g) Average time constant measured in 5 flies for all conditions as presented in (b-c;e-f).

The same stimulus protocol as described above was repeated for CDM application. The results are illustrated in figure 3.14. It turned out that, in the case of CDM application, some cells showed a strong after-hyperpolarization after the presentation of the moving grating. In these cases, the adapted impulse response could not be measured because the observed time course is a mixture between the actual impulse response and the hyperpolarization after the stimulus, which could not be entangled. To solve this problem, one could measure the hyperpolarization occuring after the presentation of a

moving grating separately. This was not performed for the experiments of flying flies because the problem did not occur to a significant extent. The after-hyperpolarization was rather weak or not present (fig. 3.5). Due to the time limitation given by the duration of flight, the decision was made to perform more stimulus presentations rather than to attempt to measure the after-hyperpolarization. To keep the data comparable, the same stimulus protocol was used as for the flight experiments in order to perform the CDM experiments and exclude the data sets with a strong hyperpolarization after the presentation of a moving grating. Therefore, only the data from 3 flies are shown in figure 3.14, which corresponds to about 50% of the recorded flies. For the single fly chosen as an example, the response to an isolated impulse looks very similar before and after CDM application (fig. 3.14 a). Moreover, the time course of the response does not differ significantly (fig. 3.14 b-c). The overall response strength, evaluated by the maximum firing rate, decreased after the presentation of an adaptation stimulus for both conditions. When an adaptation stimulus is presented beforehand, the impulse response is shorter for the CDM application condition compared to before application of CDM (fig. 3.14 d-f). This observation is opposite to what was expected from the experiments on flying flies. Whereas flying led to an increase of the high-pass time constant, CDM led to a decrease in the high-pass time constant.

Before the application of CDM, on average the time constant of the impulse response after adaptation had a value about 2/3 of the impulse response before adaptation. The application of CDM lead to a stronger adaptation of the time constant; the value was only about half of the isolated impulse response (fig. 3.14 g).

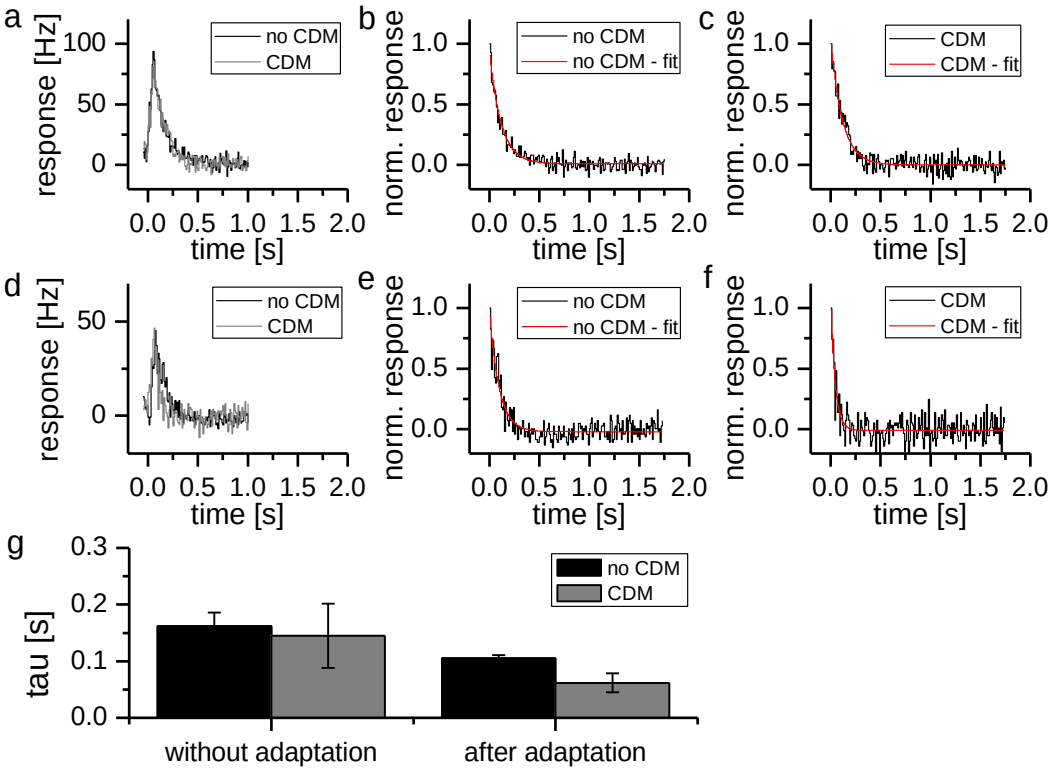

Figure 3.14: Impulse Response before and after the Presentation of a Moving Sine Grating. a-f) Impulse responses and fits obtained from a single fly are shown. a) Impulse response during before-CDM and CDM conditions. b) Data and fit to the impulse response during the before-CDM condition. c) Data and fit to the impulse response during the CDM condition. d) Impulse response 200 ms after the presentation of a moving grating (5 Hz) during the before-CDM and CDM conditions. e) Data and fit to the impulse response 200 ms after the presentation of a moving grating (5 Hz) during the before-CDM condition. f) Data and fit to the impulse response 200 ms after the presentation of a moving grating (5 Hz) during the CDM condition. g) Average time constant measured in 3 flies for all conditions measured as presented in (b-c; e-f).

The output Reichardt detector model was fitted to the steady-state response with equation (1). I used the high-pass time constant measured after the presentation of a moving grating as a parameter in the detector model; the low-pass time constant was fitted using the method of least mean squares. The experimental results for the flight experiments as well as for the CDM experiments are plotted together with the outcome of the fit in figure 3.15.

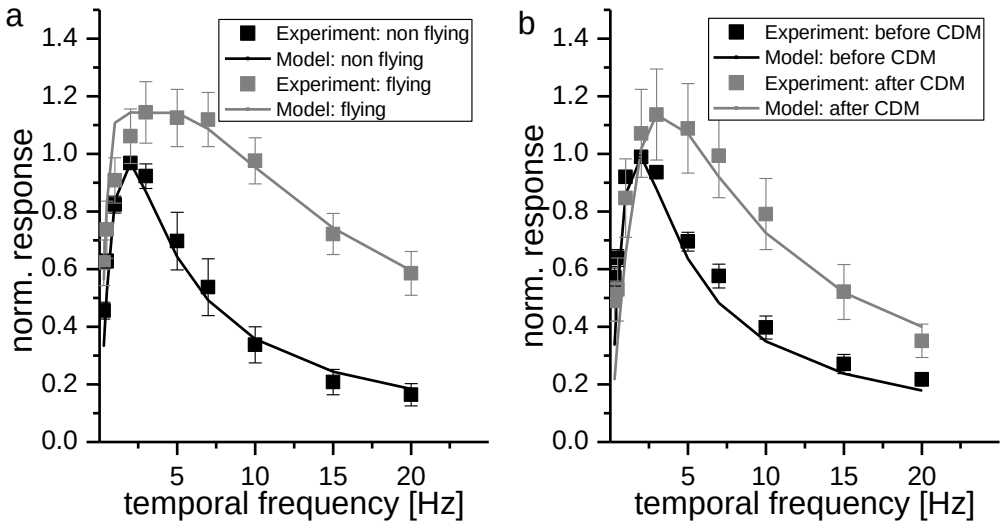

Figure 3.15: Comparison between the Experimentally Measured and Fitted Temporal Frequency Tuning Curves. a) The steady-state frequency tuning curve measured for the non-flight and flight conditions are shown together with the corresponding fits of the Reichardt detector model. The same experimental data are shown as in fig. 3.3 b; however, the responses were normalized by the maximum peak of the non-flight condition. The fit of the Reichardt detector model was performed on the normalized data sets. b) The steady-state frequency tuning curve measured for the before-CDM and CDM conditions are shown together with the corresponding fits of the Reichardt detector model. The same experimental data are shown as in fig. 3.8 b; however, the responses were normalized by the maximum peak of the before-CDM condition. The fit of the Reichardt detector model was performed on the normalized data sets.

The best fit for the non-flight condition could be obtained with a low-pass time constant of 0.069 s. For the flight condition, the best fit was a low-pass time constant of 0.024 s. Therefore, the results indicate that the low-pass time constant has to decrease during flight. The best fit for the before-CDM condition could be reached with a low-pass time constant of 0.077 s. As expected, this is very similar to the non-flight condition. For the CDM condition, the best fit was reached with a low-pass time constant of 0.036 s. This is a slightly higher value than for the flight condition.

If one considers the error function of the fit, it becomes evident that for the non-flight as well as for the before-CDM condition the curve is much shallower than for the flight or the CDM condition (fig. 3.16). Therefore, even though the fits for the non-flight and the before-CDM conditions do not result in exactly the same low-pass time constant, the

small differences in the time constant are not surprising. However, on the other hand, the difference in the fitted low-pass time constant between the flight and the CDM conditions is more significant.

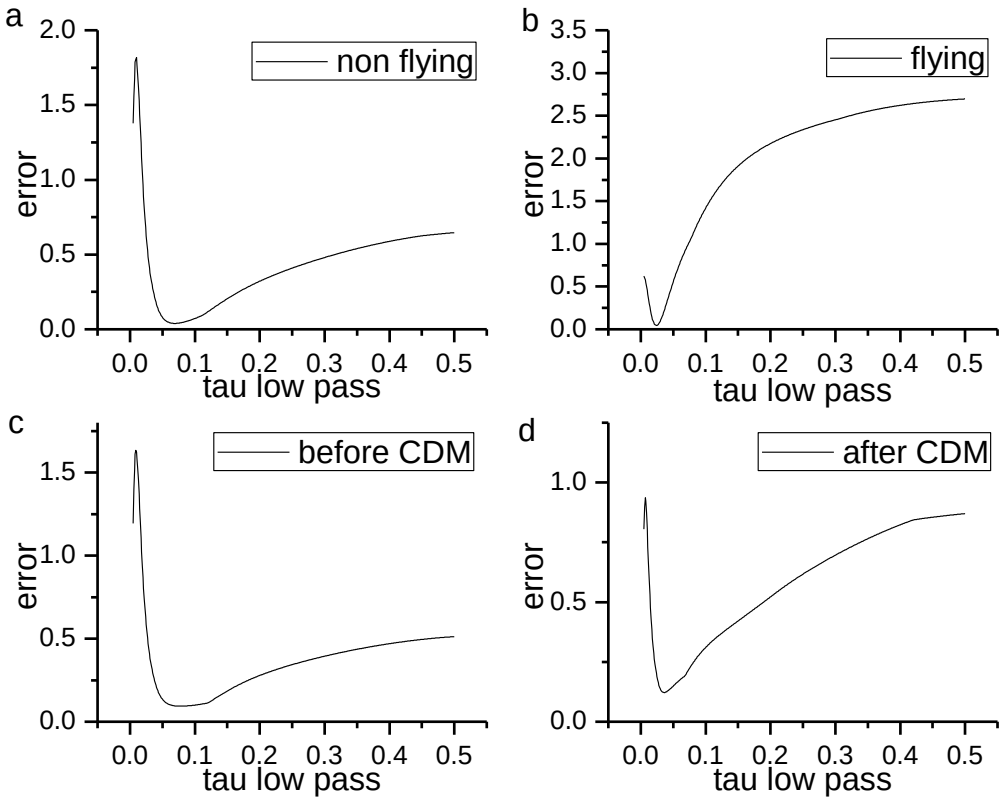

Figure 3.16: Error Function of the Low-pass Time Constant. a) The least mean square error is plotted against τ_{low}-non-flight; τ_{high}-non-flight was held fixed at the value measured from the impulse response. b) The least mean square error is plotted against τ_{low}-flight; τ_{high}-flight was held fixed at the value measured from the impulse response. c) The least mean square error is plotted against τ_{low}-before-CDM; τ_{high}-before-CDM was held fixed at the value measured from the impulse response. d) The last mean square error is plotted against τ_{low}-CDM; τ_{high}-CDM was held fixed at the value measured from the impulse response.

The good fit of the steady-state response between the model and the experimental data is only one aspect of the High-pass model. To test whether the step response could also be explained by the High-pass model, the previously determined time constants were used to calculate the transient response characteristics (equation 2).

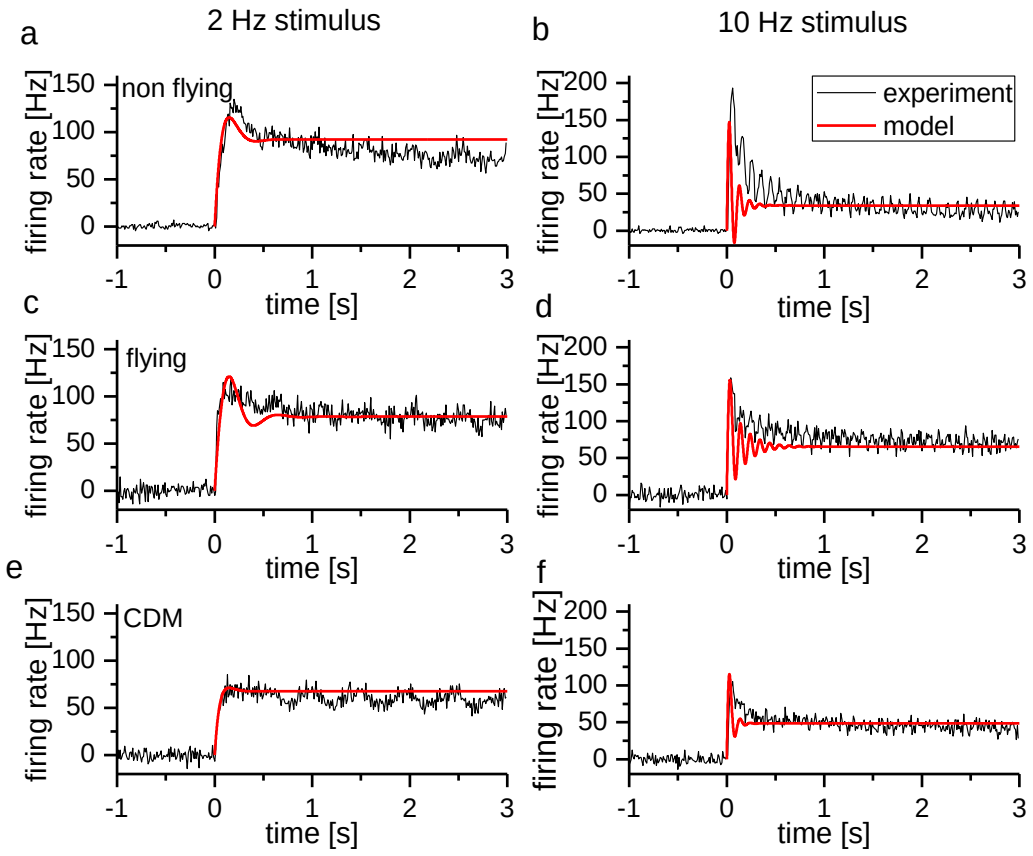

Figure 3.17: Model Prediction of the Step Response to Visual Stimulation. a-b) Experimental data and model predictions of the transient response for the non-flight condition. The temporal frequency of the moving pattern was 2 Hz (a) or 10 Hz (b), respectively. c-d) same as in (a-b), but for the flight condition. e-f) same as in (a-b), but for the CDM application condition.

The transient response of the non-flight, flight and CDM conditions were compared with the results of the High-pass detector model for a sine-wave grating moving with a constant speed of 2 Hz and 10 Hz (figure 3.17). The peak response of the modeled results fit quite well to the experimental data. The difference between experimental data and model was largest for the non-flight condition. The transient response properties were not captured as well by the model as the steady-state and peak response.

4. Discussion

In this work I investigated how visual motion processing is modulated by the behavioral state of the fly. First, I studied how visual motion processing is modulated during flight. Therefore, I measured the response of the lobula plate tangential cell H1 to visual stimulation during non-flight and during flight. Furthermore, by using the same stimulus protocol I investigated whether some of the observed effects of the flight condition can be mimicked by octopamine. To test this I applied the octopamine agonist CDM into the hemolyphme of the brain and recorded the change in response properties of H1. Flight, as well as the application of CDM, increased the spontaneous activity of the cell. Both also broadened the frequency tuning curve of H1 towards higher frequencies. In the last part of the work, I examined what parameters had to be adjusted in the Reichardt model for elementary motion detection to explain the difference in the tuning properties of H1 between the non-flight/before–CDM and flight/CDM condition.

4.1 Methodology

4.1.1 Cut Experiments

This set of experiments was performed to show whether there exist a feedback from the motor system to the LPTCs. The idea came from previous observation in which the cutting of the connective in the neck of the fly led to an abolishment of the responses of certain neurons in the lobula plate (fig. 4.1; Haag, unpublished). This led to the

hypothesis that ascending projections from the motor system are necessary for the survival and function of lobula plate tangential cells.

In these experiments, graded response neurons were recorded intracellularly (Haag, unpublished). The experiment itself consisted of three steps. First, a cell was recorded with an electrode containing Alexa 488. Then, the fly was removed from the set-up and the connective was cut with scissors. At the end, the fly was placed back in the set-up. A second set of recordings of the same cell were made, using an electrode containing Alexa 568. The resulting double staining confirmed that before and after the cutting procedure the same cell was recorded. However, it was impossible to cut the connective while recording the cells since this would have most likely resulted in losing the cell. Recording from spiking neurons changed the situation and it was possible to cut the neck connective while recording. As described in the Methods section above, a hair was attached to the neck connective; by pulling the hair with forceps the connective was destroyed. The success of this procedure was confirmed after completion of the experiments under a microscope. Of course, a strong fixation of the head to the thorax as well as a very stable attachment of the fly within the set-up is absolutely crucial for the success of the process. Even under the best circumstances brain movements cannot be completely avoided but only minimized. Therefore, all the obtained results from the experiments have to be interpreted with caution. Changes in the response properties after cutting the connective might not only be attributed to the effect of ascending projections from the motor or mechanosensory system but also be induced by a destruction of parts of the brain caused by relative movements between the reference electrode and the brain or by an increased level of arousal.

Many of the first experiments were unsuccessful; the cell was lost during cutting and often also the lobula plate appeared to be silent after the procedure. Most of the variability in the data could be attributed to differences in the success of the experimental procedure rather than to intrinsic variability of flies or cells. Therefore, no statistics on the data were performed. Nevertheless, the results obtained in the work from the cutting experiment are in strong disagreement with previous observations (fig. 4.1).

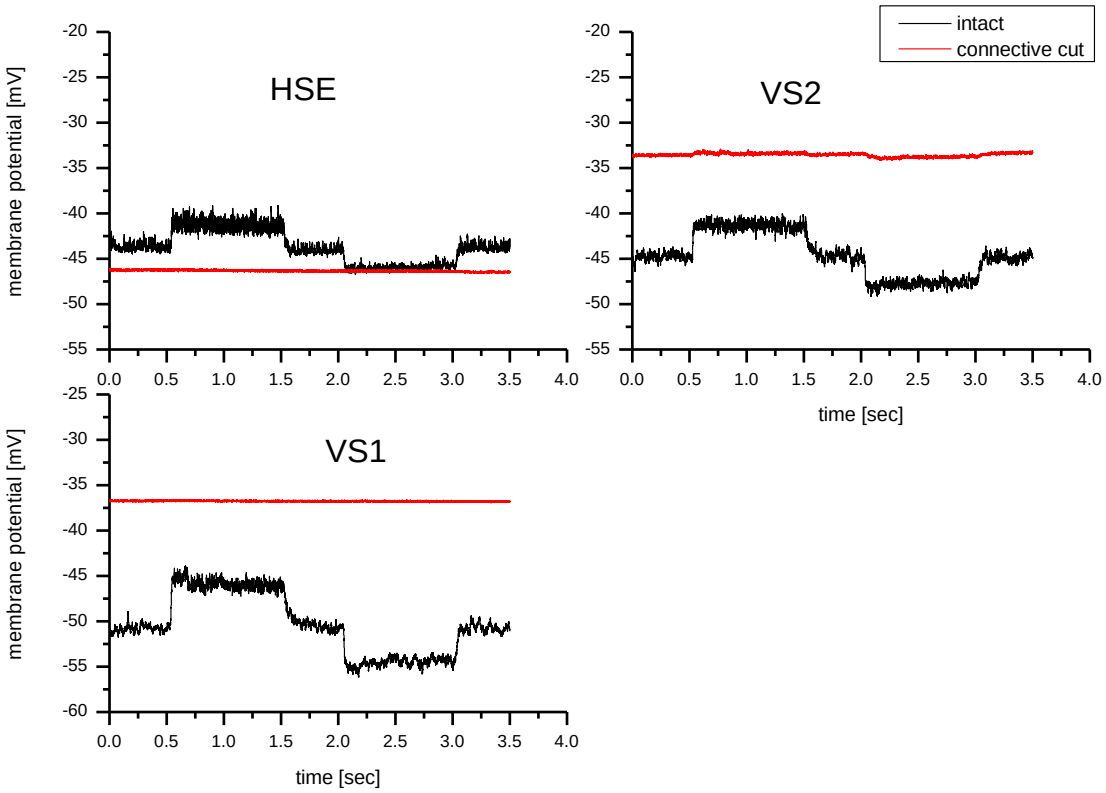

Figure 4.1: Intracellular Recording of Lobula Plate Tangential Cells before and after Cutting the Connective. The cells were simulated with a pattern either moving in their preferred direction (0.5-1.5 sec) or in the null direction (2.0-3.0 sec). Before the connective was cut, a clear response to the pattern movement could be observed which diminished completely (HSE, VS1) or almost completely (VS2) after the connective was cut (picture taken from J. Haag).

The experiments were initially only performed with H1. Here, in a few cases a temporary increase in firing rate and small changes in the response properties were observed. It is difficult to draw conclusions about the underlying mechanisms causing these changes of the response of H1. The fact that the changes observed were not permanent speaks for the hypothesis that the cell or other brain regions might have been slightly damaged during that procedure or the arousal level increased.

The results obtained from the H1 recordings were completely unexpected considering previous data suggesting that the lobula plate tangential cells (HSE and VS) become silent after cutting the connective (fig. 4.1;, Haag, unpublished). The additional data from V1 further support the conclusion that previous observations of lost of

responsiveness of LPTCs to motion stimuli are artifacts caused by the experimental procedure rather than being caused by actually cutting the connective. V1 is coupled to VS1 via electrical synapses (Haag and Borst, 2008); therefore, it would be almost impossible that the strong effects observed in VS1 are not reflected to a great extent in V1. The specific reason for the different results still remains unclear. However, it might be possible that during previous work other structures in the neck essential for the survival of lobula plate cells might have been destroyed such as air sacks or the heart tube.

One very important point I want to address is that the discussed results do not exclude the possibility that the neuronal projections in the neck connective, including ascending projections from the motor system, have an important function during flight or arousal. To test this one could, for example, simultaneously record the flight activity and record from LPTCs, or stimulate ascending neurons while recording from LPTCs (Heide, 1983). Experiments pointing in these directions were recently published (Haag et al., 2010; Rosner et al., 2010). LTPCs or descending neurons were recorded while the halteres were either moving actively or passively. However, the rather short sequences of haltere beating did not cause much change in the response properties of the LTPCs.

4.1.2 Extracelluar Recordings in Tethered Flying Flies

Extracellular recordings from tethered flying insects are not that uncommon. However, most studies so far have been conducted in locusts. In these studies, the neurons recorded were usually postsynaptic to the lobula complex (Rind et al., 2008; Santer et al., 2006; Santer et al., 2005). Something one has to consider is that the robustness of a preparation as well as the motivation to fly is highly dependent on the animal species. The great success of experiments in locusts could be attributed to the fact that these animals are well suited for such kind of experiment.

One of the major problems that occurred when performing extracellular recordings in tethered flying flies was the increased level of noise. In contrast to a previous study (Heide, 1983) I fixed the head directly on the thorax. Vibration and other movement

artifacts were reduced by minimizing the angle between head and thorax. Having a relatively large hole in the cuticula in the back of the head made it possible to determine during the preparation whether small vibrations will occur during experiments.

In order to reduce the time period needed to find H1, low resistance electrodes of 0.5 MOhms were used. This increased the motivation of flying in the flies but had the drawback that more background activity was recorded as well. Based on background activity, flying increased the activity of neurons in the lobula plate. This increased the risk of recording the activity of multiple units. Therefore, the ISI were checked carefully. In addition, data were only used from recordings where the electrode did not have to be adjusted within the experimental session and the same threshold criteria were used for the flight and non-flight condition. Performing recordings in the lobula plate of blowflies has the advantage that this brain area is very well characterized (Borst and Haag, 2002). Identification of H1 is easy since only one other neuron (H2) has been described that has the same preferred direction and similar projection patterns (Eckert, 1980; Haag and Borst, 2003).

The behavioral data obtained with the high-speed camera confirmed that extracellular recording from LPTCs does not affect the wingbeat frequency and the optomotor response. The wingbeat frequency was only a few Hz different from values previously reported in blowflies (Balint and Dickinson, 2001). The optomotor response was robust. Most experimental data were obtained with a lower contrast pattern than the optomotor response; however, it has to be noted that for technical reasons the background illumination was also higher during the recording with the high-speed camera.

Extracellular recordings are a usefulmeans of obtaining relatively fast information about changes in motion processing related to the behavioral state. In contrast to calcium-imaging and patch clamp, extracellular recording has the advantage that it is a relatively easy method to apply. In addition, it is possible to hold the cells over a long time period, and therefore the recording time was only limited by the flight durations. Hence, similar to studies previously done on fixed flies, tools like information theory etc. can be used.

4.1.3 Application of CDM

CDM was used as an octopamine agonist. It was investigated whether the application of CDM has a similar effect on the visual system as flight.

The first question, of course, is why the application of CDM/octopamine should have similar effects on neuronal processing in the visual system as flight. There are numerous studies indicating that octopamine plays an important role during flight (Brembs et al., 2007; Buhl et al., 2008; Orchard, 1982; Orchard et al., 1993). Furthermore, it has also been shown that octopamine can modulate the response properties of neurons involved in vision (Erber and Kloppenburg, 1995; Erber and Sandeman, 1989; Kloppenburg and Erber, 1995; Longden and Krapp, 2009). In addition, anatomical projections of octopaminergic neurons into the lobula complex and medulla are known (Sinakevitch and Strausfeld, 2006; Busch et al., 2009). Taken together, all three points justify the assumption that the release of octopamine might explain, at least partially, the effect of flight on the response properties of lobula plate tangential cells.

It is well known that CDM can be used as a tissue-permeable octopamine agonist; this has already been tested in a number of studies (Duch and Pfluger, 1999; Kinnamon et al., 1984; Longden and Krapp, 2009; Vierk et al., 2009). A good description about the binding properties of the octopamine receptor can be found in (Hiripi et al., 1999). However, it has to be asked whether the method of application is suitable as an experimental condition. Bath application itself of course is a relatively crude method, e.g., it does not give much information about the actual place of function of octopamine. However, the fact that octopamine is increased in the hemolymphe during flight (Orchard, 1982; Orchard et al., 1993) indicates that bath application of CDM should at least result in some effects. A great advantage of the method is that it is simple and easy to apply. In addition, the application procedure does not disturb the animal at all. This is of critical importance since octopamine is known to be released during arousal (Davenport and Evans, 1984; Roeder, 1999; Stevenson et al., 2005). Therefore, bath application seems to be suitable as an initial experiment to address the question of whether octopamine contributes to some of the observed effects in flight. The CDM concentration used in this work was more towards the lower end of the range used in

previous studies (Duch and Pfluger, 1999; Kinnamon et al., 1984; Stevenson et al., 2005; Vierk et al., 2009). It was in the same order of magnitude as used previously in studies on flies (Longden and Krapp, 2009). Since this earlier work already suggested that the spontaneous activity increases after the application of octopamine, a concentration was chosen that induced a stable increase in spontaneous firing rate over the duration of the stimulus protocol.

4.2 State-Dependent Modulation of Visual Processing in the Fly

In the current work, the response properties of the lobula plate tangential cell H1 to visual motion stimuli were recorded under different behavioral states of the fly. Two conditions have been used as a non-active state – the non-flight condition and the fixed fly condition before the application of CDM. The other behavioral states are the flight condition and the CDM application condition. In the following I will compare the findings of this study with previous work (Heide, 1983) and recent literature on the effect of the behavioral state in flies (Chiappe et al., 2010; Haag et al., 2010; Longden and Krapp, 2009; Longden and Krapp, 2010; Maimon et al., 2010; Rosner et al., 2010).

4.2.1 H1 Recordings of Tethered Flying *Calliphora*

Heide (1983) in collaboration with his colleagues Foster and McCann also recorded from a lobula plate tangential cell which they assumed to be H1. Taking into account the result from this work it is rather surprising that Heide did not observe changes in the activity of H1 related to the locomotor state. As a stimulus they presented a pattern moving either in the preferred or null direction of H1. The firing rate – close to 300 Hz during non-flight and flight conditions – they reported when the pattern was moved in the preferred direction indicates a rather strong stimulus. A pattern movement in the null direction of H1 completely suppressed the firing rate for the non-flight condition but not for the flight condition (Heide, 1983; fig. 5: firing rate 5-20 Hz). Since the difference in the firing rate in response to visual stimulation was rather small for the non-flight and for the flight condition they concluded that flight does not alter the response properties

of H1. How can this strong disagreement with my findings be explained? I never used a stimulus which resulted in a similar strong response in the firing rate for the non-flight condition as Heide and colleagues. Nevertheless, figure 3.2 shows that differences, for non-flight and flight conditions, in the firing rate as a response to a pattern moving in the preferred and null directions decrease for very strong stimuli. This is especially true if one considers only the first two seconds of the stimulus presentation. In the current work neither in the non-flight nor in the flight condition were firing rates above 300 Hz observed over a time period longer than a few milliseconds. For both stimulus directions, the input-output relations in the experiments presented by Heide (1983) are probably saturated. Unfortunately, Heide (1983) did not report any spontaneous activity.

4.2.2 The Behavioral State Changes the Level of Spontaneous Activity and the Directional Tuning Range

In this work a strong increase in the spontaneous firing rate of H1 due to a change in the behavioral state of the animal was observed. While the increase in the firing rate after the application of CDM was about 3-fold, the increase associated with flying was about 6-10-fold. An increase in spontaneous activity is in accordance with work done in parallel on state-dependent influences of other lobula plate tangential cells in *Drosophila* and *Calliphora* (Chiappe et al., 2010; Haag et al., 2010; Longden and Krapp, 2009; Longden and Krapp, 2010; Maimon et al., 2010; Rosner et al., 2010). In principle, four different behavioral states were investigated: application of CDM (Longden and Krapp, 2009), passive and active movement of the halteres (Haag et al., 2010; Rosner et al., 2010), walking (Chiappe et al., 2010) and flying (Maimon et al., 2010). Three of these studies included work on spiking neurons, which makes a quantitative comparison possible (Haag et al., 2010; Longden and Krapp, 2009; Rosner et al., 2010).

The application of CDM in *Calliphora vicina* resulted in an increase of spontaneous activity of V1 and V2 cells (Longden and Krapp, 2009). The increase in spontaneous activity was on the same order of magnitude as in the CDM experiment of the current study. The difference might be attributed to various causes such as fly species, cell type,

different end concentration of CDM in the hemolymphe, different diffusion properties within the tissue, etc.

Halteres are known to oscillate during walking and flying, indicating locomotor behavior (Miller, 1977; Sandeman and Markl, 1980; Schneider, 1953). However, haltere movements were also reported during grooming (Rosner et al., 2010) or even without any locomotoractivity (Miller, 1977). Rosner et al. (2010) recorded from lobula plate tangential cells while monitoring active haltere movements. The baseline activity of lobula plate tangential cells (CH, HS, H1, V1) increased during haltere movement. Interestingly, the increase in baseline activity of H1 was rather weak (Rosner et al., 2010; fig. 4,~ 3 fold) compared to the results from flying flies, but similar to the changes reported after the application of CDM. The major focus of the work from Haag et al. (2010) was on an identified motorneuron, the ventral cervical nerve motorneuron (VCNM). This neuron integrates information from multiple sensory modalities (halteres, vision, wind). Active haltere movement resulted in a strong depolarization of VCNM (~20.2 mV), whereas HS cells recorded in the same flies only showed a rather small depolarization (~2.3 mV). Both studies concluded that the changes in activity in the different neurons are not due to a direct feedback from the haltere to the lobula plate tangential cells but rather a result of a central input modulating both haltere movement and LPTC responses (Rosner et al., 2010; Haag et al., 2010). However, whereas Haag et al. (2010) argue that the observed baseline shift in HS cells is caused by back-propagation of activity from postsynaptic neurons via gap junction, Rosner et al. (2010) assumed that the central signal is acting directly at the level of the lobula plate or presynaptically. Nevertheless, the central signal causing the increased firing rate and haltere movement is too weak to explain the changes observed in the increased firing rate of H1 during flight.

Rosner et al. (2010) also tested the response of H1 to moving stimuli during active haltere beating. They did not find any increase in activity compared to the trials where the haltere did not move. For the spiking neurons (H1, V1, possible U element) the observed changes in the responses to different stimuli were rather weak compared to results of this study. The relative increase in the spike frequency associated with haltere

beating was more pronounced for weak stimuli. Taken together, haltere beating had a rather small effect on the response properties of lobula plate tangential cells.

Similar to flying, however, it could be shown that HS cells show a strong increase in their response gain to visual stimulation during walking compared to non-walking (Chiappe et al., 2010). This suggests that although halteres are moving actively during walking and flying, the central signals associated with haltere movement alone cannot explain the observed effects of response increase during flight, walking and, to a lesser extent, also after CDM application. Different or at least additional mechanisms must cause the strong changes observed. Nevertheless, the haltere movements are bringing the cells closer to threshold and therefore might be important in combination with additional signals. Furthermore, the work of Haag et al. (2010) demonstrated that haltere movements have a strong effect on neck motor neurons.

Maimon et al. (2010) did patch clamp recordings on VS cells in the lobula plate of *Drosophila*. In contrast to H1, VS cells are non-spiking cells and respond to visual stimulation only with a shift in their membrane potential. Qualitatively, this study and mine point into the same direction since Maimon et al. (2010) observed an increase in resting potential linked to flight. They also measured the time course with which the baseline increase during flight decays back to the baseline value measured before flight was initiated. The fast decay time (Maimon et al., 2010; fig. 6c, right) made them conclude that the baseline shift is most likely not a result of neuromodulation (e.g., octopamine) but rather of input from a central signal or sensory feedback from the mechanoreceptors.

What are the consequences of an increased spontaneous activity during flight? An increase of the spontaneous activity can have a strong effect on the neural coding properties. For the non-flight condition, the spontaneous activity of H1 is rather low, ranging from 5-20 Hz. Therefore, the tuning range in the null direction is also limited to 5-20 Hz since the firing rate cannot fall below 0 Hz. For CDM application, it has been shown that the tuning range for motion in the null direction is increased through the elevated spontaneous firing rate (Longden and Krapp, 2009). Since the effect of the behavioral state on the spatial and directional tuning curve of different lobula plate

tangential cells was already discussed in other studies (Maimon et al., 2010; Longden and Krapp, 2009), the present study did not focus on this aspect. However, preliminary data suggest, in agreement with the other findings, that the tuning range for H1 is also increased during flight (fig. 3.5). Interestingly, despite the elevated firing rate during flight, weak stimuli (low contrast) did not increase the tuning range of H1 for null direction motion. Moreover, strong stimuli (high contrast) did not lead to a symmetric response to movement in the preferred and in the null direction. This can be modeled, for example, by using a different gain for the left and right half detector at the subtraction stage of the Reichardt detector or by assuming different input-output relationships between excitatory or inhibitory synapses and H1. As for the baseline activity alone, Maimon et al. (2010) measured the time course with which the dynamic range of response to a visual stimulus decreased after the fly stopped flying. The time scale was rather long and on the order of seconds (Maimon et al. 2010; fig. 6c, left). Therefore, neuromodulation might play a role, and the time course might reflect the time needed for octopamine to diffuse out of the receptor range or to become degraded.

Furthermore, an increased spontaneous activity is an indication that a cell is closer to threshold. This might reduce the latency of a cell's response to the onset of a stimulus or even increase the stimulus sensitivity. However, these relationships are not deterministic because the level of noise in the spike train could be increased as well. The effect will also depend on where on a stimulus response curve the spontaneous firing rate is located.

Another interesting aspect comes from information theoretical work. Comparing the response to dynamic stimuli in different neurons of various animals (e.g., fly, monkey, fish) it has been suggested that the information transmitted per spike is relatively constant, varying between values of one to two bits per spike in general (Borst and Theunissen, 1999). In addition, it has been shown that the information rate of H1 increases with an elevated firing activity (Borst and Haag, 2001). This result is far from trivial because, although it might be intuitive that increasing the number of spikes for example can increase the tuning range of a cell, other aspects such as noise entropy might change as well. Longden et al. (2009) showed that for V1 cells, despite the fact

that the information rate per spike was reduced after application of CDM, the information rate per second increased. The increase of spontaneous activity during flight and after the application of CDM, in addition to findings from the previous literature, suggests an increased information transfer during flight.

Why is the spontaneous rate of H1 not increased during the non-flight condition, as well? One possible explanation is that a low spontaneous firing rate is an evolutionary adaptation for saving energy. It has been demonstrated that action potentials carry a significant metabolic cost (Laughlin, 2001). Therefore, there exists a trade-off between an increased information rate and metabolic cost. An increase in the tuning range and an elevated information rate might be a favorable and efficient adaptation to the changed visual input statistic during flight. However, keeping up a high firing throughout the lifetime of a fly might be metabolically too expensive.

4.2.3 State Dependent Broadening of the Temporal Frequency Tuning Curve

The response properties of H1 to visual motion stimuli of different temporal frequency changed in three aspects with the behavioral state of the fly:

1.) at low stimulus frequencies the latency to the stimulus onset was reduced,
2.) the level of adaptation was reduced for prolonged stimulation in a frequency-dependent manner,
3.) the tuning curve was broadened towards higher frequencies.

The first result was observed in flying flies but not after the application of CDM. It is, however, possible that this decrease in latency was simply not detected, due to the variability in the data and the small number of stimulus repetitions. This is quite likely since other work has found a reduced latency to stimulus onset at low frequencies after the application of CDM (Longden and Krapp, 2010).

The second observation was that at high frequencies the steady-state level of the visual response changes during flight and after CDM application. The increased steady-state

level during flight and after CDM application is interesting because the fly receives permanent visual motion input due to self-motion during flight. The preferred direction of H1 is back-to-front motion, a visual input that a fly usually receives only during turns. Therefore, a prolonged stimulation of H1 might not occur that often during flight. However, it is likely that an elevation of the steady-state level is common for lobula plate tangential cells since similar observations have already been obtained for V1 after the application of CDM (Longden and Krapp, 2010). In addition, the modeling results suggest that a change in the low-pass time constant in the Reichardt detector is causing the elevated steady-state level during flight and after CDM application. Since the EMD are providing the input to the lobula plate, this further indicates that all lobula plate tangential cells should be affected in the same manner. Similar to the results of the current work, Longden and Krapp (2010) showed that the differences in the steady-state level between the CDM and before-CDM application conditions depended on temporal frequency (Longden and Krapp, 2010; fig. 4). Maimon et al. (2010) did not report any changes in the time course of the response of VS cells to a stimulus presentation in the preferred direction during flight. This is not surprising since they used a rather low frequency stimulus.

The broadening of the temporal frequency tuning curve of the steady-state response was also observed after the application of CDM in VS cells (Longden et al., 2010, fig. 4) and during walking in HS cells (Chiappe et al., 2010). Chiappe at al. (2010) suggested that an increased response gain to high temporal frequencies might be a strategy that stabilizes the optomotor response. During locomotion flies are exposed to a higher range of image speeds. Therefore, an increased gain at high temporal frequencies may enable the detection of faster retinal image shifts. It remains questionable whether the increased gain at higher temporal frequencies is sufficient to explain the detection of faster images during flight. Nevertheless, the broadening of the tuning curve is interesting with respect to the optomotor response and will be discussed further.

Throughout the literature, the similarity between the optomotor response and the temporal frequency tuning curve have been emphasized. Qualitatively, the behavioral data are quite similar to the electrophysiological tuning curve acquired in LPTCs (Borst and Bahde, 1987; Duistermars et al., 2007; Fry et al., 2009; Haag et al., 2004; Hausen

and Wehrhahn, 1989; Joesch et al., 2008; Schnell et al., 2010). However, studies in *Drosophila* revealed a discrepancy between the electrophysiologically-measured temporal frequency tuning curve in lobula plate tangential cells recorded in fixed flies and the behaviorally-observed optomotor response (fig. 4.2 a & b). Whereas tuning properties of single cells showed an optimum around 1 Hz (Joesch et al., 2008; Schnell et al., 2010), behavioral analyses revealed an optimal response of 1-4 Hz for walking (Buchner, 1984; Goetz and Wenking, 1973) and 4-10 Hz for flying flies (Duistermars et al., 2007). A similar observation can be made from work on *Calliphora vicina*, although the data are less clear (fig. 4.2 c & d). If one compares the optomotor response from *Calliphora vicina* with the response of H1 to a moving grating, a discrepancy between the cellular and behavior data can be seen at high temporal frequencies (Borst and Bahde, 1987; Haag et al., 2004).

Regarding the experiments performed in *Drosophila*, a complete shift in the temporal frequency tuning curve between behavioral and electrophysiological data can be observed. In contrast, in *Calliphora* the temporal frequency tuning curve acquired during behavior is broadened towards higher frequencies compared to the cellular data (fig. 4.2). It remains to be shown whether this effect can be explained by a different data analysis or experimental procedure or whether this discrepancy is a result of a real species difference. Interestingly, however, changing the low-pass time constant in a Reichardt detector lacking the high-pass filter leads to a shift in the temporal frequency tuning curve (Borst et al., 2003; fig. 1); by adding the high-pass constant in the cross-arm, a broadening of the tuning curve is possible with only a slight effect on the low frequency tuning (fig. 3.14). As discussed, flying, as well as the application of CDM, led to a broadening of the temporal frequency tuning curve of H1. After the application of CDM, the measured frequency optimum was about 3-5 Hz; which is similar to the frequency at which the maximum response increase was reported from LPTCs in walking *Drosophila* compared to non-walking (Chiappe et al., 2010). Flying led to an even further shift of the frequency optimum to around 7 Hz. These results solve the observed discrepancy in the optomotor response between behavior and cellular response.

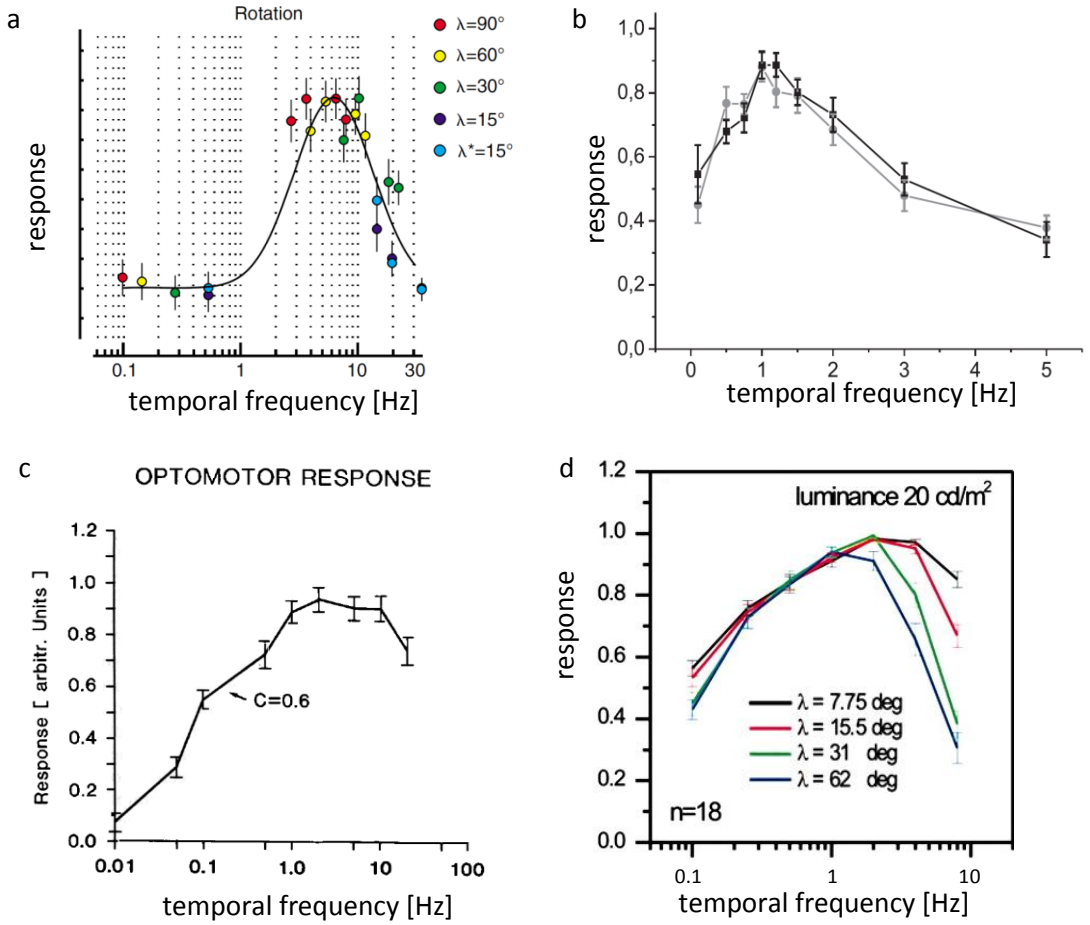

Figure 4.2: Behavioral and Cellular Temporal Frequency Tuning Curve. a) optomotor response measured in *Drosophila* (from Duistermars et al., 2007), b) temporal frequency tuning curve of HS cells measured in *Drosophila* (from Schnell et al., 2010), c) optomotor response to a motion pattern with a wavelength of 30° measured in *Calliphora* (from Borst and Bahde, 1987), d) temporal frequency tuning curve measured in H1 of *Calliphora* (from Haag et al., 2004).

4.3 Effect of Neuromodulation on Visual Processing

What mechanisms mediate the changes in visual motion processing depending on the behavioral state of an animal? Clearly, CDM could mimic some of the changes that were observed during flight in the neuronal response of H1. Since CDM is an octopamine agonist, this finding suggests that octopamine plays a role during state-dependent visual processing.

4.3.1 Physiological Action of Octopamine on the Visual System

On the single cell level, octopamine has been shown to increase the response to visual stimuli in the lobula plate of flies (Longden and Krapp, 2009; Longden and Krapp, 2010). Whether the observed effects are due to a gobal increase of octopamine in the hemolymphe or due to specific transmitter release acting only very locally at synapses presynaptic to LPTCs is not known. The fact that the specific site of octopamine application does not seem to be important speaks in favor of gobal neuromodulation (Longden and Krapp, 2009). However, anatomical studies have shown that the optic lobes of flies are highly innervated by octopaminergic neurons (Sinakevitch and Strausfeld, 2006; Busch et al., 2009). Octopaminergic neurons project into the lobula complex and the medulla. The projections to the medulla are of particular interest since visual motion processing is thought to take place mainly in this visual neuropil (Borst, 2009). To test the importance of these projections, further experiments are necessary; for example, direct electrical stimulation of octopaminergic neurons (Stern, 2009) or optogenetic activation of specific neurons.

4.3.2 Differences between Flight and CDM Condition

Both the flight condition and the application of CDM led to an increase in spontaneous activity and a shift and broadening of the temporal frequency tuning curve of H1. Generally, the effect of flight was more pronounced than the effect of CDM. However, two major differences between the flight condition and the CDM condition could be observed. First, the increase in spontaneous rate was much smaller after the application of CDM than during flight. Maimon et al. (2010) have suggested that different processes are involved in the baseline shift they observed in VS cells and the response gain during flight. Similarly, feedback from mechanoreceptors or additional central signals might explain the further increase in firing rate of H1 during flight. Second, the impulse response shortens after application of CDM, whereas the time constant for the flight condition increases compared to rest. It is possible that CDM shortens the high-pass of the Reichardt detector at the level of the medulla but additional input during flight might obscure this result.

The shift in the tuning curve was relatively similar between flying and CDM application. The small differences may be caused by several factors, even if one assumes that octopamine is solely responsible for the observed changes in the response properties of H1. First of all, the affinity of CDM to the octopamine receptor might differ from the affinity of octopamine itself (Hiripi et al., 1999). Octopamine acts as a neurohormone, neuromodulator or neurotransmitter in the invertebrate nervous system (Roeder, 1999). In particular, when considering its role as a neurotransmitter, another important aspect is that the local concentration of octopamine might be very different during bath application compared to normal synaptic transmitter release. It is very likely that the local concentration of octopamine is strongly regulated during flight. Work on *Drosophila* mutants have shown that both octopamine as well as tyramine might be involved in flight control (Brembs et al., 2007). Since CDM also binds to tyramine receptors, it is in principle possible that the bath application of CDM activates both systems. However, the affinity of CDM to the tyramine receptor is lower, so that the observed effect is most likely caused by an activation of the octopaminergic system (Hiripi et al., 1999). Nevertheless, comparing the relatively crude experiment of bath application to a behavioral state dependent neuronal transmitter release, it is surprising how well CDM application could mimic the effect of flying.

4.4 Underling Mechanisms for the Observed Change in the Tuning Properties

To model the response of H1, I used a version of the Reichardt detector which, in addition to the low-pass filter, has a high-pass filter in the cross-arm. The high-pass time constant of the model is given by the time constant of the impulse response (Borst et al., 2003). As already mentioned in the Materials and Methods section, it has been shown that the time constant of the impulse response is shortened following prolonged exposure to motion stimuli (Borst and Egelhaaf, 1987; de Ruyter van Steveninck et al., 1986; Reisenman et al., 2003). However, if one assumes an adaptation of the low-pass time constant, one expects a difference in the velocity optima for different contrasts which has not been observed (Harris et al., 1999). An adapting high-pass constant instead of an adapting low-pass constant solves this discrepancy (Borst et al., 2003). The

high-pass time constant for the flight condition was always higher than the time constant of the non-flight condition. As shown previously, measuring the impulse response before and after presenting an adapting stimulus revealed a decrease in the time constant of the impulse response (Borst and Egelhaaf, 1987; de Ruyter van Steveninck et al., 1986; Reisenman et al., 2003). The absolute amount of adaptation was stronger in the flight condition as compared to the non-flight condition. Given the slower time course of the isolated impulse response during flight, this is in agreement with the original model which proposed that the time-constant decreases more, the further it is away from the minimum value (Borst et al., 2003). Another important point of the model is that the steady-state response to low frequencies is also influenced by the high-pass time constant, whereas at high frequencies the low-pass time constant plays the most important role. Therefore, the shift of the frequency tuning curve towards higher frequencies can only be explained by a change of the low-pass time constant. Using the model, I calculated the best fit for the low-pass filter in order to explain the results. Low-pass filtering takes place in the presynaptic circuity of LPTCs, presumable in the medulla (Higgins et al., 2004). In addition, anatomical projections of octopaminergic neurons into the medulla and into the lobula complex are known (Sinakevitch and Strausfeld, 2006; Busch et al., 2009). Therefore, assuming a change in the low-pass time constant caused by octopaminergic modulation is in agreement with anatomical studies as well as with the current understanding of the processing steps underlying visual motion detection. The calculated results of the High-pass model showed a very good fit to the experimental data for high frequencies. However, for low frequencies the fit was not as good for the flight condition. Furthermore, the transient response of H1 to stimulus presentation in the preferred direction could be explained by the model to a great extent. Differences between the model predictions and the experimental data can have various explanations. The high-pass constant could only be measured approximately. The high-pass constant (as stated above) has an influence on the low frequency tuning of LTPCs as well as on the transient response (Borst et al., 2003; Reisenman et al., 2003). Hence, imprecise measurements of the high-pass constant will affect both, and might be the explanation of the difference found in the low frequency tuning and the transient response. In the non-flight condition, after presenting an adapting stimulus, the firing rate returned to the spontaneous rate after

200 ms before the onset of the impulse stimulus. In case of the flight condition, the firing rate was still slightly higher than the resting frequency (< 15 %). Therefore, the measured time constant of the impulse response was still, to some extent, influenced by the spike rate after visual stimulation, producing errors in the measurement. In previous studies this error was prevented by measuring the response to the adapting stimulus in isolation and subtracting the measured firing rate from the impulse response (Borst et al., 2003; Reisenman et al., 2003). For the flight experiment, however, this was not feasible because the length of the stimulus protocol was restricted to 20 min.

Furthermore, changing the gain in the Reichardt detector model (weighting between the left and right half detectors) also influences the transient response. Nevertheless, the results show that the high-pass time constants as well as the low-pass time constant change from non-flight to flight conditions. Given the fact that the time constant of the impulse response and the degree of adaptation are quite different between the non-flight and fight conditions, it is reasonable to suggest that there should be a significant effect in the visual response to stimuli with a lower correlation time. Thus, it would be interesting to investigate the response to more naturalistic stimuli.

4.5 State-Dependent Influences on Neuronal Processing

The results of the current work clearly demonstrated that the behavioral state has a strong influence on visual motion processing in flies. The fact, that the behavioral state of an animal can modulate neuronal processing has been known for many years. In vertebrates, the cortical activity changes dramatically during different phases of sleep and wakefulness (Gottesmann, 1999). It has also been observed that the same neurons can be involved in different behavioral tasks and in addition to that can also completely change their activity patterns. A famous example comes from work on invertebrates. In somatogastric ganglia (STG) of crabs, it has been demonstrated that neurons switch between different modes of activity depending on whether they are involved in the gastric mill rhythm or in the pyloric rhythm. The change in activity is reflected in the period of the rhythm. The period of the gastric rhythm is typically 5-10 s, whereas the period of the pyloric rhythm is approximately 1 s (Weimann et al., 1991). With a few

exceptions, in sensory processing of visual information the influence of the behavioral state has been neglected for a long time. However, it has generated more and more interest in the last couple of years.

4.6 Effect of Behavioral State on Visual Processing in Invertebrates

The first question one has to address is why there should be a behavioral effect on visual processing at all. There are several aspects related to that question. First of all, the environment an animal has to cope with is never constant. There is, for example, a strong difference between luminance levels an animal has to deal with depending on whether it is active during night or day. Though animals are usually either active at night or during the day, to have at least some visual information throughout of the circadian cycle the visual system has to be able to adapt to a wide range of light intensities. Second, the internal state of an animal might have an influence on visual processing, for example depending on whether the animal is aroused or relaxed. Last, the visual input might also be changed as a consequence of the animal's own behavior, such as locomotor activity. All these aspects are highly interconnected; the arousal state of an animal, for example, might change with the circadian cycle, or changes in the arousal state might result in a different locomotor behavior, or vice versa. Let us consider an example for all of these three different aspects: environmental, internal state, and self-motion-induced changes of visual processing.

The circadian clock is one of the few examples which has received attention for decades. The circadian clock of the horseshoe crab (*L. polyphemus*) originates in the protocerebrum. It modulates the sensitivity of the eyes through the activation of efferent optic nerve fibers. The gain in sensitivity is most likely achieved by an increase in photon catch (Barlow et al., 1977; Kass and Barlow, 1984; Kass and Barlow, 1992). Interestingly, the release of octopamine is thought to underlie the increase in visual sensitivity (Kass and Barlow, 1984). The use of an increased sensitivity regulated by the circadian rhythm becomes evident when one considers that horseshoe crabs are mainly active at night. Therefore, as many other nocturnal animals, they have a special adaptations to increase visual sensitivity during night time.

In locusts, it has been shown that, during flight, visual interneurons connected to neurons involved in escape behavior decrease their level of adaptation to looming stimuli. This aspect is explained as the result of an increased level of arousal during flight and as a mechanism to avoid collision during swarming behavior (Rind et al., 2008).

The visual input statistics also change due to self-motion. This is especially relevant for flying animals. Here the dynamic range of visual stimuli changes strongly from non-moving, to walking, to flying. Intuitively, it is clear that, for optimal coding of the stimulus, early processing steps in the visual system have to be adjusted to the input statistics. Therefore, it might not be surprising that this work has revealed differences in the encoding of the stimulus depending on the locomotor state of the animal.

Taken together, the behavioral state has a strong influence on neuronal processing. Modulating early processing stages in sensory systems might be a highly efficient strategy to adapt the animal to different situations it has to cope with.

4.7 Conclusion and Outlook

The major finding of this work is that visual motion processing is strongly modulated by the behavioral state of an animal. The fact that tethered flight and application of an octopamine agonist led to similar changes in response to the same visual stimulus hints at an important role for octopamine in state-dependent neuronal processing. Neuromodulation plays an important function in many aspects of behavioral state dependent sensory processing (e.g., Gaudry and Kristan, 2009). In addition, octopamine was already reported to play a role in visual processing in invertebrates (e.g., Kass and Barlow, 1984, Longden and Krapp, 2010). It is of high interest to investigate the mechanism that leads to changed neuronal processing during behavior. By using modeling in addition to electrophysiological recordings and pharmacological manipulations, the current work has demonstrated that these changes in neuronal processing most likely occur already very early in the sensory system. Recent studies on sensory processing suggest that similar changes can be observed throughout the animal kingdom (Maimon et al., 2010; Treue and Maunsell, 1996; Niell and Stryker, 2010; Gaudry and Kristan, 2009). Thus it is very important to study sensory processing during

behavior – by recording from behaving animals and/or studying neuromodulation – to get insights in how sensory information is processed in a behaviorally relevant situation.

Although many interesting findings could be made, this study provides only a first glimpse into the field of state-dependent visual processing in flies; further interesting results are waiting to be revealed. In the following, I will focus on questions which are still open and directly related to this study.

4.7.1 Future Experiments on the Role of Octopamine

In this study only bath application of CDM has been performed. In addition to an octopamine agonist, other neurotransmitters could be studied as well, such as serotonin, which has already been shown to have an effect on visual motion processing in insects (Donovan , 1986; Chen et al., 1999; Erber et al., 1993). Furthermore, it might be of great interest to examine the effect of octopamine antagonists. Is it, for example, possible to apply an antagonist to a flying fly and see whether specific effects of flying become reduced? This idea does not seem to be completely out of range since studies on mutants in *Drosophila* have shown that octopamine is important for flight initiation but not for flight maintenance (Brembs et al., 2007). Here, it would be interesting to see whether the spontaneous rate is still increased during flight while the broadening of the tuning curve might remain unaffected. This would suggest a different mechanism for both effects as suggested by preliminary data from Maimon et al. (2010).

The modeling results suggest that changing the low-pass time constant in the Reichardt detector presynaptic to H1 would be sufficient to explain the broadening of the tuning curve. Anatomical studies have revealed octopaminergic projections to the medulla and the lobula complex (Sinakevitch and Strausfeld, 2006; Busch et al., 2009). Are they responsible for the observed broadening of the tuning curve? Do they have an effect on the spontaneous activity of the cell? Or do the change in the time constant and the increase in the spontaneous activity have their origin in locally distinct regions? Local application of octopamine in *Calliphora* or the use of genetic tools in *Drosophila* will hopefully solve these questions.

4.7.2 Future Experiments on Tethered Flying Flies

On the experimental level, great advances have already been made. Nowadays, in addition to the possibility of recording extracellularly from flying flies, studies using intracellular recordings as well as calcium imaging have successfully addressed the question of state-dependent modulation of visual processing in flies performing different locomotor activities (Chiappe et al., 2010; Maimon et al., 2010; Seelig et al., 2010). Therefore, it seems quite likely that great progress will be made regarding the mechanisms underlying state-dependent modulations as well as the involvement of other neurons.

There are a few experiments which could be performed in the near future that are directly linked to the current study. Regarding the electrophysiological work on tethered flying flies, it would be interesting to monitor the behavior of the animal while performing recordings and, for example, to do closed loop experiments or use behavioral choice paradigms (Tang and Juusola, 2010) to establish a correlation between neuronal activity and behavior. Furthermore, measuring the response properties of lobula plate tangential cells to dynamic and even natural stimuli will give additional insights into the function of the observed effects of flying on visual processing. Here, it is also possible that other celltype-specific changes related to the behavioral state might come into play. The amount of after-hyperpolarization, spike frequency adaptation, etc., might change depending on the locomotor activity. Also, double recordings could be done from LPTCs and the motor output (Heide, 1983) or from different pairs of LPTCs. Recording from pairs of LPTCs is interesting because, considering that likely all of the LPTCs are modulated during flight, it is possible that their connectivity properties might be altered as well.

5. Reverences

Balint, CN, Dickinson, MH (2001). The correlation between wing kinematics and steering muscle activity in the blowfly Calliphora vicina. J Exp Biol, 204, 4213-4226.

Barlow, RB, Bolanowski, SJ, Brachman, ML (1977). Efferent optic-nerve fibers mediate circadian-rhythms in Limulus eye. Science, 197, 86-89.

Bausenwein, B, Fischbach, KF (1992). Activity labeling patterns in the medulla of Drosophila-melanogaster caused by motion stimuli. Cell Tissue Res, 270, 25-35.

Borst, A (2009). Drosophila's view on insect vision. Curr Biol, 19, R36-R47.

Borst, A, Bahde, S (1986). What kind of movement detector is triggering the landing response of the housefly. Biol Cybern, 55, 59-69.

Borst, A, Bahde, S (1987). Comparison between the movement detection systems underlying the optomotor and the landing response in the housefly. Biol Cybern, 56, 217-224.

Borst, A, Egelhaaf, M (1987). Temporal-modulation of luminance adapts time constant of fly movement detectors. Biol Cybern, 56, 209-215.

Borst, A, Egelhaaf, M (1989). Principles of visual motion detection. Trends Neurosci, 12, 297-306.

Borst, A, Haag, J (2001). Effects of mean firing on neural information rate. J. Computat. Neurosci, 10, 213-221.

Borst, A, Haag, J (2002). Neural networks in the cockpit of the fly. J Comp Physiol A, 188, 419-437.

Borst, A, Reisenman, C, Haag, J (2003). Adaptation of response transients in fly motion vision. II: Model studies. Vision Res, 43, 1309-1322.

Borst, A, Theunissen, FE (1999). Information theory and neural coding. Nat Neurosci, 2, 947-957.

Borst, A, Weber, F (2011). Neural action fields for optic flow based navigation: A simulation study of the fly lobula plate network. Plos One, 6.

Borst, A, Haag, J (2007). Optic flow processing in the cockpit of the fly. Cold Spring Harbor Monograph Series 49: 101-122

Borst, A, Haag, J, Reiff, DF (2010). Fly motion vision. Annu Rev Neurosci, 33, 49-70.

Borst, Abmd (2007). Correlation versus gradient type motion detectors: the pros and cons. Philos Trans R Soc Lond B, 362, 369-374.

Braitenberg, V (1967). Patterns of projection in visual system of fly .I. Retina-Lamina projections. Exp Brain Res, 3, 271-298.

Braitenberg, V, Ferretti, CT (1966). Landing reaction of Musca Domestica induced by visual stimuli. Naturwiss, 53, 155.

Braitenberg, V (1970). Ordnung und Orientierung der Elemente im Sehsystem der Fliege. Kybernetik, 7, 235-242.

Brembs, B, Christiansen, F, Pfluger, HJ, Duch, C (2007). Flight initiation and maintenance deficits in flies with genetically altered biogenic amine levels. J Neurosci, 27, 11122-11131.

Brenner, N, Strong, SP, Koberle, R, Bialek, W, van Steveninck, RRD (2000). Synergy in a neural code. Neural Comput, 12, 1531-1552.

Buchner, E (1984). Behavioural analysis of spatial vision in insects. In Photoreception and vision in invertebrates. Ali, MA (ed). Plenum Press: New York, London, pp. 561-621.

Buchner, E, Buchner, S, Bulthoff, I (1984). Deoxyglucose mapping of nervous activity induced in Drosophila brain by visual movement .1. Wildtype. J Comp Physiol A, 155, 471-483.

Budick, SA, Reiser, MB, Dickinson, MH (2007). The role of visual and mechanosensory cues in structuring forward flight in Drosophila melanogaster. J Exp Biol, 210, 4092-4103.

Buhl, E, Schildberger, K, Stevenson, PA (2008). A muscarinic cholinergic mechanism underlies activation of the central pattern generator for locust flight. J Exp Biol, 211, 2346-2357.

Bullock, TH, Behrend, K, Heiligenberg, W (1975). Comparison of jamming avoidance responses in Gymnotid and Gymnarchid electric fish - case of convergent evolution of behavior and its sensory basis. J Comp Physiol, 103, 97-121.

Bullock, TH, Hamstra, RH, Scheich, H (1972). The jamming avoidance response of high frequency electric fish. J Comp Physiol A, 77, 1-22.

Busch, S, Selcho, M, Ito, K, Tanimoto, H (2009). A map of octopaminergic neurons in the Drosophila brain. J Comp Neurol, 513, 643-667.

Chen, B, Meinertzhagen, IA, Shaw, SR (1999). Circadian rhythms in light-evoked responses of the fly's compound eye, and the effects of neuremodulators 5-HT and the peptide PDF. J Comp Physiol A, 185, 393-404.

Chiappe, ME, Seelig, JD, Reiser, MB, Jayaraman, V (2010). Walking modulates speed sensitivity in Drosophila motion vision. Curr Biol, 20, 1470-1475.

Clark, DA, Bursztyn, L, Horowitz, MA, Schnitzer, MJ, Clandinin, TR (2011). Defining the computational structure of the motion detector in Drosophila. Neuron, 70, 1165-1177.

Collett, TS, Paterson, CJ (1991). Relative motion parallax and target localization in the Locust, Schistocerca-Gregaria. J Comp Physiol A, 169, 615-621.

Cook, T, Desplan, C (2001). Photoreceptor subtype specification: from flies to humans. Semin Cell Dev Biol, 12, 509-518.

Davenport, AP, Evans, PD (1984). Stress-induced changes in the octopamine levels of insect hemolymph. Insect Biochem, 14, 135-143.

David, CT (1982). Compensation for height in the control of groundspeed by Drosophila in a new, Barbers pole wind-tunnel. J Comp Physiol, 147, 485-493.

de Ruyter van Steveninck, R, Zaagman, WH, Mastebroek, HAK (1986). Adaptation of transient responses of a movement-sensitive neuron in the visual system of the blowfly Calliphora-Erythrocephala. Biol Cybern, 54, 223-236.

Douglass, JK, Strausfeld, NJ (1995). Visual-motion detection circuits in flies - peripheral motion computation by identified small-field retinotopic neurons. J Neurosci, 15, 5596-5611.

Douglass, JK, Strausfeld, NJ (2003). Anatomical organization of retinotopic motion-sensitive pathways in the optic lobes of flies. Microsc Res Tech, 62, 132-150.

Donovan, LA, Thompson, PM, Shaw, SR (1986). Light Adaptation Serotonin and Efferent Neurons All Way Affect Visual Responsiveness in A Circadian-Insensitive Insect Retina. Society for Neuroscience Abstracts, 12, 856.

Duch, C, Pfluger, HJ (1999). DUM neurons in locust flight: a model system for amine-mediated peripheral adjustments to the requirements of a central motor program. J Comp Physiol A, 184, 489-499.

Duistermars, BJ, Chow, DM, Condro, M, Frye, MA (2007). The spatial, temporal and contrast properties of expansion and rotation flight optomotor responses in Drosophila. J Exp Biol, 210, 3218-3227.

Eckert, H (1980). Functional-properties of the H1-neurone in the 3Rd optic ganglion of the blowfly, Phaenicia. J Comp Physiol, 135, 29-39.

Egelhaaf, M, Borst, A (1989). Transient and steady-state response properties of movement detectors. J Opt Soc Am A -Optics Image Science and Vision, 6, 116-127.

Eichner, H, Joesch, M, Schnell, B, Reiff, DF, Borst, A (2011). Internal structure of the fly elementary motion detector. Neuron, 70, 1155-1164.

Elyada, YM, Haag, J, Borst, A (2009). Different receptive fields in axons and dendrites underlie robust coding in motion-sensitive neurons. Nat Neurosci, 12, 327-332.

Erber, J, Kloppenburg, P (1995). The modulatory effects of serotonin and octopamine in the visual-system of the honey-bee (Apis-mellifera L.) .I. Behavioral-analysis of the motion-sensitive antennal reflex. J Comp Physiol A, 176, 111-118.

Erber, J, Kloppenburg, P, Scheidler, A (1993). Neuromodulation by serotonin and octopamine in the honeybee - behavior, neuroanatomy and electrophysiology. Experientia, 49, 1073-1083.

Erber, J, Sandeman, DC (1989). The effect of serotonin and octopamine on the optokinetic response of the crab Leptograpsus-Variegatus. J Neurobiol, 20, 667-680.

Exner S (1891) Die Physiologie der Facettirten Augen vou Krebsen and Insecten. Deuticke. Leipzig.

Farooqui, T (2007). Octopamine-mediated neuromodulation of insect senses. Neurochemical Res, 32, 1511-1529.

Farrow, K, Borst, A, Haag, J (2005). Sharing receptive fields with your neighbors: Tuning the vertical system cells to wide field motion. J Neurosci, 25, 3985-3993.

Fischbach, KF, Dittrich, APM (1989). The Optic Lobe of Drosophila-Melanogaster .1. A Golgi analysis of Wild-Type Structure. Cell Tissue Res, 258, 441-475.

Franceschini, N., Riehle, A., and Le Nestour, A. (1989). Directionally selective motion detection by insect neurons. In Facets of Vision, D.G. Stavenga and R.C. Hardie, eds. (Berlin: Springer), pp. 360–390.

Franz, MO, Krapp, HG (2000). Wide-field, motion-sensitive neurons and matched filters for optic flow fields. Biol Cybern, 83, 185-197.

Fry, SN, Rohrseitz, N, Straw, AD, Dickinson, MH (2009). Visual control of flight speed in Drosophila melanogaster. J Exp Biol, 212, 1120-1130.

Frye, MA, Dickinson, MH (2001). Fly flight: A model for the neural control of complex behavior. Neuron, 32, 385-388.

Gabbiani, F, Jones, PW (2011). A genetic push to understand motion detection. Neuron, 70, 1023-1025.

Gao, SY, Takemura, SY, Ting, CY, Huang, SL, Lu, ZY, Luan, HJ, Rister, J, Thum, AS, Yang, ML, Hong, ST, Wang, JW, Odenwald, WF, White, BH, Meinertzhagen, IA, Lee, CH (2008). The neural substrate of spectral preference in Drosophila. Neuron, 60, 328-342.

Gaudry, Q, Kristan, WB (2009). Behavioral choice by presynaptic inhibition of tactile sensory terminals. Nat Neurosci, 12, 1450-1457.

Geiger, G (1974). Optomotor responses of fly Musca-domestica to transient stimuli of edges and stripes. Kybernetik, 16, 37-43.

Geiger, G, Nassel, DR (1981). Visual orientation behavior of flies after selective laser-beam ablation of interneurones. Nature, 293, 398-399.

Gewecke, M (1967). Die Wirkung Von Luftströmung auf die Antennen und das Flugverhalten der blauen Schmeissfliege (Calliphora Erythrocephala). Z Vergl Physiol , 54, 121-&.

Goetz, KG, Hengstenberg, B, Biesinger, R (1979). Optomotor control of wing beat and body posture in Drosophila-melanogaster. Biol Cybern, 35, 101-112.

Goetz, KG (1968). Flight control in Drosophila by visual perception of motion. Kybernetik, 4, 199-208.

Goetz, KG (1972). Principles of optomotor reactions in insects. Bibl Ophthalmol, 82, 251-259.

Goetz, KG, Wenking, H (1973). Visual control of locomotion in walking fruitfly Drosophila. J Comp Physiol, 85, 235-266.

Goodman, LJ (1960). The landing responses of insects .1. the landing response of the fly, Lucilia-sericata, and other Calliphorinae. J Exp Biol, 37, 854-878.

Gottesmann, C (1999). Neurophysiological support of consciousness during waking and sleep. Prog Neurobiol, 59, 469-508.

Haag, J, Borst, A (1997). Encoding of visual motion information and reliability in spiking and graded potential neurons. J Neurosci, 17, 4809-4819.

Haag, J, Borst, A (2001). Recurrent network interactions underlying flow-field selectivity of visual interneurons. J Neurosci, 21, 5685-5692.

Haag, J, Borst, A (2003). Orientation tuning of motion-sensitive neurons shaped by vertical-horizontal network interactions. J Comp Physiol A, 189, 363-370.

Haag, J, Borst, A (2004). Neural mechanism underlying complex receptive field properties of motion-sensitive interneurons. Nat Neurosci, 7, 628-634.

Haag, J, Borst, A (2008). Electrical coupling of lobula plate tangential cells to a heterolateral motion-sensitive neuron in the fly. J Neurosci, 28, 14435-14442.

Haag, J, Denk, W, Borst, A (2004). Fly motion vision is based on Reichardt detectors regardless of the signal-to-noise ratio. Proc natl Acad Sci USA, 101, 16333-16338.

Haag, J, Wertz, A, Borst, A (2007). Integration of lobula plate output signals by DNOVS1, an identified premotor descending neuron. J Neurosci, 27, 1992-2000.

Haag, J, Wertz, A, Borst, A (2010). Central gating of fly optomotor response. Proc natl Acad Sci USA, 107, 20104-20109.

Hardie, RC (1979). Electro-physiological analysis of fly retina .1. Comparative properties of R1-6 and R7 and 8. J Comp Physiol, 129, 19-33.

Harris, RA, O'Carroll, DC, Laughlin, SB (1999). Adaptation and the temporal delay filter of fly motion detectors. Vision Res, 39, 2603-2613.

Hassenstein, B, Reichardt, W (1951). Funktionsanalyse der Bewegungsperzeption eines Käfers. Naturwiss, 38, 507.

Hassenstein, B, Reichardt, W (1956a). Functional structure of a mechanism of perception of optical movement. In Proceedings of the first international congress on cybernetics: Namur, pp. 797-801.

Hassenstein, B, Reichardt, W (1956b). Systemtheoretische Analyse der Zeit-, Reihenfolgen- und Vorzeichenauswertung bei der Bewegungsperzeption des Rüsselkäfers Chlorophanus - A theoretical analysis of the system of time-, sequence- and sign evaluation in the perception of movement in the snout beetle Chlorophanus. Zeitschr Naturforsch, llb, 513-524.

Hausen, K (1982a). Motion sensitive interneurons in the optomotor system of the fly .1. the horizontal cells - structure and signals. Biol Cybern, 45, 143-156.

Hausen, K (1982b). Motion sensitive interneurons in the optomotor system of the fly .2. the horizontal vells - receptive-field organization and response characteristics. Biol Cybern, 46, 67-79.

Hausen, K (1984). Photoreception and vision in invertebrates. The lobula-complex of the fly: structure, function and significance in visual behaviour. NATO ASI (Advanced Science Institutes) Series Series A Life Sciences, 74, 523-559.

Hausen, K, Wehrhahn, C (1983). Microsurgical lesion of horizontal cells changes optomotor yaw responses in the blowfly Calliphora-erythrocephala. Proc R Soc Lond B, 219, 211-216.

Hausen, K, Wehrhahn, C (1989). Neural circuits mediating visual flight control in flies .1. Quantitative comparison of neural and behavioral-response characteristics. J Neurosci, 9, 3828-3836.

Hausen, K (1993). Decoding of retinal image flow in insects. Rev Oculomot Res, 5, 203-235.

Heide, G (1983). Neural mechanisms of flight control in Diptera. In Insect Flight II-Insektenflug II (BIONA report 2). Nachtigall, W (ed). Gustav Fischer: Stuttgart,New York, pp. 35-52.

Heisenberg, M, Wonneberger, R, Wolf, R (1978). Optomotor-Blindh31 - Drosophila mutant of lobula plate giant neurons. J Comp Physiol, 124, 287-296.

Hengstenberg, R (1982). Common visual response properties of giant vertical cells in the lobula plate of the blowfly Calliphora. J Comp Physiol, 149, 179-193.

Hengstenberg, R (1988). Mechanosensory control of compensatory head roll during flight in the blowfly Calliphora-Erythrocephala Meig. J Comp Physiol A, 163, 151-165.

Hengstenberg, R, Hausen, K, Hengstenberg, B (1982). The number and structure of giant vertical cells (Vs) in the lobula plate of the blowfly Calliphora-Erythrocephala. J Comp Physiol, 149, 163-177.

Higgins, CM, Douglass, JK, Strausfeld, NJ (2004). The computational basis of an identified neuronal circuit for elementary motion detection in dipterous insects. Vis Neurosci, 21, 567-586.

Hildreth, EC, Koch, C (1987). The analysis of visual motion from computational theory to neuronal mechanisms. Ann Rev Neurosci 10, 477.

Hiripi, L, Nagy, L, Hollingworth, RM (1999). In vitro and in vivo effects of formamidines in locust (Locusta migratoria migratorioides). Acta Biol Hung, 50, 81-87.

Horstmann, W, Egelhaaf, M, Warzecha, AK (2000). Synaptic interactions increase optic flow specificity. Acta Biol Hung J Neurosci, 12, 2157-2165.

Jarvileh, M, Zellter, F (1971). Localized intracellular potentials from presynaptic and postsynaptic components in external plexiform layer of an insect retina. Z Vergl Physiol , 75, 422-&.

Jarvileh, M, Zettler, F (1973). Electrophysiological-histological studies on some functional properties of visual cells and second-order neurons of an insect retina. Zeitschrift für Zellforschung und Mikroskopische Anatomie, 136, 291-306.

Joesch, M, Plett, J, Borst, A, Reiff, DF (2008). Response properties of motion-sensitive visual interneurons in the lobula plate of Drosophila melanogaster. Curr Biol, 18, 368-374.

Joesch, M, Schnell, B, Raghu, SV, Reiff, DF, Borst, A (2010). ON and OFF pathways in Drosophila motion vision. Nature, 468, 300-U186.

Kass, L, Barlow, RB (1984). Efferent neurotransmission of circadian-rhythms in Limulus lateral eye .1. Octopamine-induced increases in retinal sensitivity. J Neurosci, 4, 908-917.

Kass, L, Barlow, RB (1992). A circadian clock in the Limulus brain transmits synchronous efferent signals to all eyes. Vis Neurosci, 9, 493-504.

Katsov, AY, Clandinin, TR (2008). Motion processing streams in Drosophila are behaviorally specialized. Neuron, 59, 322-335.

Kimmerle, B, Egelhaaf, M (2000). Performance of fly visual interneurons during object fixation. J Neurosci, 20, 6256-6266.

Kinnamon, SC, Klaassen, LW, Kammer, AE, Claassen, D (1984). Octopamine and chlordimeform enhance sensory responsiveness and production of the flight motor pattern in developing and adult moths. J Neurobiol, 15, 283-293.

Kirschfeld, K (1973). Das neuronale Superpositionsauge. Fortschritte der Zoologie, 21, 228-257.

Kloppenburg, P, Erber, J (1995). The modulatory effects of serotonin and octopamine in the visual-system of the honey-bee (Apis-mellifera L.) .II. Electrophysiological analysis of motion-sensitive neurons in the lobula. J Comp Physiol A, 176, 119-129.

Kral, K, Poteser, M (1997). Motion parallax as a source of distance information in locusts and mantids. J Insect Behav, 10, 145-163.

Krapp, HG, Hengstenberg, B, Hengstenberg, R (1998). Dendritic structure and receptive-field organization of optic flow processing interneurons in the fly. J Neurophysiol, 79, 1902-1917.

Krapp, HG, Hengstenberg, R (1996). Estimation of self-motion by optic flow processing in single visual interneurons. Nature, 384, 463-466.

Krapp, HG, Hengstenberg, R, Egelhaaf, M (2001). Binocular contributions to optic flow processing in the fly visual system. J Neurophysiol, 85, 724-734.

Land, MF (1999). Compound eye structure: matching eye to environment. In: Adaptive mechanisms in the ecology of vision. Archer, S.N.; Djamgoz, M.B.A.; Loew, E.R.; Partridge, J.C.; Vallerga, S. (ed). Kluwer Academic Publishers: Dordrecht, Boston & London, pp. 51-71

Land, MF (1997). Visual acuity in insects. A Rev Entomol, 42, 147-177.

Land, MF, Fernald, RD (1992). The evolution of eyes. Annu Rev Neurosci, 15, 1-29.

Laughlin, SB (2001). Energy as a constraint on the coding and processing of sensory information. Curr Opin Neurobiol, 11, 475-480.

Laughlin, SB, Osorio, D (1989). Mechanisms for neural signal enhancement in the blowfly compound eye. J Exp Biol, 144, 113-146.

Longden, KD, Krapp, HG (2009). State-dependent performance of optic-flow processing interneurons. J Neurophysiol, 102, 3606-3618.

Longden, KD, Krapp, HG (2010). Octopaminergic modulation of temporal frequency coding in an identified optic flow-processing interneuron. Front Syst Neurosci, 4: 153.

Maddess, T (1986). Afterimage-like effects in the motion-sensitive neuron H1. Proc R Soc Lond B, 228, 433-459.

Maddess, T, Laughlin, SB (1985). Adaptation of the motion-sensitive neuron H1 is generated locally and governed by contrast frequency. Proc R Soc Lond B, 225, 251-275.

Maimon, G, Straw, AD, Dickinson, MH (2010). Active flight increases the gain of visual motion processing in Drosophila. Nat Neurosci, 13, 393-U29.

Matsubara, J, Heiligenberg, W (1978). How well do electric fish electro-locate under jamming. J Comp Physiol, 125, 285-290.

Mayer, M, Vogtmann, K, Bausenwein, B, Wolf, R, Heisenberg, M (1988). Flight control during free yaw turns in Drosophila-Melanogaster. J Comp Physiol A, 163, 389-399.

Meinertzhagen, IA, O'Neil, SD (1991). Synaptic organization of columnar elements in the lamina of the wild type in Drosophila-melanogaster. J Comp Neurol, 305, 231-263.

Miller, PL (1977). Haltere activity in a flightless hippoboscid fly, Crataerina-pallida. J Insect Physiol, 23, 855-860.

Montell, C, Jones, K, Zuker, C, Rubin, G (1987). A 2nd opsin gene expressed in the ultraviolet-sensitive R7 photoreceptor cells of Drosophila-melanogaster. J Neurosci, 7, 1558-1566.

Morris, OT, Duch, C, Stevenson, PA (1999). Differential activation of octopaminergic (DUM) neurones via proprioceptors responding to flight muscle contractions in the locust. J Exp Biol, 202, 3555-3564.

Murakami, M, Kashiwadani, H, Kirino, Y, Mori, K (2005). State-dependent sensory gating in olfactory cortex. Neuron, 46, 285-296.

Nalbach, G (1993). The halteres of the blowfly Calliphora .1. Kinematics and dynamics. J Comp Physiol A, 173, 293-300.

Nalbach, G, Hengstenberg, R (1994). The halteres of the blowfly Calliphora .2. 3-Dimensional organization of compensatory reactions to real and simulated rotations. J Comp Physiol A, 175, 695-708.

Nelson, ME, Maciver, MA (1999). Prey capture in the weakly electric fish Apteronotus albifrons: Sensory acquisition strategies and electrosensory consequences. J Exp Biol, 202, 1195-1203.

Niell, CM, Stryker, MP (2010). Modulation of visual responses by behavioral state in mouse visual cortex. Neuron, 65, 472-479.

Orchard, I (1982). Octopamine in insects - neurotransmitter, neurohormone, and neuromodulator. Can J Zool, 60, 659-669.

Orchard, I, Lange, AB (1984). Cyclic-AMP in locust fat-body - correlation with octopamine and adipokinetic hormones during flight. J Insect Physiol, 30, 901-904.

Orchard, I, Ramirez, JM, Lange, AB (1993). A multifunctional role for octopamine in locust flight. A Rev Entomol, 38, 227-249.

Otsuna, H, Ito, K (2006). Systematic analysis of the visual projection neurons of Drosophila melanograster. I. Lobula-specific pathways. J Comp Neurol, 497, 928-958.

Ramirez, JM, Pearson, KG (1991). Octopaminergic modulation of interneurons in the flight system of the locust. J Neurophysiol, 66, 1522-1537.

Reichardt, W (1961). Autocorrelation, a principle for the evaluation of sensory information by the central nervous system. In Sensory Communication. Rosenblith, WA (ed). The M.I.T. Press and John Wiley & Sons: New York, London, pp. 303-317.

Reichardt, W (1987). Evaluation of optical motion information by movement detectors. J Comp Physiol A, 161, 533-547.

Reichardt, W (1969) Movement perception in insects. In: Processing of optical data by organisms and by machines (ed. W. Reichardt). New York: Academic Press

Reichardt, W, Varjú, D (1959). Übertragungseigenschaften im Auswertesystem für das Bewegungssehen. Z. Naturforsch., 14b, 674-689.

Reichert, H, Rowell, CHF, Griss, C (1985). Course correction circuitry translates feature detection into behavioral action in locusts. Nature, 315, 142-144.

Reiff, DF, Plett, J, Mank, M, Griesbeck, O, Borst, A (2010). Visualizing retinotopic half-wave rectified input to the motion detection circuitry of Drosophila. Nat Neurosci, 13, 973-U92.

Reisenman, C, Haag, J, Borst, A (2003). Adaptation of response transients in fly motion vision. I: Experiments. Vision Res, 43, 1291-1307.

Reiser, MB, Dickinson, MH (2008). A modular display system for insect behavioral neuroscience. J Neurosci Methods, 167, 127-139.

Rind, FC, Santer, RD, Wright, GA (2008). Arousal facilitates collision avoidance mediated by a looming sensitive visual neuron in a flying locust. J Neurophysiol, 100, 670-680.

Rister, J, Pauls, D, Schnell, B, Ting, CY, Lee, CH, Sinakevitch, I, Morante, J, Strausfeld, NJ, Ito, K, Heisenberg, M (2007). Dissection of the peripheral motion channel in the visual system of Drosophila melanogaster. Neuron, 56, 155-170.

Roeder, T (1999). Octopamine in invertebrates. Prog Neurobiol, 59, 533-561.

Rosenberg, LA, Glusman, JG, Libersat, F (2007). Octopamine partially restores walking in hypokinetic cockroaches stung by the parasitoid wasp Ampulex compressa. J Exp Biol, 210, 4411-4417.

Rosner, R, Egelhaaf, M, Warzecha, AK (2010). Behavioural state affects motion-sensitive neurones in the fly visual system. J Exp Biol, 213, 331-338.

Sandeman, DC, Markl, H (1980). Head movements in flies (Calliphora) produced by deflection of the halteres. J Exp Biol, 85, 43-60.

Sanes, JR, Zipursky, SL (2010). Design principles of insect and vertebrate visual systems. Neuron, 66, 15-36.

Santer, RD, Rind, FC, Stafford, R, Simmons, PJ (2006). Role of an identified looming-sensitive neuron in triggering a flying locust's escape. J Neurophysiol, 95, 3391-3400.

Santer, RD, Simmons, PJ, Rind, FC (2005). Gliding behaviour elicited by lateral looming stimuli in flying locusts. J Comp Physiol A, 191, 61-73.

Schneider, G (1953). Die Halteren der Schmeissfliege (Calliphora) als Sinnesorgane und als mechanische Flugstabilisatoren. Z Vergl Physiol , 35, 416-458.

Schnell, B, Joesch, M, Forstner, F, Raghu, SV, Otsuna, H, Ito, K, Borst, A, Reiff, DF (2010). Processing of horizontal optic flow in three visual interneurons of the Drosophila brain. J Neurophysiol, 103, 1646-1657.

Seelig, JD, Chiappe, ME, Lott, GK, Dutta, A, Osborne, JE, Reiser, MB, Jayaraman, V (2010). Two-photon calcium imaging from head-fixed Drosophila during optomotor walking behavior. Nat Methods, 7, 535-U77.

Sherman, A, Dickinson, MH (2003). A comparison of visual and haltere-mediated equilibrium reflexes in the fruit fly Drosophila melanogaster. J Exp Biol, 206, 295-302.

Sherman, A, Dickinson, MH (2004). Summation of visual and mechanosensory feedback in Drosophila flight control. J Exp Biol, 207, 133-142.

Simmons, P (1980). A locust wind and ocellar brain neuron. J Exp Biol, 85, 281-294.

Sinakevitch, I, Strausfeld, NJ (2006). Comparison of octopamine-like immunoreactivity in the brains of the fruit fly and blow fly. J Comp Neurol, 494, 460-475.

Skingsley, DR, Laughlin, SB, Hardie, RC (1995). Properties of histamine-activated chloride channels in the large monopolar cells of the dipteran compound eye - A comparative-study. J Comp Physiol A, 176, 611-623.

Srinivasan, M, V (1990). Generalized gradient schemes for the measurement of two-dimensional image motion. Biol Cybern, 63, 421-432.

Srinivasan, MV, Lehrer, M, Kirchner, WH, Zhang, SW (1991). Range perception through apparent image speed in freely flying honeybees. Vis Neurosci, 6, 519-535.

Srinivasan, MV, Poteser, M, Kral, K (1999). Motion detection in insect orientation and navigation. Vision Res, 39, 2749-2766.

Srinivasan, MV, Zhang, SW, Lehrer, M, Collett, TS (1996). Honeybee navigation en route to the goal: Visual flight control and odometry. J Exp Biol, 199, 237-244.

Stern, M (2009). The PM1 neurons, movement sensitive centrifugal visual brain neurons in the locust: anatomy, physiology, and modulation by identified octopaminergic neurons. J Comp Physiol A, 195, 123-137.

Stevenson, PA, Dyakonova, V, Rillich, J, Schildberger, K (2005). Octopamine and experience-dependent modulation of aggression in crickets. J Neurosci, 25, 1431-1441.

Straka, H, Ammermuller, J (1991). Temporal resolving power of blowfly visual-system - effects of decamethonium and hyperpolarization on responses of laminar monopolar neurons. J Comp Physiol A, 168, 129-139.

Strausfeld, NJ (1976). Atlas of an insect brain. Springer: Berlin, Heidelberg.

Straw, AD, Lee, S, Dickinson, MH (2010). Visual control of altitude in flying Drosophila. Curr Biol, 20, 1550-1556.

Sugiura, H, Dickinson, MH (2009). The generation of forces and moments during visual-evoked steering maneuvers in flying Drosophila. Plos One, 4.

Takemura, SY, Lu, ZY, Meinertzhagen, IA (2008). Synaptic circuits of the Drosophila optic lobe: The input terminals to the medulla. J Comp Neurol, 509, 493-513.

Tammero, LF, Dickinson, MH (2002). The influence of visual landscape on the free flight behavior of the fruit fly Drosophila melanogaster. J Exp Biol, 205, 327-343.

Tang, S, Juusola, M (2010). Intrinsic Activity in the fly brain gates visual information during behavioral choices. Plos One, 5

Treue, S, Maunsell, JHR (1996). Attentional modulation of visual motion processing in cortical areas MT and MST. Nature, 382, 539-541.

Uusitalo, RO, Juusola, M, Weckstrom, M (1995). Graded responses and spiking properties of identified first-order visual interneurons of the fly compound eye. J Neurophysiol, 73, 1782-1792.

Uusitalo, RO, Weckstrom, M (2000). Potentiation in the first visual synapse of the fly compound eye. J Neurophysiol, 83, 2103-2112.

vanSteveninck, RRD, Lewen, GD, Strong, SP, Koberle, R, Bialek, W (1997). Reproducibility and variability in neural spike trains. Science, 275, 1805-1808.

Vierk, R, Pflueger, HJ, Duch, C (2009). Differential effects of octopamine and tyramine on the central pattern generator for Manduca flight. J Comp Physiol A-, 195, 265-277.

von Frisch, K (1947). The dances of the honey bee. Bull Animal Behavior [London], 5, 1-32.

von Frisch, K. (1993). The dance language and orientation of bees. Cambridge, MA: Harvard University.

Wallace, GK (1959). Visual Scanning in the desert locust Schistocerca-Gregaria Forskal. J Exp Biol, 36, 512-525.

Warrant, EJ (1999). Seeing better at night: life style, eye design and the optimum strategy of spatial and temporal summation. Vision Res, 39, 1611-1630.

Watanabe, A, Takeda, K (1963). Change of discharge frequency by A.C. Stimulus an weak electric Fish. J Exp Biol, 40, 57-&.

Weber, F, Machens, CK, Borst, A (2010). Spatiotemporal response properties of optic-flow processing neurons. Neuron, 67, 629-642.

Wehrhahn, C, Hausen, K (1980). How is tracking and fixation accomplished in the nervous-system of the fly - a behavioral-analysis based on short-time stimulation. Biol Cybern, 38, 179-186.

Weimann, JM, Meyrand, P, Marder, E (1991). Neurons that form multiple pattern generators - identification and multiple activity patterns of gastric pyloric neurons in the crab stomatogastric system. J Neurophysiol, 65, 111-122.

Weismann, A. (1864). Die nachembryonale Entwicklung der Musciden nach Beobachtungen an Musca vomitoria und Sarcophaga carnaria. Zeitschr wiss Zool, 14: 187-336

Wertz, A, Borst, A, Haag, J (2008). Nonlinear integration of binocular optic flow by DNOVS2, a descending neuron of the fly. J Neurosci, 28, 3131-3140.

Wiegmann, BM, Trautwein, MD, Winkler, IS, Barr, NB, Kim, JW, Lambkin, C, Bertone, MA, Cassel, BK, Bayless, KM, Heimberg, AM, Wheeler, BM, Peterson, KJ, Pape, T, Sinclair, BJ, Skevington, JH, Blagoderov, V, Caravas, J, Kutty, SN, Schmidt-Ott, U, Kampmeier, GE,

Thompson, FC, Grimaldi, DA, Beckenbach, AT, Courtney, GW, Friedrich, M, Meier, R, Yeates, DK (2011). Episodic radiations in the fly tree of life. Proc natl Acad Sci USA, 108, 5690-5695.

Yamaguchi, Shhd, Wolf, R, Desplan, C, Heisenberg, M (2008). Motion vision is independent of color in Drosophila. Proc natl Acad Sci USA, 105, 4910-4915.

Zanker, JM, Srinivasan, MV, Egelhaaf, M (1999). Speed tuning in elementary motion detectors of the correlation type. Biol Cybern, 80, 109-116.

Zbikowski, R (2005). Fly like. Ieee Spectrum, 42, 46-51.

Zhu, Y, Nern, A, Zipursky, SL, Frye, MA (2009). Peripheral visual circuits functionally segregate motion and phototaxis behaviors in the fly. Curr Biol, 19, 613-619.

Zuker, CS, Montell, C, Jones, K, Laverty, T, Rubin, GM (1987). A rhodopsin gene expressed in photoreceptor cell R7 of the Drosophila eye - homologies with other signal-transducing molecules. J Neurosci, 7, 1550-1557.

6. Curriculum Vitae

Sarah Nicola Jung

Date of Birth: 04.04.1982

Nationality: German

Education

Oct 2007 – present	**PhD Project** Max Planck Institute of Neurobiology, Munich, Germany Department of Systems and Computational Neurobiology Project: Visual Motion Detection in Tethered Flying Flies Supervisors: Dr. Jürgen Haag & Prof. Dr. Alexander Borst
Sept 2006 – June 2007	**Diploma Project/Research Assistant** University of Missouri St. Louis, St. Louis, USA Center for Neurodynamics Project: Response properties of electrosensory units in the midbrain tectum of the paddlefish (Polyodon spathula, Walbaum)
July – Dec 2005	**Study Abroad** University of Adelaide, Adelaide, Australia
Oct. 2001 – Sept 2007	**Diploma Studies** Rheinische Friedrich-Wilhelms-Universität, Bonn, Germany Major: Biology; Degree: Diplom - grade 1.3 (top grade 1.0)
1992 – 2001	**A-levels (Abitur)** Aggertalgymnasium in Engelskirchen Majors: Mathematics, Biology

Teaching

Oct 2003 – Aug 2006	**Tutor for "Mathematics in Biology"** (5 semesters) Rheinische Friedrich-Wilhelms-Universität, Bonn, Germany

Awards & Memberships

June 2008 – present	**DFG Research Training Group** Orientation and Motion in Space: Fellowship
Oct 2007 – present	**International Max Planck Research School** for Molecular and Cellular Life Sciences, Munich
Jan 2009 – present	**Bernstein Center for Computational Neuroscience,** Munich

International Graduate Courses (selected participants)

June 2010 – July 2010	**Neural Systems & Behaviour** Summer course at Marine Biology Lab (Woods Hole) Duration: 8 weeks
Jan 2009	**Structure and Function of Neural Circuits** Winter School at Obergurgl, Austria (PENS) Duration: 1 week (lecture based)
Aug 2007	**Methods in Computational Neuroscience** Summer course at Marine Biology Lab (Woods Hole) Duration: 4 weeks
June 2007 – July 2007	**Neuroethology: The Neural Basis of Natural Behavior Using an Invertebrate System** Summer course at Friday Harbor Marine Biology Lab, University of Washington Duration: 4 weeks

Organization of Events

April 2009	**PhD -Symposium Interact** – http://www.munich-interact.org/ Function: Head of the Steering Committee Participation: approximately 400 PhD students

Publications

Full Paper

Jung SN, Borst A, Haag J (2011) Flight activity alters velocity tuning of fly motion-sensitive neurons. J Neurosci 31: 9231-9237

Hofmann MH, **Jung SN,** Chagnaud BP, Preissner M, Siebenaller U, Wilkens LA (2008) Response properties of electrosensory units in the midbrain tectum of the paddlefish (*Polyodon spathula*). J Exp Biol 211:773-779

Hofmann MH, **Jung SN**, Wilkens LA (2007) Resonant properties in the paddlefish electrosensory system caused by delayed feedback. Biological Cybernetics 97: 413-421. PMID: 17926062

Talk

Jung SN (2010) Visual motion detection in tethered flying flies. Joint Graduate School Symposium – 'Networks', Berlin, Germany.

Jung SN (2011) Visual motion detection in tethered flying flies. University of Bielefeld, Department of Neurobiology, Bielefeld, 14th of July 2011.

Poster Presentations

Jung SN, Borst A, Haag J (2011) Visual motion detection in tethered flying flies. 9th Göttingen Meeting of the German Neuroscience Society. Göttingen, Germany.

Jung SN, Borst A, Haag J (2009) Visual motion detection in stationary flying flies. Autumn School – 'Space, Time, and Numbers'. Seeon, Germany.

Jung SN, Wilkens LA, Hofmann MH (2007) Response properties of electrosensory units in the midbrain tectum of the paddlefish. Satellite Meeting Electroreception. Vancouver, Canada & International Congress of Neuroethology. Vancouver, Canada.

7. Acknowledgements

I would like to thank my PhD-advisors Prof. Dr. Alexander Borst and Jürgen Haag for having me in the lab and for giving me the opportunity to work independently on this interesting project. It was an awesome experience for me to be at the MPI and I highly appreciate the great working atmosphere in the lab. I want to thank them for fast feedback regarding applications, manuscripts, posters, etc. Thanks in particular, for supporting me to take part at various Summer- and Winter-Schools throughout my PhD. My direct supervisor Dr. Jürgen Haag, I want to thank for his constant support throughout the years, for never losing patience and always being open for questions and discussions regarding the project.

Furthermore, I would like to thank Prof. Dr. Sonya Bahar - whom I already know from my Diplom thesis - for being there and supporting me in many ways whenever needed. I would like to thank Prof. Dr. Andreas Herz for being part on my thesis committee and giving me feedback on various aspects related to the project as well as to applications.

I would like to thank Renate Gleich for taking care of the flies, preparing solutions and in every aspect being of great technical assistance. Thanks especially for all the extra work you do for the lab. Thanks to Hubert Eichner and Franz Weber for all the support and questions they answered me about programming and taking care of our fly meeting. I would like to thank Johannes Plett for his help on the LED-arena.

Most of all, I would like to thank my colleagues and friends in the lab for the great atmosphere. Thanks to Bettina, my involuntary senior, for any scientific conversation we had. Thanks for your patience and moral support throughout the last couple of years - thesis and non-thesis related. Thanks to Susu, for always making the world a bit brighter

around you. Thanks to all the people who shared the office with me Thorben, Elisabeth, Katarina, Erika, Kristina, Matthew and Marcel. It was just great working with you.

Thanks to Amrita and Gayanne for all the discussions about science and life. Thanks to Yong for listening. Thanks to Hanna for helping me settle down in Munich and giving me an introduction to Estonia.

I would like thank the whole Borst and Griesbeck lab for the excellent scientific environment.

My work was supported through a doctoral fellowship (2008-2011) of the DFG which gave me the possibility to realize my dissertation within the graduate college 'Orientation and Motion in Space'. I also want to thank the coordinators of the International Max Planck Research School - Hans-Joerg Schaefer, Maximiliane Reif and Ingrid Wolf - for the great work they do for PhD-students in Munich. IMPRS gave me the possibility to extent my 'soft skills' related to science and took part in financing several of the conferences and schools I attended.

Finally, I would like to thank my family for their unconditional support throughout all the years.

Ehrenwörtliche Versicherung

Ich versichere hiermit ehrenwörtlich, dass die vorgelegte Dissertation von mir selbständig und ohne unerlaubte Hilfe angefertigt ist.

München, den _____ _____

Erklärung

Hiermit erkläre ich, dass die Dissertation nicht ganz oder in wesentlichen Teilen einer anderen Prüfungskommission vorgelegt worden ist und dass ich mich anderweitig einer Doktorprüfung ohne Erfolg nicht unterzogen habe.

München, den _____ _____